MODELING AND VALIDATION OF FULL SCALE CRASH TESTING FOR OPEN-FACED AESTHETIC CONCRETE BARRIER

By

ANDREW WAGDY WASSEF

A thesis submitted to the

Graduate School-New Brunswick

Rutgers, The State University of New Jersey

In Partial Fulfillment of the Requirements

For the degree of

Master of Science

Graduate Program in Civil & Environmental Engineering

Written under the direction of

Dr. Hani H. Nassif

And approved by

_____

_____

_____

New Brunswick, New Jersey

May 2017

ABSTRACT OF THE THESIS

MODELING AND VALIDATION OF FULL-SCALE CRASH TESTING FOR OPEN-FACED AESTHETIC CONCRETE BARRIER

By ANDREW WAGDY WASSEF

Thesis Director:

Dr. Hani H. Nassif

As bridges built in the 1930's and 1940's begin to reach the end of their design and service lives, the concrete and embedded steel reinforcement of balustrades show noticeable signs of deterioration, which affects their performance. Many of these old bridges are historic and the aesthetics must be preserved to keep it as a historic landmark. The Historic Preservation Office (HPO) mandated that a new balustrade for use on historic bridges must retain the appearance of the original one while also satisfying the requirements of the crash test level AASHTO MASH TL-4, which was adopted by the FHWA on January 1, 2011.

This study addresses the issue that the state of New Jersey does not currently have any open-faced balustrade standard specifications. A new design was developed, for

which the aesthetics have been approved by the HPO, and a detailed finite element model was developed using LS-DYNA software for crash test simulation. The capacity of the barrier was checked using the design procedures outlined in section 13 of the AASHTO Bridge Design Specifications. A parametric study of the balustrade was performed using the finite element model, adjusting parameters such as height, post width, and window opening width. Occupant risk factors such as ridedown accelerations, and occupant impact velocities were evaluated using these models.

Based on the results of the simulations, a final design was selected and chosen for full scale crash testing. A single unit truck, pickup truck, and small passenger car were crash tested at TTI and successfully met all the AASHTO MASH TL-4 requirements. All risk factors were well below the maximum permissible values for the car and pickup truck, and the single unit truck was successfully contained.

After these successful crash tests, the model was calibrated to more accurately duplicate the impact response of the vehicle and barrier. The models were also validated using traditional methods, as well as the statistical comparison program, Roadside Safety Verification and Validation Program (RSVVP), which was developed under NCHRP Project 22-24.

ACKNOWLEDGEMENTS

TABLE OF CONTENTS

Contents

LIST OF TABLES

LIST OF FIGURES

CHAPTER I

1. INTRODUCTION

1.1. PROBLEM STATEMENT

As many bridges built in the 1930's start to reach the end of their design service lives, the need for repairs and maintenance becomes more and more apparent, and when the state of the bridges becomes more deficient, there comes a need to rehabilitate, or in some cases, completely replace the bridge. Some bridges that are old may have historical significance to the city they are in, and city council members may create roadblocks that do not allow for a full removal and replacement. A bridge may not be completely replaced if it is considered a national landmark, if it has become part of the "character" of a city, or even if it is just an aesthetically pleasing part of the city view.

One bridge that has historical significance has been undergoing rehabilitation since April of 2014 is the Pulaski Skyway in Jersey City, Hudson County, NJ. The Hoboken Viaduct, also known as NJ Route 139, was opened in 1932 and is part of the Route 1&9 Historic Corridor. Along its length is an open-faced concrete balustrade barrier to prevent vehicles from driving off the bridge. The current barrier in place is as old as the bridge itself and is deteriorating rapidly because of its age. Because of this,

there is a need to replace the old barrier with a new one that was designed and tested to pass today's rigorous safety standards.

The open-faced design of this barrier adds an aesthetic element to the bridge because more recently designed barriers are solid and do not provide the pleasing appearance that the original one does. Because of this, the Historic Preservation Office (HPO) has expressed opposition to using the solid barrier. One of the solutions to this problem is to retain the original barrier on the bridge, but have an approved crash tested metal barrier between the lanes and itself. This way, the open bridge rail will still be there providing the aesthetics and the passengers on the bridge will still have a crashworthy barrier to help prevent injury or death.

This solution, though, is not optimal because the view of the original rail would be obstructed. But what if the original aesthetics could be retained without the need for a second barrier? The only way for this to occur is if there was an aesthetically pleasing bridge rail design that has been crash tested and approved by the Federal Highway Administration (FHWA). The objective of this research is to create an aesthetically pleasing open faced bridge rail design that meets the aesthetic requirements of the HPO and the safety standards of the FHWA. The safety standard that must be met to receive approval from the FHWA is to pass a Test Level 4 (TL-4) collision specified in the American Association of State Highway Transportation Officials Manual for Assessing Safety Hardware (AASHTO MASH).

1.2.   RESEARCH OBJECTIVES AND SCOPE

The purpose of this research is to develop an aesthetic, open-faced concrete balustrade design that is also safe, and can sustain a MASH TL-4 collision. Because full-

scale crash testing is very time-consuming and expensive, computer simulations will be used prior to construction and testing. A detailed finite element model using the dynamic non-linear Finite Element Analysis (FEA) software LS-DYNA will be utilized to predict the behavior for different scenarios. A parametric study will be performed using this model to evaluate different design alternatives. Parameters that will be changed and investigated include total height, post height, post width, window opening width, and concrete strength. During this study, factors such as occupant risk, barrier damage, vehicle response and occupant response will be investigated. Once the study is concluded, a final design will be chosen and used for construction. After the final design is chosen, the barrier will be constructed and tested at an FHWA accredited facility, and a final pass/fail grade will be determined. Once the barrier passes, the finite element models will be calibrated and validated. The barrier will become a standard NJDOT specification and will be able to be used anywhere in the state where historic barriers need replacement

1.3. THESIS ORGANIZATION

This thesis will be organized as follows:

Chapter I introduces the problem statement, research objectives and scope, and thesis organization.

Chapter II covers the background and literature review of work performed by others in historic bridge rehabilitation, finite element crash test simulation, and crash testing.

Chapter III covers the barrier design, Finite Element Model development, and the parametric study results.

Chapter IV covers the full-scale barrier construction, crash testing, results, and finite element model calibration and validation.

Chapter V covers the summary, and conclusions.

CHAPTER II

2. LITERATURE REVIEW

2.1.   INTRODUCTION

Before any piece of roadside safety hardware is approved for use on the road, it must first pass the appropriate crash test. In the past few decades, researchers have begun using finite element models which have become a widespread and commonly used method of analysis. Software such as LS-DYNA has revolutionized the way highway barriers are analyzed and evaluated. By utilizing finite element models, the process of designing and optimizing any piece of safety hardware is faster than ever because in many cases, some designs may be ruled out before they are constructed or tested. Limiting the number of full scale tests performed greatly reduces the cost of developing and implementing safety hardware.

The methods of physically testing this safety hardware have also grown to be much more sophisticated and consistent.   Many facilities, such as Texas A&M Transportation Institute (TTI), have performed countless tests on a varying array of safety hardware and have nearly perfected the art of crash testing. The use of highly accurate accelerometers, rotational transducers, and high-speed cameras has revolutionized the way the data is processed and analyzed.

This chapter will discuss work performed by others in the area of bridge rehabilitation, finite element modeling, and full-scale crash testing.

2.2.   BRIDGE REHABILITATION

As historic bridges become older and the need to rehabilitate or replace them becomes more and more apparent, there are many things that must be considered. To retain aesthetics, the components of the bridges that are to be replaced must look similar to the original ones, and most of the standard specifications, such as those for barriers, must be redesigned to look similar, which adds to the project time and cost. These redesigned components must also fulfill the safety requirements set forth by the Federal Highway Administration (FHWA). This is usually the challenging part of historic bridge rehabilitation because the safety requirements are changed periodically and never stay constant for a long period of time. These requirements are ever-changing because safety is a top concern for engineers and with every change to the requirements, the level of safety is improved.

Demond (1996) provides six alternative solutions to rehabilitate bridges when replacing a bridge is not desirable. The six alternatives are listed and briefly described below:

1) **Rehabilitation (widening)** – Widening the existing structure (usually an overdesigned truss) to accommodate larger traffic volume.

2) **Rehabilitation (complimentary)** – Making traffic on the existing structure one way and building a similar bridge next to the original to handle traffic in the other direction.

3) **Twinning** – Similar to complimentary rehabilitation, but the new bridge as identical as possible to the original.

4) **Adaptive reuse** – Using the original bridge for something besides transportation.

5) **National landmark rehabilitation** – Maintaining the original appearance with minimal alterations to accommodate current highway standards.

6) **Removal and replacement with mitigation** – Salvaging components from the old bridge for use on a new bridge. This is done when functional requirements are too unreasonable to attain.

2.3.   OPEN FACED BALUSTRADE DESIGN

There are many different types of bridge rails used across the United States made out of different materials including wood, concrete, steel, aluminum, or a combination of these materials. Barriers made of concrete are typically used for a higher level of crash resistance than those made of wood or metal. Table 1 shows a list of tested and approved concrete barriers from the AASHTO ARTBA-AGC Task Force 13 bridge rail guide. The concrete bridge rails in Table 1 have all been tested and approved under the previously accepted criteria of NCHRP Report 350.

Table 1: Bridge railings using cast-in-place concrete [http://guides.roadsafellc.com]

Name/Designator	Image	Mounting Type	Aesthetic	See Through	Test Spec./ Test Level
SBC04d TL-4 F Shape		Deck	No	No	R350/TL4
SBC04e TL-5 F Shape		Deck	No	No	R350/TL5
SBC05d TL-4 Safety Shape		Deck	No	No	R350/TL4
SBC05e TL-5 Safety Shape		Parapet	No	No	R350/TL5
SBC07b TX T411		Parapet	Yes	Yes	R350/TL3
SBC07c Natchez Trace Bridge Rail		Parapet	Yes	Yes	R350/TL3
SBC07d TX F411		Deck	Yes	Yes	R350/TL4
SBC12b CA Type 80 SW		Parapet	Yes	Yes	R350/TL2

SBC12d CA Type 80		Parapet	No	Yes	R350/TL4
SBC13d CA Type 732		Parapet	No	No	R350/TL4

2.4.   FINITE ELEMENT MODELING

Because full scale crash tests are very costly and time consuming, there is an urgent need for accurate numerical computer solutions. Advances in non-linear dynamic modeling have occurred with the greatest progress during the 1990's when these models became more widely-used. Eskandarian et. al. (1997) modeled, tested, and validated a bogie used as a surrogate crash test vehicle for impact with roadside objects. The bogies used for full scale tests have a crushable nose with honeycomb material, and can be reused several times while only replacing the nose. Because the popularity of non-linear finite element programs is on the rise, a validated bogey model is necessary. Bogies are very versatile because the nose can easily be changed to represent different vehicle types, and the vehicle weight can be easily adjusted. The honeycomb material was validated using the impact of the nose with a rigid pole as the baseline for comparison. Showing proper behavior when impacting a narrow object is important because narrow objects (signs, poles, etc.) can cause injury often times, and it is a better measure of performance for model behavior (Eskandarian et. al, 1997).

Consolazio et. al. (2002) modified an NCAC model of the 2000P vehicle to accurately simulate different crash testing conditions. A low profile barrier for use in

construction zones was and modeled in the highway vehicle object simulation model (HVOSM) and later confirmed using LS-DYNA. The NCAC model was accurate for tall longitudinal barriers, but was not meant to simulate large deformations in the front suspension. The front suspension springs were modified to make the truck behavior more realistic. The barrier was constructed and a full scale test was performed, and successful. The model was validated, and a comparison of the test and model is shown in Figure 1. When modeling crash scenarios, it is important to make sure all critical failures are modeled properly to ensure an accurate result (Consolazio et. al, 2002).
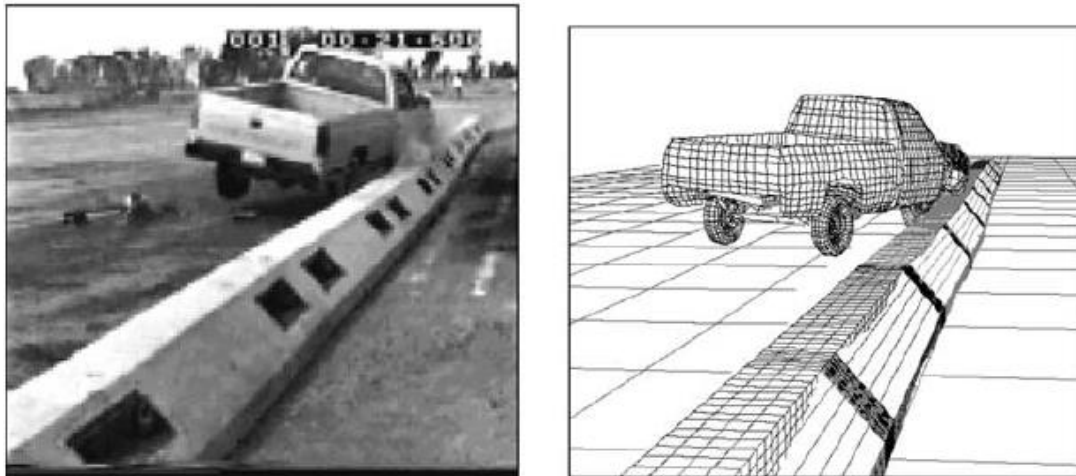
Figure 1: Comparison of crash test results and simulation results for 2000P vehicle
(Consolazio et. al, 2002)

Borovinsek et. al (2007) evaluated the use of computer simulations to evaluate barrier designs according to European standard EN 1317. EN 1317 criteria defines safety in terms of containment level, impact severity, and deformation of the barrier after impact. Two vehicles are used to evaluate the barrier, a 900 kg personal car and a high mass vehicle such as a heavy goods vehicle or a bus. The heavy weight vehicle properties depend on the containment level being evaluated. Accelerometers were defined at the center of gravity of the vehicle and the barriers were modeled using mainly

shell elements. Bolted connections were modeled with beam elements. Soil conditions are difficult to accurately model because they are always changing and hard to predict. Soil conditions were modeled with spring elements in different directions where the barrier was secured to the ground, and is shown in Figure 2. Contacts were defined where applicable and different reinforcements were evaluated. The reinforcements evaluated included a longitudinally placed tension belt, wheel guidance profile, and a single wire rope, which are shown in Figure 3.
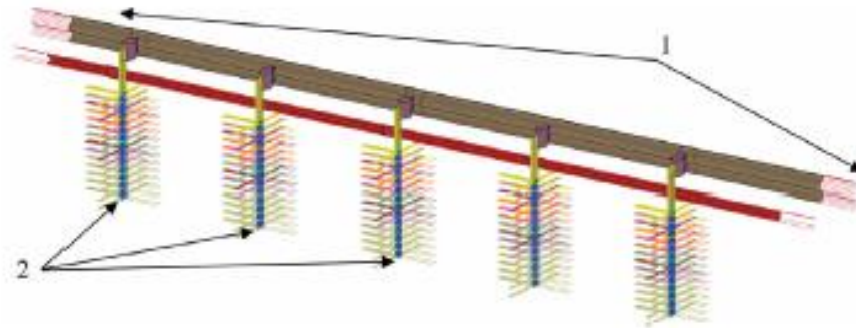
Figure 2: Spring elements used to simulate soil conditions (Borovinsek et. al (2007))
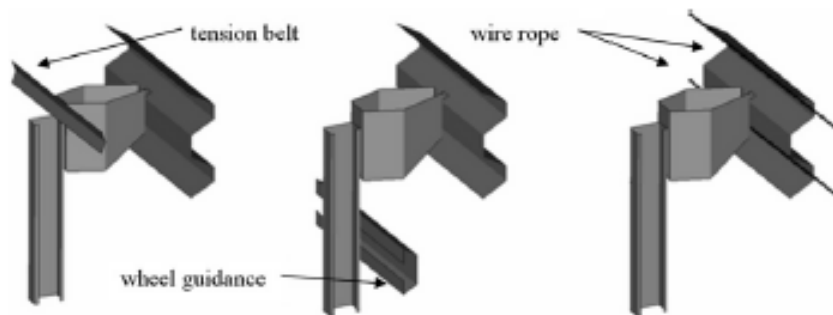
Figure 3: Guardrail reinforcement options evaluated (Borovinsek et. al (2007))

The wheel guidance system was chosen as the best option for containment level H1 and was certified later with a large scale test. The barrier performed acceptably and safely redirected the truck without any major parts separating from the barrier. The finite

element models were compared to the experimental results and the Acceleration Severity Index (ASI) time dependencies were in fairly good agreement and the values differed by less than the acceptable 10% margin. It was concluded that the computer simulations can be used to evaluate the experimental parameters with reasonable accuracy, and the use of simulations reduces the development and testing costs of new barrier designs (Borovinsek et. al, 2007).

Ren and Vesenjak (2005) compared results of an LS-DYNA simulation and full scale crash test of a metal barrier according to European Standard EN 1317. The rail evaluated was composed of a W-shaped guardrail, distance spacers, and posts with 2/3 of their height rammed into the soil. Each section of the guard rail is 4.2 m long with a 0.2 m splice at each section. The material was defined using tensile test results of S 235 steel and an effective plastic strain of 0.28. When the effective plastic strain reaches this level, the load carrying capability of the element becomes zero, effectively removing it from the model. Viscoelastic springs were defined on the posts to simulate soil, and linear springs were defined at the ends of the guardrail to simulate the continuation of the rail. The vehicle evaluated and tested was a Fiat uno impacting at 100 km/h at 20 degrees. When the full scale test and simulation were compared, there was very good agreement in the results and the model and it was determined that the model could be used for computational evaluation of other road safety barriers in the place of performing full scale tests (Ren and Vesenjak, 2005).

Itoh et. al. (2007) performed a simulation and full scale crash test for a 1.1 meter high F-shaped barrier. As per Japanese testing standards, the vehicle to be used is a 25,000 kg truck impacting at 100 km/h at 15 degrees to produce 650 kJ of energy.

However, due to limited pulling power available, the truck used was only 20,000 kg and the angle was changed to 17 degrees to produce 660 kJ of energy. In the model, the subgrade of the barrier was modeled with springs, and the simulation was run. The barrier showed satisfactory performance in the model, and when tested full-scale, the barrier was shown to meet all safety requirements. The results from the models and experimental results were in good agreement, as shown in Figure 4 (Itoh et. al, 2007).
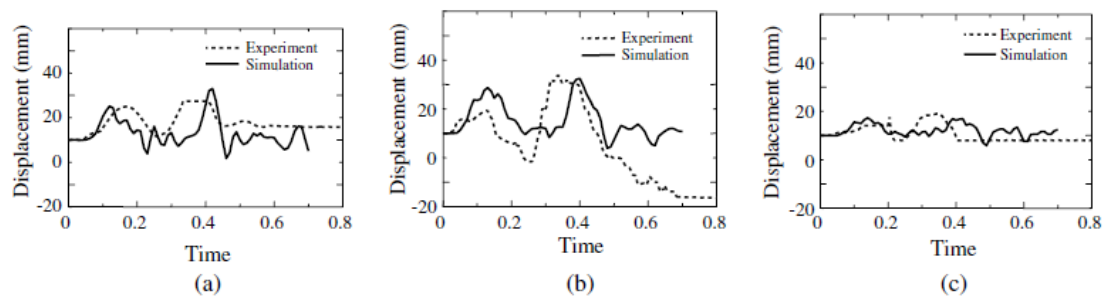
Figure 4: Comparison of experimental and simulation results (Itoh et. al, 2007)

Marzougui et. al. (2012) evaluated the practicality of using finite element models to evaluate barrier retrofits. During NCHRP Project 22-14(3), seven barriers previously accepted under NCHRP Report 350 were tested under MASH conditions, and three of them failed the pickup truck collision (Test 3-11). These collisions were then modeled using LS-DYNA and validated. Different retrofit options were then evaluated using these models to find a functional retrofit option. The FHWA recently announced that crash simulation results would be considered acceptable for evaluating improvements to previously tested barriers, which means there would be no need for another crash test. Barrier models were modeled in LS-DYNA using exactly the same geometry and connection details as the barriers tested. The finite element model of the Chevy Silverado was tested and was accepted as an acceptable surrogate for the 2270P vehicle previously used. Two of the barriers that were investigated for retrofits include the G9

Thrie-beam barrier and the G4 median barrier. The G4 median barrier failed because the truck overrode the installation and the Thrie-beam barrier failed because the wheel snagged on the bottom of the barrier and caused the truck to roll 360 degrees. A comparison of between the models and tests is shown in Figure 5. The visual comparison shown in Figure 5 is only the first step in validating the models and showing that they are successfully able to replicate the full-scale collisions. The second step to validation was to compare the graphs of the accelerations, and the roll, pitch, and yaw of the vehicle. The third step is to statistically compare the models with the experimental results by the use of Phenomena Importance Rating Tables (PIRT's). PIRT tables look at a variety of parameters measured to evaluate whether the values in the model fall close enough to the experimental values to be deemed valid. After evaluating different retrofit options, it was shown that the Thrie-beam rail could be retrofitted with a half-blockout to reduce roll, and the G4(1S) median barrier could be improved by increasing the height 3 inches to prevent the truck from overriding the barrier (Marzougui et. al, 2012).
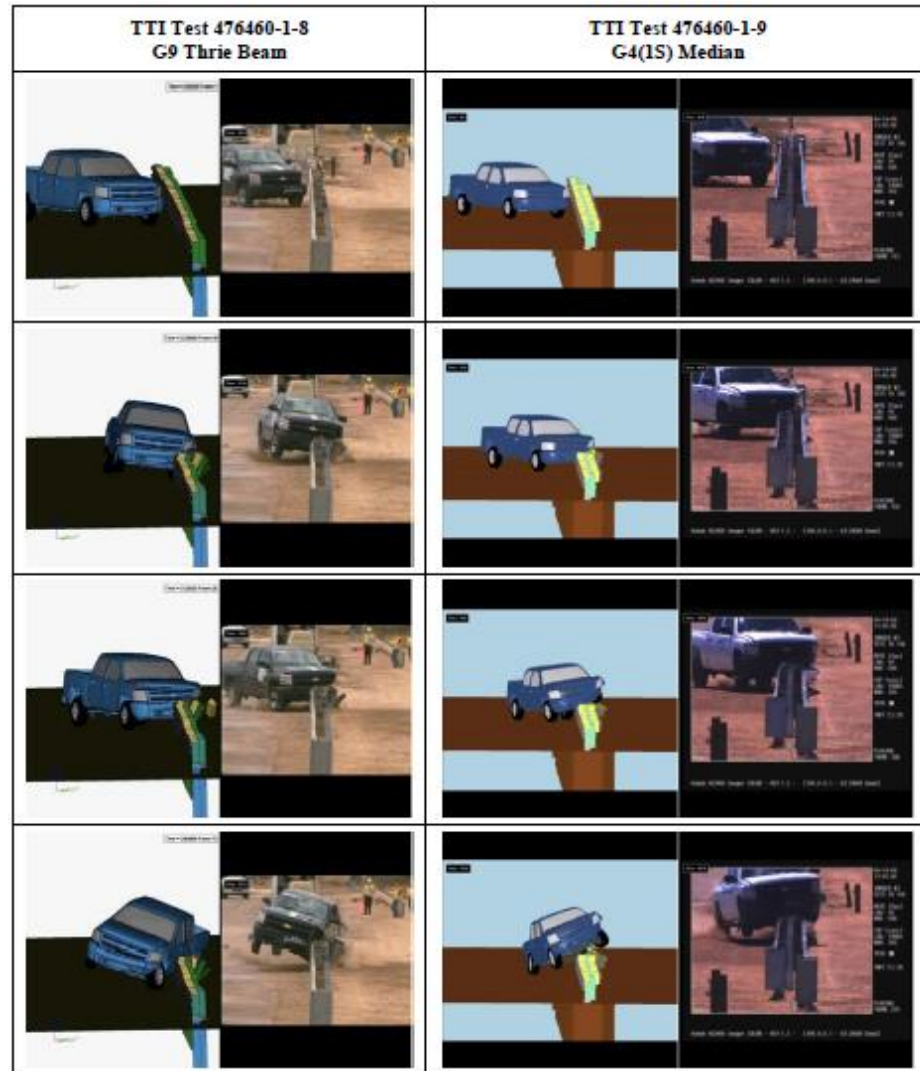
Figure 5: Comparison between computer models and full scale tests for G9 Thrie Beam
and G4(1S) barriers (Marzougui et. al, 2012)

Marzougui et. al (2014) evaluated the crashworthiness of roadside barriers
previously accepted under NCHRP Report 350. The adoption of the new MASH
requirements raises the question of whether this hardware still fulfills the safety
requirements of the new standard. Because many of these previously accepted barriers
are already in use, finite element models were used to investigate the crashworthiness
under the new conditions. The 32-inch New Jersey shaped barriers were evaluated under
the MASH conditions. Tests 3-10 and 3-11 using a small car and pickup truck,

respectively, were modeled in LS-DYNA, and compared to full-scale results. The barrier was modeled using rigid shell material because the deformation is very small when these vehicles are used, and the barrier was fixed at the bottom. Rigorous validation efforts were not undertaken for the research because the New Jersey shaped barriers were extensively used in other simulation studies. The models were compared using visual comparisons, traditional metric comparison, and analytical comparisons using procedures outlined in NCHRP Project 22-24. The simulations for both tests were stable, showed no unusual behavior, and traditional and analytical validation efforts showed good agreement between the models and experimental results. The conclusion of this study was that finite element simulations provide a good representation of experimental setups, and that the New Jersey shaped barrier in question still passes the new MASH requirements (Marzougui et. al, 2014).

Abu-Odeh (2008) conducted a study regarding how different concrete material models behaved in a bridge rail subjected to a bogie impact. In the past, concrete barriers were modeled using a rigid or elastic material characterization because it would reduce the computing time needed, and because there were no models that could accurately predict the behavior of the concrete that were not difficult to use. The author developed a finite element model of the TxDOT type T501 bridge rail and simulated a 5000 lb. bogie vehicle impacting it at 20 miles per hour using LS-DYNA. Three material models for concrete were simulated to investigate the accuracy of the predicted behavior. Each of these models required varying input to simulate. Some only required the unconfined compressive strength and density, while others required additional information. The conclusion of this study was that the models all predict, with reasonable accuracy, the

behavior and deformation of the concrete after the impact with the bogie. The crack pattern each model predicted is very approximate, and none of them correctly mapped it, but the overall damage location they predicted was accurate (Abu-Odeh, 2008).

Borrvall et al (2011) investigated and evaluated the RHT concrete model that is available in LS-DYNA. They conducted a study to compare how the RHT model performed when a reinforced concrete plate was modeled and subjected to a blast load. The findings of this experiment were that the experimental results and model were in good agreement. When the damage is displayed in the simulation, there is good qualitative agreement between it and the experimental results. The pressure measured at the center of the block was higher than what the simulation displayed, but it was still in close enough agreement to be deemed acceptable. It was noted that this model could still be developed further to more accurately predict spalling, scabbing and crack prediction, but as far as showing overall damage and failed sections, this model is good (Borrvall et. al, 2011).

When modeling rebar, there are two methods that can be used: smeared and explicit. Schwer (2014) discussed these two methods in great detail and how they are input into models. Schwer provided a breakdown of the different methods of reinforcement shown in Figure 6.
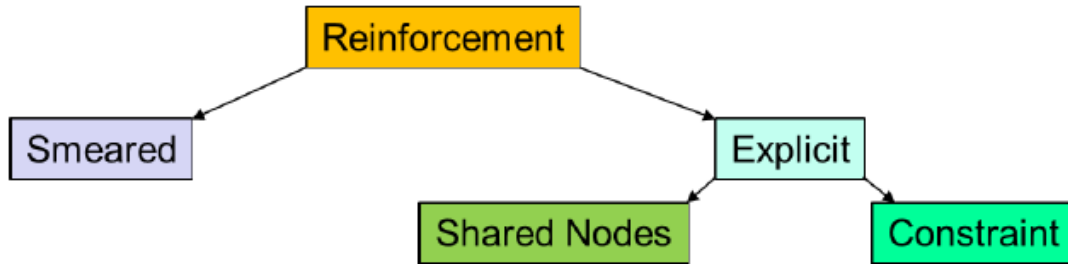
Figure 6: Breakdown of reinforcement modeling methods (Schwer, 2014)

Smeared reinforcement works well when the stress does not go too far beyond the yield stress. The reinforcement is modeled within the mesh of the concrete, and elements of concrete are given different material properties to act as steel. The concept of smeared reinforcement is that elements containing reinforcement are given volume fraction average of material properties, e.g. yield strength, shear modulus, bulk modulus, etc. One material model used to model smeared reinforcement is *MAT_PSEUDO_TENSOR. The property averaging for this material is calculated via the relation

$$K_k = (1 - f_R)K_c + f_R K_R$$

Where K_k is the volume averaged bulk modulus, K_c is the concrete bulk modulus, K_R is the reinforcement bulk modulus, and f_R is the volume fraction of the reinforcement. The same format of averaging is used for all other material properties. Using this volume fraction average for the elements containing reinforcement treats these elements as a composite material. This method of averaging is accurate until yield occurs, and homogenization is lost.

The second method of including reinforcement is explicit reinforcement. To explicitly model reinforcement, section properties must be defined, and this section can then be used to model the rebar as either truss elements or beam elements. It can be

modeled by using shared nodes or constraint methods. When using shared nodes, the meshing effort can become overwhelming, especially when there are multiple layers of reinforcement. When using this method, all nodes of the rebar must be coincident with nodes of concrete to be combined with them. This requires a lot of time and is very tedious.

The other method of explicitly modeling rebar is by the use of constraint methods. When using this method, the meshes of the concrete and reinforcement are completely independent of one another, and there is no need to have any coincident nodes. This makes the meshing very easy and fast. After the meshes are defined, the rebar is simply placed at the right location inside the concrete, and constrained. LS-DYNA provides the *ALE_COUPLING_NODAL_CONSTRAINT keyword which locks the acceleration and velocity of the reinforcement nodes to the concrete nodes. In doing this, the relative motion of both materials is the same and this allows the concrete and steel to act as one unit, as they do in real life. The author found that using a constraint method was the easiest and fastest method of modeling. Because the mesh refinement of the steel and concrete were performed independently of one another, it is accomplished faster than the smeared models, and the rebar placement is easier to accurately perform (Schwer, 2014).

2.5.   FULL SCALE CRASH TESTING

Beginning in 1993, bridge rails have been tested according to the standards set forth in NCHRP Report 350. Before this report was used, bridge rails were evaluated using the testing criteria set forth in the AASHTO Guidelines for testing bridge railings, NCHRP Report 230, or NCHRP Report 239. When NCHRP 350 was released, however, the testing of all roadside safety hardware was standardized. All safety hardware listed in

NCHRP 350 was classified into six different test levels to accommodate different vehicle types and collisions (Ross et. al, 1993).

The AASHTO Manal for Assessing Safety Hardware (MASH) is currently the standard manual used for testing safety devices used on highways in the United States. It was adopted by the FHWA on January 1, 2011, and is what is used when evaluating safety devices. There were many changes in crash testing criteria made between Report 350 and MASH including vehicle mass, impact angle, speed, and other factors. The new criteria set forth in MASH provides higher crash severity than Report 350. The TL-4 criteria has also been changed; the speed for the single unit truck was increased from 80 km/h to 90 km/h, the impact angle for the pickup truck and small car was increased from 20 to 25 degrees, and the mass of the vehicles has been increased. Table 2 summarizes the criteria for the six test levels used in MASH.

Table 2: Summary of crash test levels for bridge railings from MASH (AASHTO, 2016)

Test Level	Vehicle	Velocity	Angle
TL-1	1100C (passenger car) 2270P (pickup truck)	31 mi/hr [50 km/hr] 31 mi/hr [50 km/hr]	25° 25°
TL-2	1100C (passenger car) 2270P (pickup truck)	44 mi/hr [70 km/hr] 44 mi/hr [70 km/hr]	25° 25°
TL-3	1100C (passenger car) 2270P (pickup truck)	62 mi/hr [100 km/hr] 62 mi/hr [100 km/hr]	25° 25°
TL-4	1100C (passenger car) 2270P (pickup truck) 10000S (single-unit truck)	62 mi/hr [100 km/hr] 62 mi/hr [100 km/hr] 56 mi/hr [90 km/hr]	25° 25° 15°
TL-5	1100C (passenger car) 2270P (pickup truck) 36000V (tractor-van trailer)	62 mi/hr [100 km/hr] 62 mi/hr [100 km/hr] 50 mi/hr [80 km/hr]	25° 25° 15°
TL-6	1100C (passenger car) 2270P (pickup truck) 36000T (tractor-tanker trailer)	62 mi/hr [100 km/hr] 62 mi/hr [100 km/hr] 50 mi/hr [80 km/hr]	20° 25° 15°

Bullard et. al. (2008) performed a MASH 4-12 test with a 32 in NJ barrier. This barrier was previously tested under NCHRP Report 350 TL-4 conditions and passed marginally, but when tested again under the more severe MASH TL-4 conditions, the single unit truck rolled over that same barrier and failed. Figure 7 shows the failed MASH 4-12 test of the 32 in high Jersey barrier (Bullard et. al, 2008).
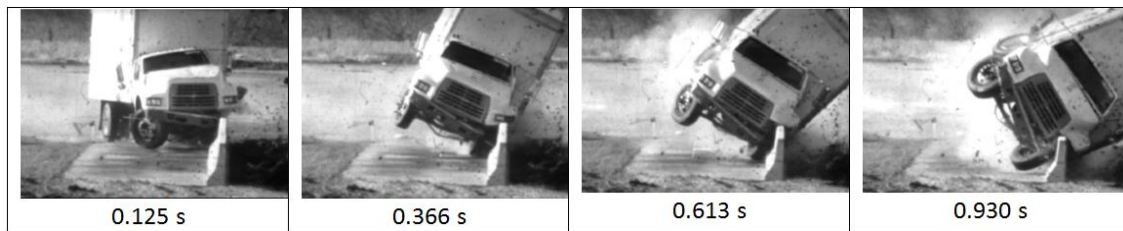
Figure 7: Test photos for failed MASH 4-12 test for 32 in barrier (Bullard et. al, 2008)

In response to this failed test, Sheikh et al. (2012) investigated and found that the minimum required rail height for longitudinal barriers in TL-4 impact conditions for AASHTO MASH is different from NCHRP Report 350. The impact conditions that were changed include the vehicle mass, velocity at impact, and center of gravity of the single unit truck. A comparison of the test conditions is shown in Table 3.

The minimum height specified in the AASHTO design specifications for TL-4 impact conditions is 32 in (AASHTO, 2012), but with the increased impact severity, this height may not be sufficient. Finite element models were used to simulate collisions for barriers of the following heights: 42, 39, 38, 37, and 36 inches. The barrier was modeled using a rigid shell material because the deformation of the test article is very small. As expected, the 42 in barrier provided the most stability because it was the tallest. As the height decreased, so did the stability of the vehicle. The 36 in rail was marginally stable and passed the MASH TL-4 collision and the truck did not roll over. It was determined that any further reduction in height from 36 inches would allow the rear axle to pass over

the barrier, and allows the truck to roll over. For this reason, 36 inches was chosen as the

minimum allowed barrier height for a TL-4 level collision (Sheikh et. al, 2011) and

(Sheikh et. al, 2012).

Table 3: Comparison of NCHRP Report 350 and MASH TL-4 impact conditions for
Single Unit Truck (Ross et. al, 1993) and (AASHTO, 2016)

Parameter	NCHRP Report 350	AASHTO MASH
Vehicle Mass	17,640 lb.	22,050 lb.
Impact Velocity	50 mph	56 mph
Impact Angle	15°	15°
CG height of vehicle ballast	63 in	67 in

Pfeifer et. al. (1996) evaluated the Minnesota Combination Bridge Rail subjected

to TL-4 conditions according to NCHRP Report 350. This rail was initially meant to be

used on low service level roadways, but it was determined that with modifications, the

rail would be able to withstand R350 TL-4 conditions. The first iteration of the redesign

process included increasing the size of the weld at the base of the post to increase the post

capacity, and changing anchor bolt details. The full scale test of this first design failed

due to snagging, so a second iteration of the design was necessary. The second iteration

of modifications included extending the tubular rail and concrete parapet 4 in toward the

roadway. These modifications were retrofitted to the existing system. The barrier was

extended by dowelling into the existing parapet, and the tube was extended by welding an

additional steel tube to the original top rail. Because the tube used for the retrofit was not

readily available from steel suppliers, the final iteration replaced the two tubes welded

together with one larger tube to accomplish the same 4 in clearance. The most notable

changes in the design from the original to the iteration are the width of the concrete

portion increasing from 1'-0" to 1'-4" and the width of the steel tube increasing from 6 in to 10 in (Pfeifer et. al, 1996).

Buth et. al. (1998) tested a Texas T411 to NCHRP R350 TL-3. Previously tested under NCHRP R230, it needed to be tested again under NCHRP R350 to ensure the structural adequacy for the new standards. Under R230, TL-3 tests included an 808 kg passenger car traveling at 96.9 km/h at 21.2 degrees, and a 2043 kg passenger car traveling at 100.1 km/h at 26 degrees. Under NCHRP R350, the 808 kg passenger car did not change, and the 2043 kg passenger car was replaced with a 2000 kg pickup truck traveling at 100 km/h at 25 degrees. The vehicle used for the test was a 1993 Chevrolet 2500 pickup truck. All requirements were met, except the occupant risk because the occupant compartment deformation was extensive and could cause serious injury. Figure 8 shows images of the failed test due to excessive deformations.
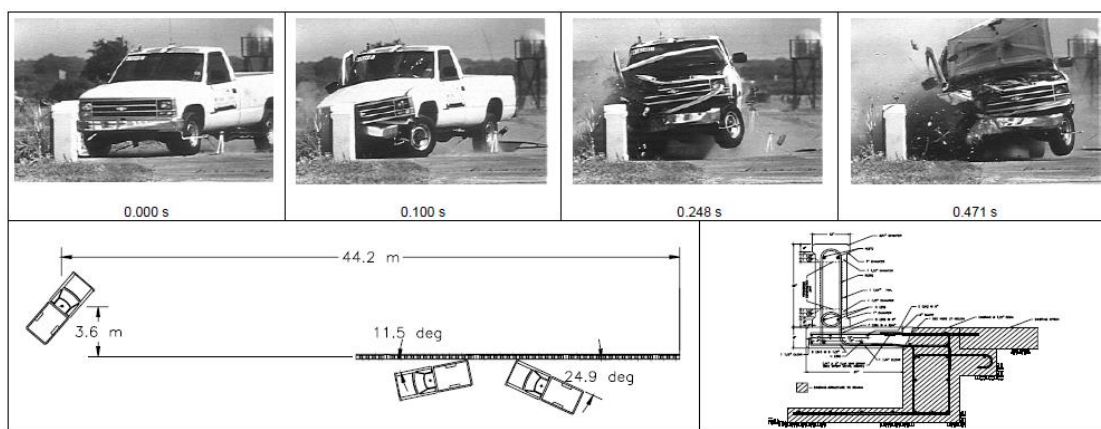
Figure 8: Failed pickup truck test of the Texas T411 bridge rail (Buth et. al, 1998)

Bullard et. al. (2002) designed two aesthetically pleasing, open-faced bridge rails that were constructed and tested full scale. One of them, the Texas F411, successfully met R350 TL-3 requirements. The other one, the TX T77, failed due to vehicle snagging

at the rail splice, which caused excessive vehicle deformation. See Figure 9 and Figure 10 (Bullard et. al, 2002).
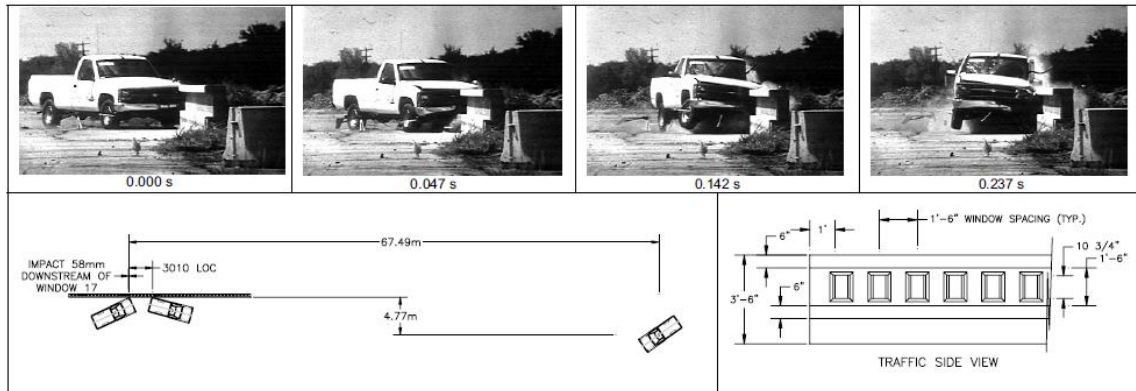
Figure 9: Test photos for NCHRP Report 350 Test 3-11 (Bullard et. al, 2002)
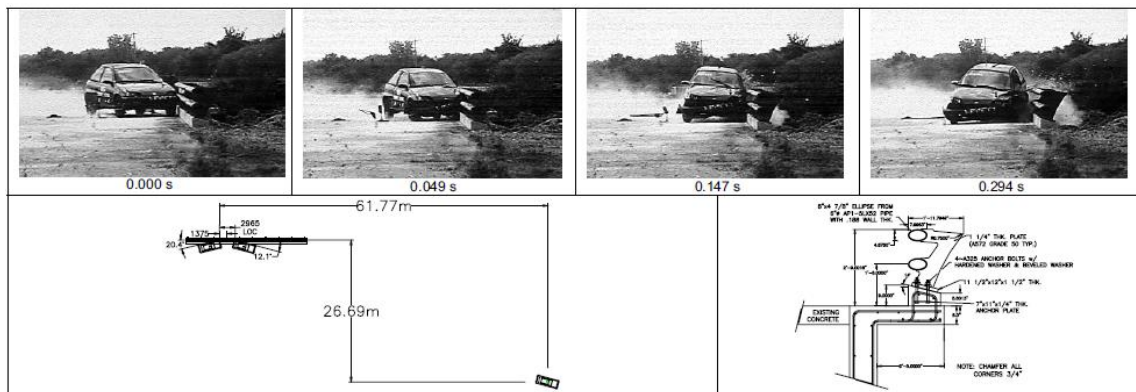
Figure 10: Test photos for Texas T77 bridge rail (Bullard et. al, 2002)

Albertson et. al. (2004) conducted a full scale crash test for the Texas F-411 bridge rail at NCHRP Report 350 TL-4, higher than the tests performed by Bullard in 2002. The 18,000 lb single unit truck impacting at 49.7 mph at 16.9 degrees was successfully contained and redirected as shown in Figure 11. This passing bridge rail is also very aesthetically pleasing due to the open-faced design. Figure 12 shows an image of the Texas F411 rail that was tested.
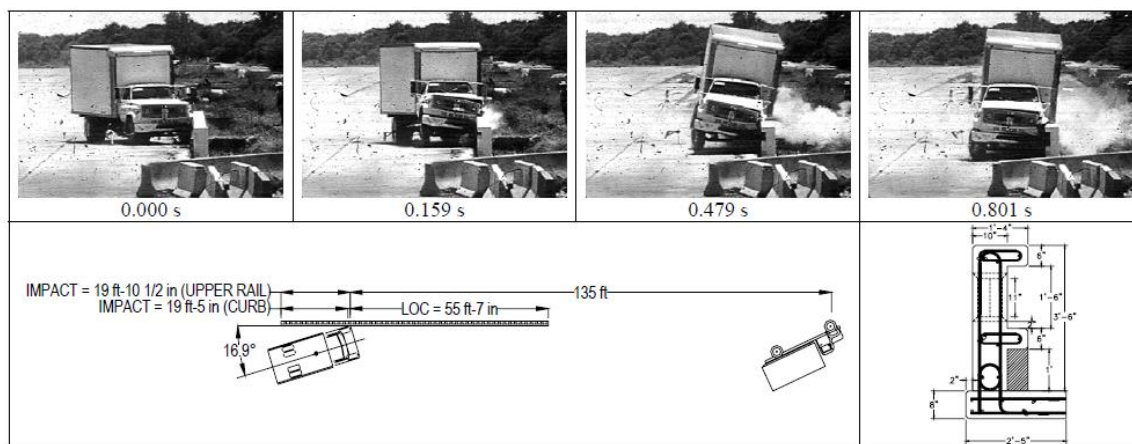
Figure 11: Test photos for NCHRP Report 350 Test 4-12 of the Texas F411 barrier (Albertson et. al, 2004)

Figure 12: Texas F411 bridge rail that was tested (Albertson et. al, 2004)

CHAPTER III

3. MODEL DEVELOPMENT AND PARAMETRIC STUDY

3.1.   INTRODUCTION

Before construction and testing anything, a parametric study was performed using the finite element analysis software LS-DYNA. By using this program, many design alternatives can be simulated and analyzed to determine the best design based on barrier and vehicle damage, occupant risk and other MASH criteria. The height was the first variable adjusted, and then different post width/window opening width combinations were tested. The initial design was calculated to have enough resistance for a TL-4 collision. After the parametric study was completed, the barrier was constructed and tested to ensure its crashworthiness according to MASH standards.

3.2.   OPEN-FACED BALUSTRADE DESIGN

The Pulaski Skyway was built in 1932, and has a historic open-faced concrete balustrade along the length of the road shown in Figure 13. This barrier has a column width to window opening ratio of 1:1, which gives the bridge a nice aesthetic touch. NJDOT developed a preliminary design that has slight changes from the original one, and is shown in Figure 14.

Figure 13: Existing open-faced balustrade on Pulaski Skyway (provided by NJDOT)
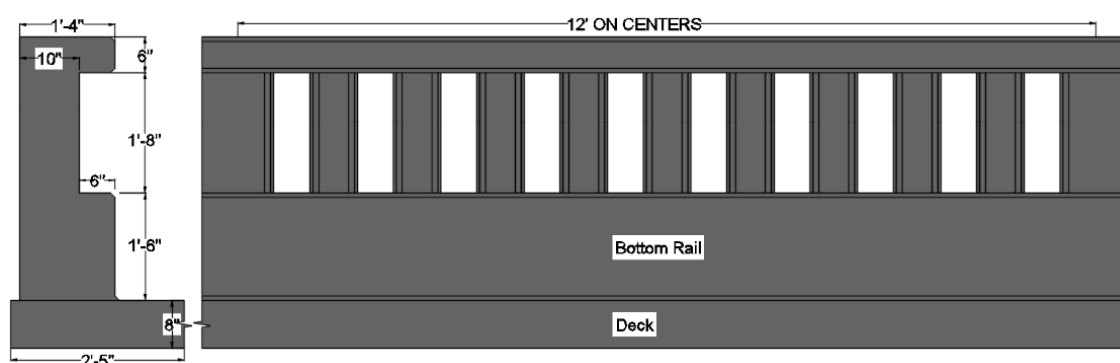
Figure 14: Proposed open-faced balustrade design (plan)

The new barrier design will be modified and parameters such as dimensions, material properties, post spacing, and reinforcement details will be adjusted accordingly. The barrier will have the necessary strength to resist a TL-4 collision as per AASHTO Bridge Design Specifications. This preliminary design is similar to an existing aesthetic balustrade developed by Texas DOT called the Texas F411.

Although this design has been proven to withstand the impact, there were still additional changes to the design that needed to be made. This design, although very similar to the Texas F411, needed modifications to meet all of the specifications set forth in the NJDOT bridge design manual. The design consultant, AECOM, checked the preliminary design, and made changes and improvements to it to ensure that the bridge

rail fulfills all requirements set forth by NJDOT. The specification that forced design changes was section 20.8 in the deck slab design manual, that specify that a 2 ½ inch top deck cover is preferred, and a minimum 2 inch cover for all rebar (NJDOT, 2009). The deck slab specification also moves the rebar ½ inch down in the deck, but the 2-inch cover does change the aesthetics of the barrier. A lot of the design changes are inside the concrete and not seen, such as the change in shape and size of some rebars, but the only visible change in the design is the increase in top-rail height, from 6 inches to 7 inches. This in turn makes the height of the posts 1 inch shorter to maintain the same total height of 44 in. The rebar details AECOM changed are as follows:

1)   Vertical bars in the posts were increased from #5's to #6's, their length was increased to develop a stronger bond, and the radius at the hoop was decreased to maintain the 2 in cover requirement

2)   The three #5 u-bars at 9 in were replaced with a #6 c-bar and #5 d-bar at 8 in. This change reduces the labor needed to tie the rebar because there is only two bars instead of three sticking up from the deck

3)   m-bars were eliminated

4)   w-bars in the bottom rail were eliminated

5)   An extra 5 ft deck bar was added at 8 in on the top alternating with the deck reinforcement

6)   Deck bar spacing was decreased from 9 in to 8 in

7)   Top deck rebar was moved down ½ in

All of these changes increase the capacity of the barrier, while also reducing the labor required to assemble it because there are less total bars to bend and tie. Figure 16 shows the original and modified rebar details.

When designing the balustrade, it is important for safety that it satisfies all the requirements set forth in section 13 of the AASHTO LRFD bridge design specifications. Section 13 is about bridge rails; it defines all the design forces to use, and sets forth the strength requirements of the railing. This procedure is required for checking the capacity of the rail, and for checking if the rail will remain stable when it is subjected to impact. Before the parametric study was performed using finite element analysis, all the designs to be considered were first checked using the criteria set forth in section 13. This was done because the final design must conform to these specifications to ensure the structural integrity of the rail, and to be approved for a MASH TL-4 collision. After AECOM made changes to the proposed design in Figure 14, it was found that the rail does have the capacity to handle the collision, and was set as the baseline for the parametric study. Figure 15 shows the aesthetic appearance of the new design and Figure 16 shows a comparison of the details for the design before and after AECOM modified it.
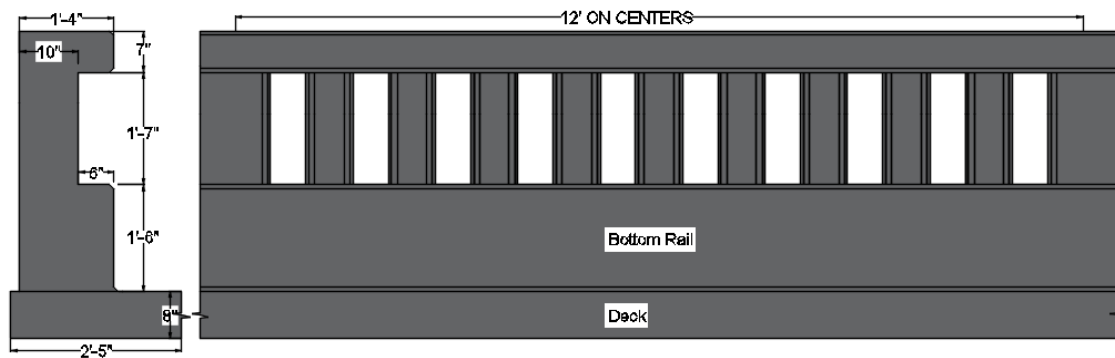
Figure 15: Modified open-faced balustrade design (plan)

Figure 16: Details for the original design (top) and for the modified design (bottom)

3.3.   FINITE ELEMENT ANALYSIS USING LS-DYNA SOFTWARE

Before performing the full scale crash tests to check if the new balustrade satisfies the requirements of AASHTO MASH TL-4, a parametric study was performed to compare the behavior and performance of different barrier shapes. By performing these simulations, different parameters of the balustrade were optimized to make it look as historic as possible while still fulfilling all FHWA Requirements. Utilizing this software also allows many different designs to be analyzed without needing to physically test them, which saves time and money.

3.3.1. LS-DYNA software

LS-DYNA is the finite element software that is being utilized for the modeling and analysis of the Pulaski Skyway balustrade. Its dynamic non-linear finite element code makes it very practical for simulating real-world situations.   This non-linear program is very popular in the automotive industry for simulating vehicle crashes which include large deformations of the chassis, and failure of several components within the vehicle and on whatever the vehicle is impacting. LS-DYNA also has features such as accelerometers that can measure accelerations in all three axes, and measure motions such as rotation, pitch, roll, and yaw. This software was used to carry out the parametric study of the balustrade to optimize the design. The input for the analysis was prepared using the preprocessor provided with the LS-DYNA software package called LS-PrePost.

3.3.2. Modeling

When modeling the balustrade, there are many things that need to be taken into consideration. Because both steel and concrete are present in the barrier, they need to be modeled together to create an accurate model. The two materials are very different from

each other by nature, and must be modeled accordingly. Steel is an isotropic material that can handle tension, compression, and bending, while concrete is only good in compression, but not bending or tension.

Because of the long and narrow shape of rebar and the modes by which it is able to carry load, all of the rebar was modeled as beam elements. Because steel is an isotropic material, it was not difficult to define the parameters in LS-DYNA. The only parameters needed to model it are the stress-strain relationship curve, modulus of elasticity, yield strength, density, and plastic strain curve.

Concrete was modeled as solid elements because more detail in the model can be created easier and more detailed information about deformation and stresses can be obtained. The material model *MAT_RHT was used in the models for the parametric study. This material model is desirable to use because it is stable, can predict behavior of concrete very well, the input needed is very limited, and it has shown to be the most reliable out of all the concrete models that have been used. The only parameters needed for this model are density and compressive strength, unlike other material models that require much more input data.

The concrete and steel occupy the same space, so the two need to be joined to one another. A nodal constraint method was used because it is faster, easier, and more accurate than using shared nodes or smeared reinforcement. The rebar was originally constrained to the concrete using the *ALE_COUPLING_NODAL_CONSTRAINT which locks the acceleration and velocity at the nodes of the concrete and steel together in order to act as one unit when strain occurs (Schwer, 2014). When creating this

constraint, the concrete is set as the master, and the steel bars are set as the slave coupled to the concrete (Schwer, 2014) and (Tay et. al, 2016). This constraint method works well, but there were a few bugs that came along with it. For example, in some models, some of the deck rebar did not couple correctly, and fell out of the deck and barrier for no apparent reason. Not having a portion of the rebar act in the concrete causes problems because the capacity of the barrier would be lowered. In order for the calculations to be accurate, all rebar must be present and acting to give the correct solution. Rebar can be seen falling out of the deck in Figure 17.
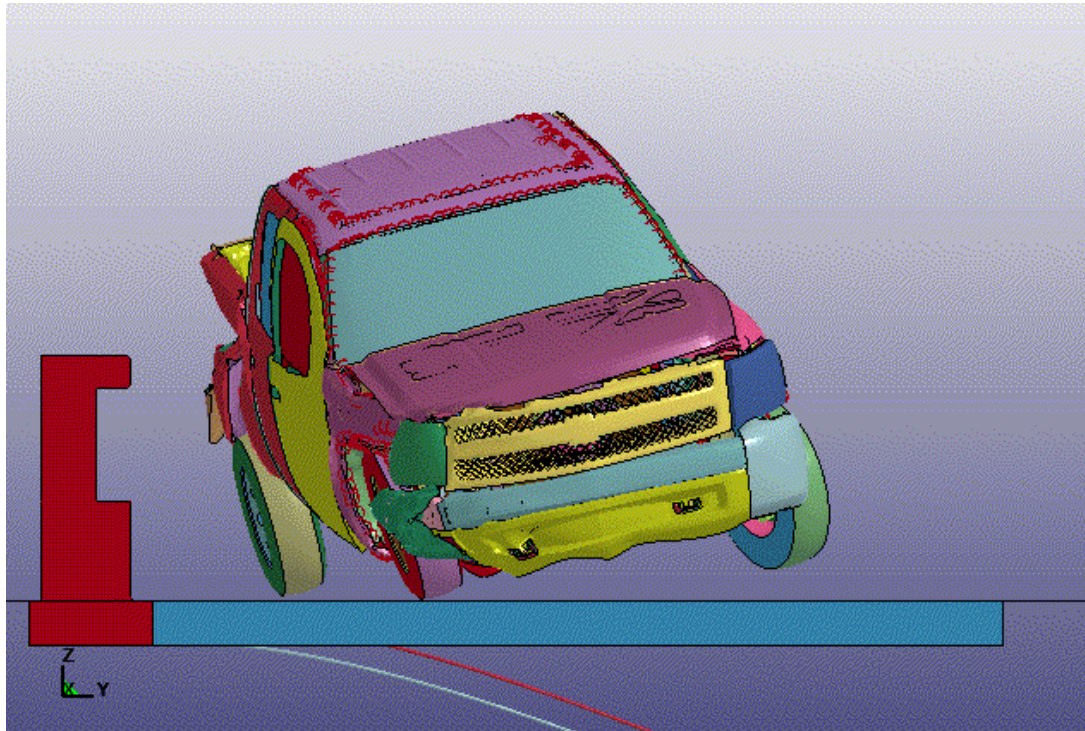
Figure 17: Rebar falling out of deck

To solve this issue, *ALE_COUPLING_NODAL_CONSTRAINT was replaced with *CONSTRAINED_BEAM_IN_SOLID which did not have any noticeable issues. This constraint method accomplishes the same task as the ale coupling constraint, but none of the rebar falls out when this one is used. The *CONSTRAINED_BEAM_IN_SOLID

card is an overhauled constraint method that is more attractive than *CONSTRAINED_LANGRANGE_IN_SOLID, or *ALE_COUPLING_NODAL_CONSTRAINT (LSTC, 2016).

3.3.3. Data Collection

When collecting data about the vehicle accelerations and rotations, accelerometers are defined in the model at the center of gravity of each vehicle. The center of gravity of each vehicle is where the accelerometers will be placed during the full-scale test to collect the data. These accelerometers record data in the directions shown in Table 4. A graphical representation of the directions for each vehicle is shown in Figure 18.

Table 4: Accelerometer data collected

Axis	Data Collected	Data Collected
Longitudinal (x-axis)	x-acceleration	Roll Rate
Transverse (y-axis)	y-acceleration	Pitch Rate
Vertical (z-axis)	z-acceleration	Yaw Rate
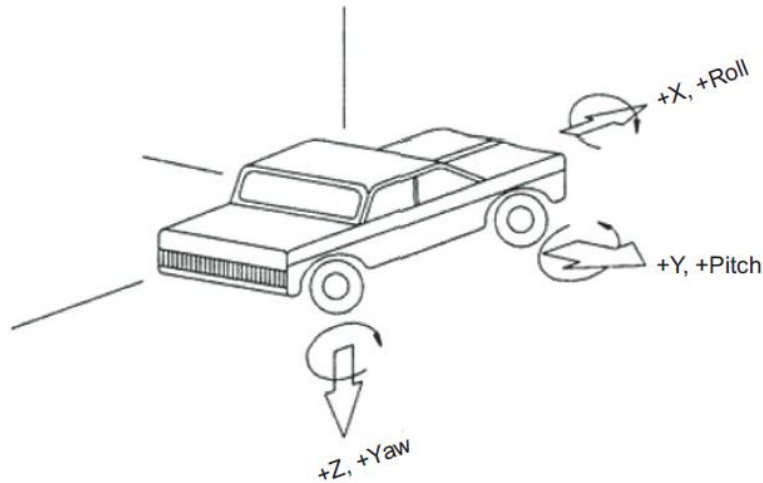
Figure 18: Recommended vehicle coordinate system (AASHTO, 2016).

The data collected when the model is run is extracted via the Nodeout file generated in the output. The acceleration and angular rotation data is filtered using an SAE-180 Hz filter to clean it up before it is processed further. After the acceleration and

angular rotation rates are extracted from the nodeout file and saved in Microsoft Excel .csv file format, they are input to the TRAP program developed by TTI.

The Test Risk Assessment Program (TRAP) is a program developed by TTI used for processing acceleration and rotational data in finite element models and full scale tests. The input required for the TRAP program includes:

1)   x, y, and z- accelerations at the center of gravity of the vehicle

2)   Roll, pitch, and yaw angular rates at the center of gravity of the vehicle

3)   Vehicle mass, speed immediately before impact, angle of impact

After all of these parameters are input, occupant risk parameters (such as theoretical head impact velocity, occupant impact velocity, ridedown accelerations) are calculated, and the angular rates are integrated to calculate the rotational angles at different times. This acceleration and rotational data is then put into excel and KaleidaGraph to generate the collision plots shown throughout this thesis.

3.4.   PARAMETRIC STUDY

The Pulaski Skyway has a balustrade that is unique in that it has a very historic appearance. It does not look like a typical Jersey barrier that is just a simple solid wall-looking item, it has an open-faced design with window openings shown in Figure 13. In order to keep the appearance of the barrier as close as possible to the original one while still fulfilling the safety requirements of AASHTO MASH TL-4, a parametric study must be performed. The parametric study focused on the proposed design changing the following three parameters:

1)   Total Barrier Height

2)   Post Width

3)   Window Opening Width

The Texas F411 has a height of 42 inches, a post width of 12 inches, and a window opening of 6 inches. This post width to window opening ratio is 1:2, which is not acceptable for the historical appearance of the Pulaski barrier. To make the design acceptable, the baseline design for the parametric study had started with a height of 42 inches, a post width of 8 inches, and a window opening of 6 inches. This makes the post width to window opening ratio 4:3, which is close enough to the original Pulaski barrier's ratio of 1:1 for the Historical Preservation Office to approve the aesthetic design. Table 5 shows a parameter matrix of the values for each parameter that were changed and simulated.

Table 5: list of parameters and values to be simulated

Test Level	Value 1	Value 2	Value 3
Barrier Height (in)	42	43	44
Post Width (in)	8	10	12
Window Opening (in)	6	8	10

3.4.1. Height Adjustment

The first parameter changed was the total barrier height. The height was adjusted by changing the height of the posts in the barrier. The height of the previously tested TL-4 passed Texas F411 barrier is 42 inches, but in the full-scale crash test, the truck seems to start tipping over the barrier. The truck never fully overturns over the barrier, but there is a noticeable risk of overturning. When adjusting the height for the parametric study, the heights tested were 42 in, 43 in, and 44 in.

The distance from the ground to the bottom of the box on the truck is approximately 43.5 inches, and with this being higher than the barrier, the truck tires hit the barrier when the back of the truck swings towards it. When this happens, the truck starts to "trip" over the barrier and begins the rolling motion over it. Figure 19 shows the gap between the SUT box and the top of the 42" barrier and that the tires are the first part in the rear of the vehicle to make contact with the barrier.
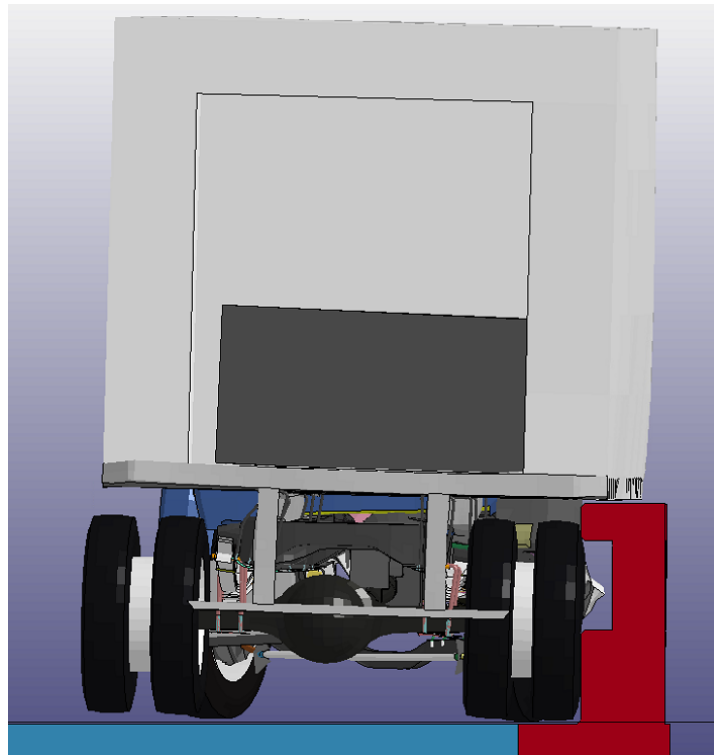
Figure 19: Rear view of SUT tires contacting the 42 in barrier

This gap, although small, has a huge effect on the kinematics of the truck during and after the collision. The height of the barrier determines which part of the truck in the rear will hit first, and ultimately determines how the truck will behave. If the height is low, the tires will hit the barrier and the box will ride on it for a longer time. On the other hand, if the barrier is high, the box will hit first and more effectively keep the truck on the correct side. When the box hits the barrier first, the truck is also deflected away faster,

and does not tip over the barrier. This is shown in the collision with the 44 inch barrier. Figure 20 shows a comparison of single unit truck collisions, with the 42 inch barrier on the left, the 43 inch barrier in the middle, and the 44 inch barrier on the right. As seen in the 44 in barrier case, the box hits the barrier instead of the tires, and this causes all the rolling motion to occur on the correct side of the barrier.

42 in barrier	43 in barrier	44 in barrier
0.000 s	0.000 s	0.000 s
0.170 s	0.170 s	0.170 s
0.570 s	0.570 s	0.570 s
0.880 s	0.880 s	0.880 s
1.100 s	1.100 s	1.100 s
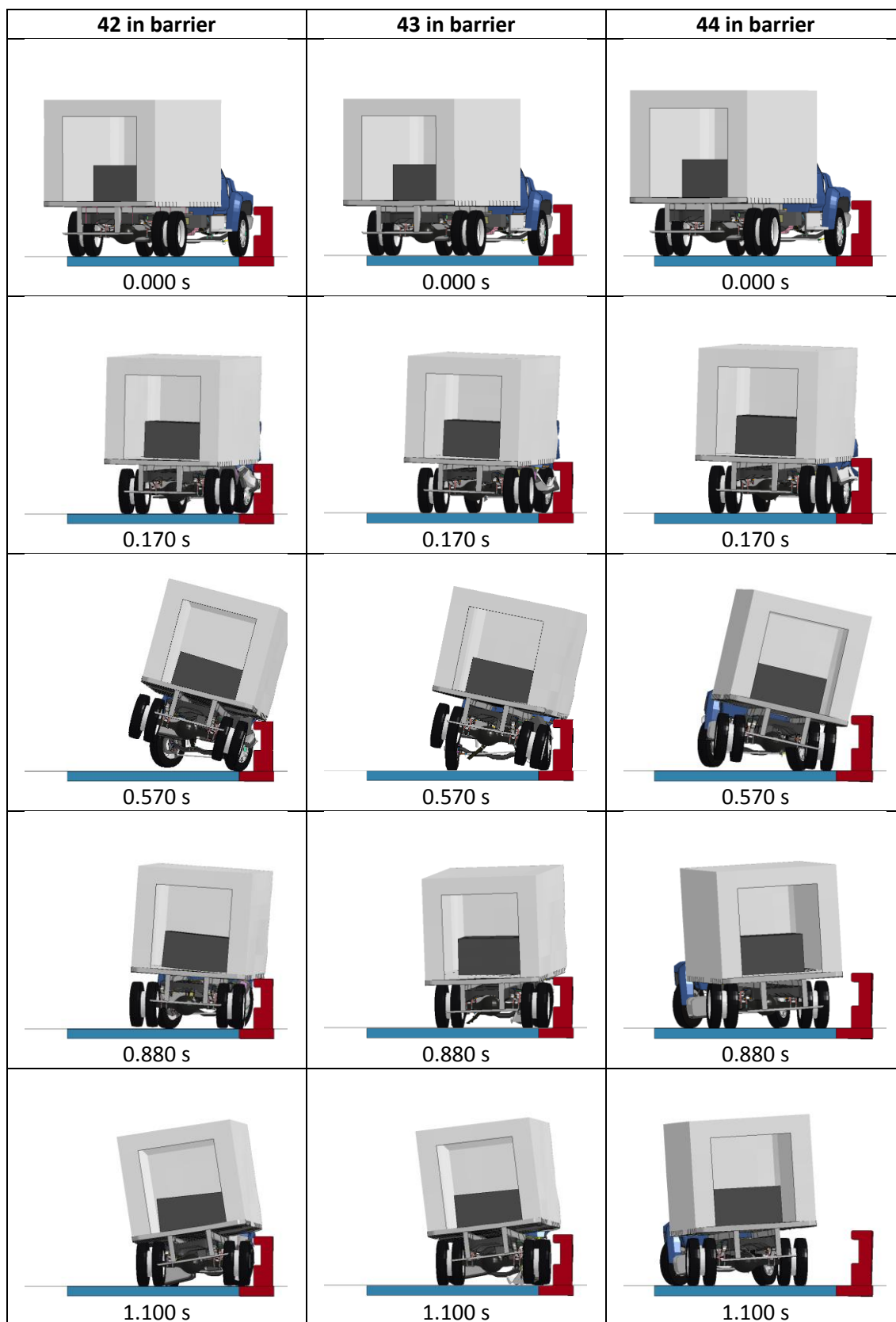
Figure 20: SUT collisions with the 42, 43, and 44 inch barriers, respectively

As shown in Figure 20, the 42 inch and 43 inch barriers cause the truck to tip partially over to the other side, but the 44 inch barrier contains all of the rolling on the traffic side. Table 6 lists the data collected in the SUT collisions of different height barriers.

Table 6: SUT collision data for different height barriers

Occupant Risk Factors		42 in barrier	43 in barrier	44 in barrier
		FEA	FEA	FEA
Occupant Impact Velocity (m/s)	x-direction	2.1	1.9	2.3
	y-direction	2.4	2.5	3.6
	at time	at 0.2226 seconds on right side of interior	at 0.2095 seconds on right side of interior	at 0.1966 seconds on right side of interior
THIV (m/s)		3.2 at 0.2226 seconds on right side of interior	3.1 at 0.2095 seconds on right side of interior	4.3 at 0.1966 seconds on right side of interior
Ridedown Acceleration (g's)	x-direction	-4.7 (1.0077 - 1.0177 seconds)	-3.7 (0.2460 - 0.2560 seconds)	-4.6 (0.2372 - 0.2472 seconds)
	y-direction	-10 (0.2930 - 0.3030 seconds)	-9.3 (0.2581 - 0.2681 seconds)	-11.5 (0.2501 - 0.2601 seconds)
PHD (g's)		10.3 (0.2929 - 0.3029 seconds)	9.4 (0.2580 - 0.2680 seconds)	11.5 (0.2501 - 0.2601 seconds)
ASI		0.64 (0.2531 - 0.3031 seconds)	0.63 (0.0921 - 0.1421 seconds)	0.8 (0.2503 - 0.3003 seconds)
Maximum Angular Disp. (deg)	Roll	16.8 (0.6067 seconds)	12.9 (0.5854 seconds)	14.7 (0.4934 seconds)
	Pitch	-3 (0.6148 seconds)	2.5 (0.9293 seconds)	3.8 (0.2572 seconds)
	Yaw	-13.7 (0.3294 seconds)	-12.7 (0.2698 seconds)	-22.9 (0.8766 seconds)

When looking at Table 6, at first glance it appears that the performance of each barrier does not differ much from the other two. This conclusion is initially drawn because it only displays the maximum values of acceleration, pitch, roll, and yaw. Figure 21 shows

plots comparing acceleration values for all three axes and how they change for each barrier height. For the most part, the height does not change the acceleration in any direction very much, except in the y-axis. The y-axis is normal to the inside face of the barrier, and is affected when the height increases from 43 inches to 44 inches. This 1 inch height increase causes the box to come in contact with the barrier first instead of the tires, and when this occurs, the truck is quickly deflected away from the barrier instead of tilting over it. This sudden change in direction causes a significantly higher acceleration in the y-direction. This spike in acceleration is seen at a time of about 0.25 seconds after the collision.

Except for in the y direction, the height of the barrier does not have a significant effect on the acceleration, but it does however have a very significant impact on the kinematics and direction of movement of the truck. The roll, pitch, and yaw of the truck change drastically when the height of the barrier is changed. The roll in the 44 inch collision is about the same as the other barriers, but what you don't see on the graph is that although the roll angle is about the same, all of the rolling in the 44 inch barrier collision is contained on the traffic side of the barrier with the box leaning on it, while in the 42 inch barrier collision, the truck tips over the barrier and the rolling occurs on top of the barrier. Because the truck does not get stuck on top of the barrier for a long time in the 44 in case, the pitch also differs dramatically because the box of the truck is not kept leaning forward on top of the barrier like in the other cases. Figure 22 shows the graphs comparing the yaw, roll, and pitch for each collision.
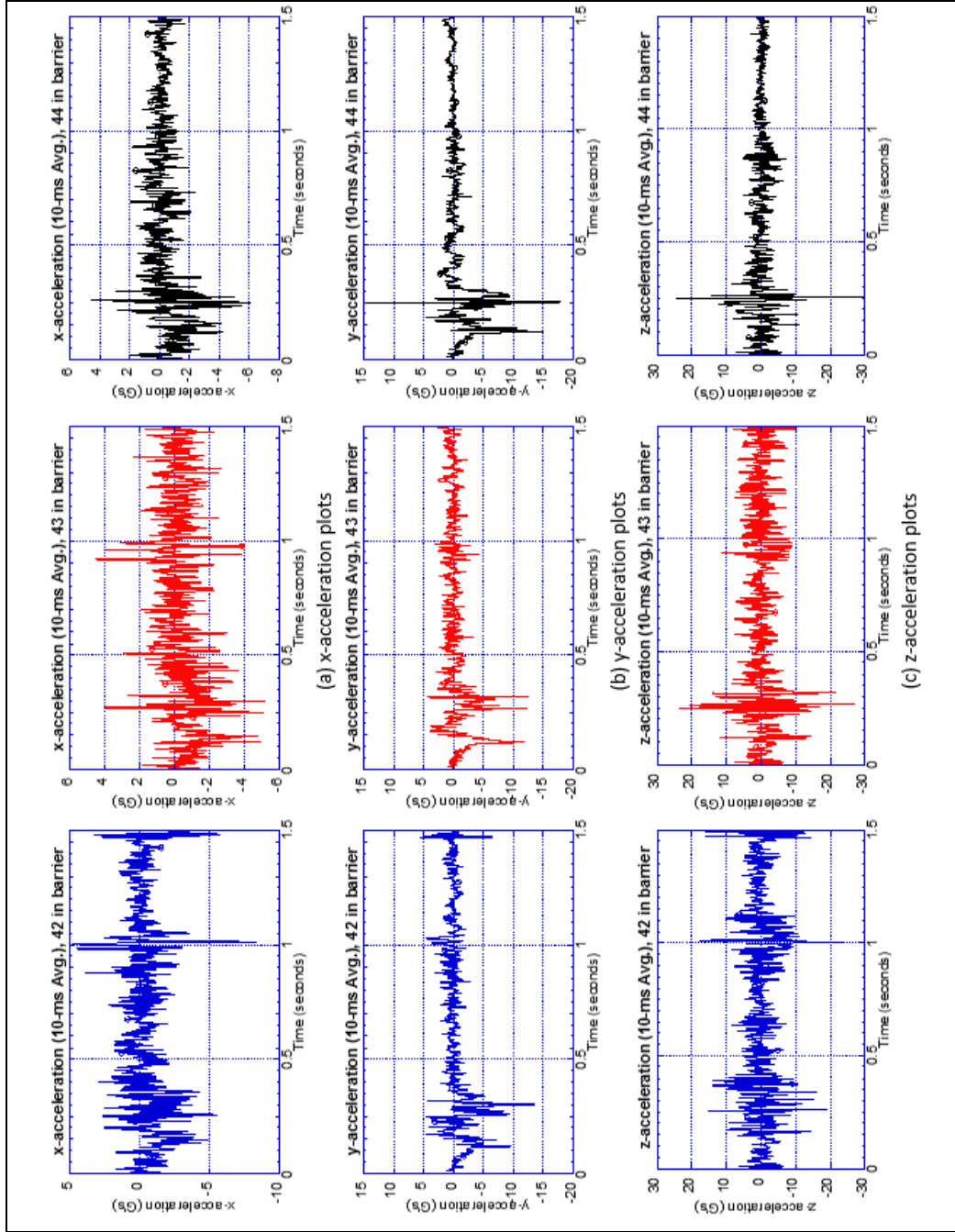
Figure 21: SUT collision comparison of accelerations for different height barriers: (a) x-acceleration plots; (b) y-acceleration plots; (c) z-acceleration plots
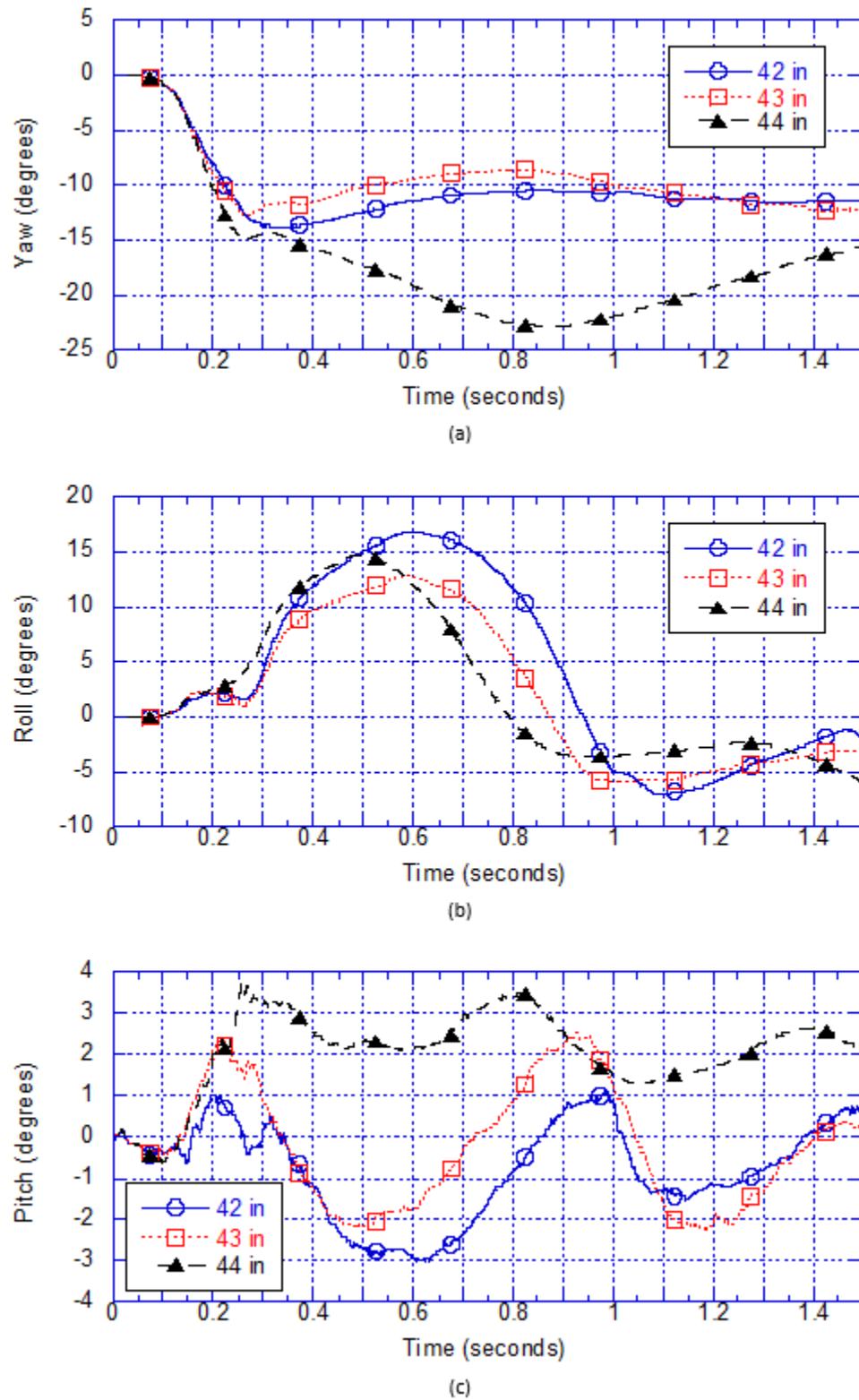
Figure 22: SUT collision comparison of axial rotations for different height barriers: (a) Yaw angles vs time; (b) Roll angles vs time; (c) Pitch angles vs time.

3.4.2. Post Width / Window Opening Adjustment

When adjusting the post width and window opening width, it is very important to keep in mind that the ratio of post width to window opening must stay close to 1:1. Keeping this in mind, it must be noted that not all combinations in the parameter matrix can be used. For example, a post width of 12 in cannot be combined with a window opening of 6 in or 8 in. The only combinations of post width and window openings that can be considered for use are shown in Table 7.

Table 7: Compatible post and window combinations

Compatible Combinations	Post Width (in)	Window Opening (in)	Window Opening (in)
1	8	6	8
2	10	8	10
3	12	10	12

These combinations represent the ones that have an acceptable ratio close enough to 1:1 to satisfy the Historical Preservation Office's requirements. Some of these still must be eliminated though. The combinations in row 3 are all unsuitable because a post width of 12 in is too large and does not look like the original balustrade that is trying to be replicated. The 10 in post width is large, but is not too large to completely rule out. Although a 10 in window opening would make the ratio 1:1, this wide of an opening would look too wide for the appearance of the barrier. After eliminating these cases, we are left with only three combinations that are acceptable. These are shown in Table 8.

Table 8: Acceptable post and window combinations

Combination	Post Width (in)	Window Opening (in)
1	8	6
2	8	8
3	10	8

Although combination number three in Table 8 is still viewed as acceptable, it is still not considered very desirable because the thinner post width of 8 inches is better aesthetically. All three combinations with a height of 44 in were simulated, and it was found through analyzing results that the post and window-opening widths did not have much of an effect on how the truck behaved when the collision occurs. After the height of 44 in was selected, combinations one and two from Table 8 were compared to see which one is preferable.

After these two barriers were simulated, the results were processed and both performed very similarly. Figure 23 shows the comparison of the collisions between the two combinations. As seen in Figure 23, the window opening width had virtually no effect on the behavior of the truck during or after the collision. With this being said, it can be seen in Figure 24 and Figure 25 that the accelerations in every direction and the rotations about every axis do not vary by a significant margin.

6 in window	8 in window
0.000 s	0.000 s
0.170 s	0.170 s
0.570 s	0.570 s
0.880 s	0.880 s
1.100 s	1.100 s
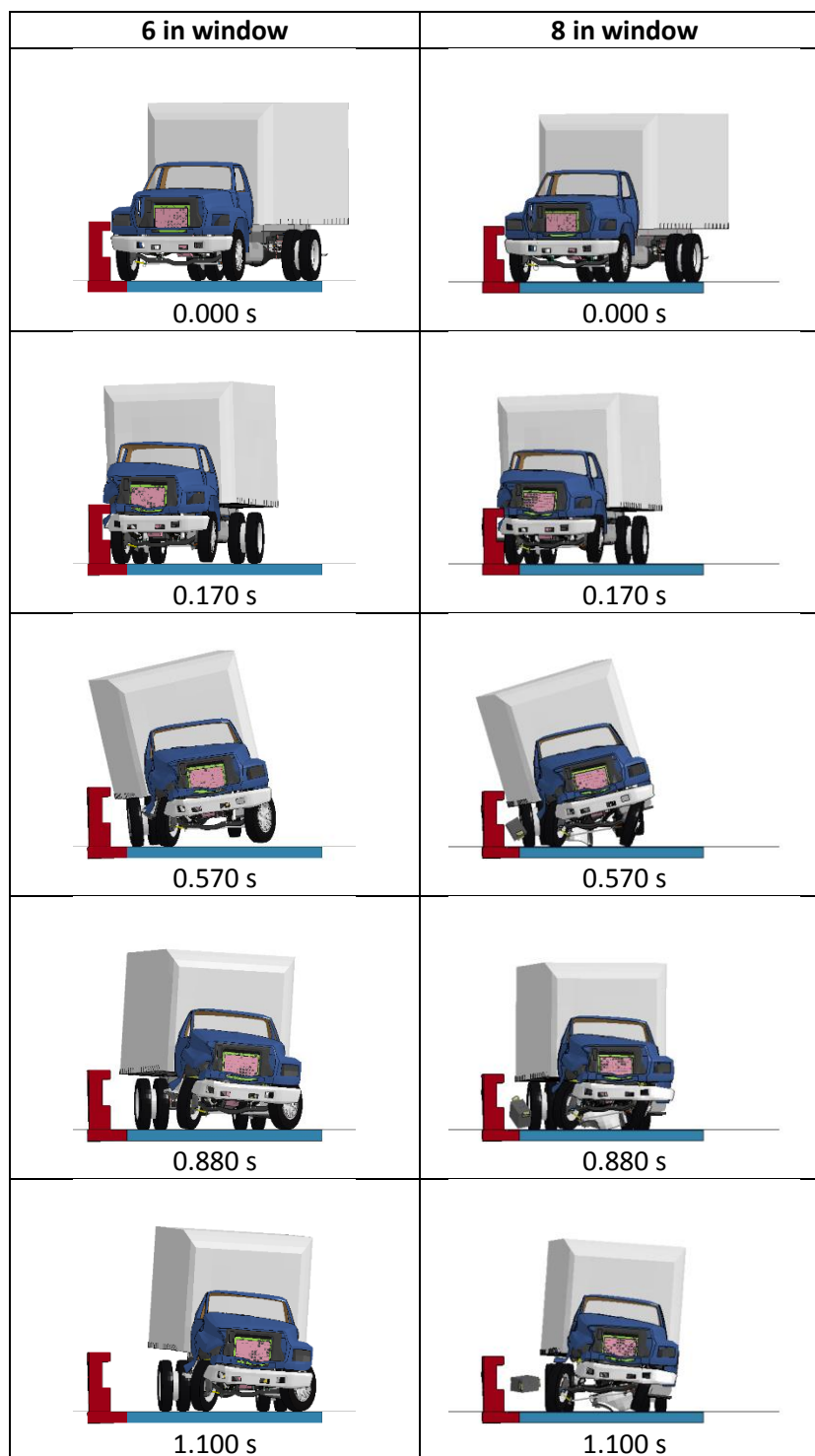
Figure 23: Comparison of 44 in high barrier with a 6 in window (left) and 8 in window (right)
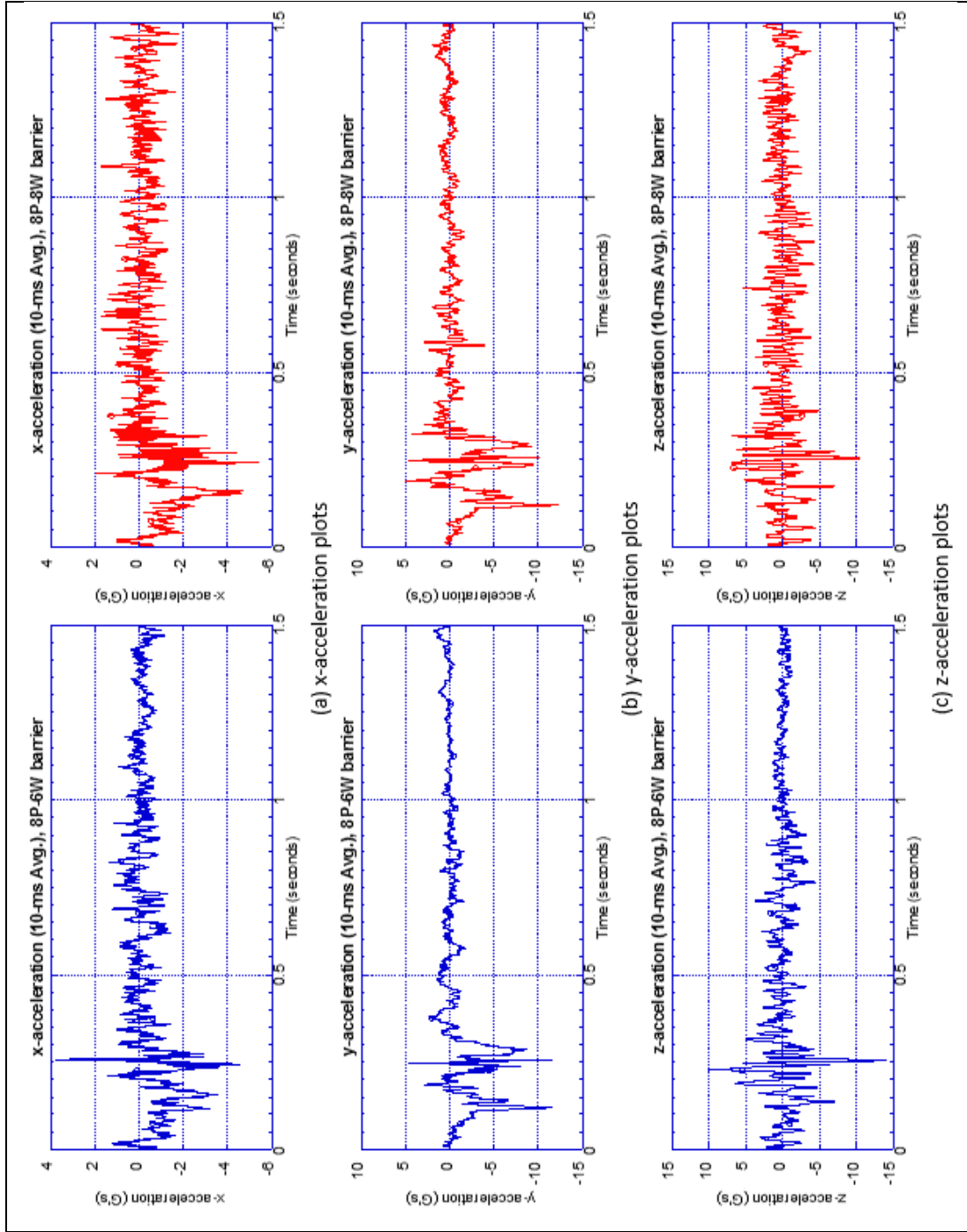
Figure 24: SUT collision comparison of accelerations for different post and window widths: (a) x-acceleration plots; (b) y-acceleration plots; (c) z-acceleration plots

Figure 25: SUT collision comparison of axial rotations for different post and window widths: (a) Yaw angles vs time; (b) Roll angles vs time; (c) Pitch angles vs time.

Table 9: SUT collision data for different window openings

Occupant Risk Factors		8P-6W	8P-8W
		FEA	FEA
Occupant Impact Velocity (m/s)	x-direction	2.3	2.6
	y-direction	3.6	3.4
	at time	at 0.1966 seconds on right side of interior	at 0.1927 seconds on right side of interior
THIV (m/s)		4.3	4.3
		at 0.1966 seconds on right side of interior	at 0.1927 seconds on right side of interior
Ridedown Acceleration (g's)	x-direction	-4.6 (0.2372 - 0.2472 seconds)	-5.4 (0.2363 - 0.2463 seconds)
	y-direction	-11.5 (0.2501 - 0.2601 seconds)	-10.1 (0.2499 - 0.2599 seconds)
PHD (g's)		11.5 (0.2501 - 0.2601 seconds)	10.5 (0.2500 - 0.2600 seconds)
ASI		0.8 (0.2503 - 0.3003 seconds)	0.72 (0.2500 - 0.3000 seconds)
Maximum Angular Disp. (deg)	Roll	14.7 (0.4934 seconds)	17.2 (0.5171 seconds)
	Pitch	3.8 (0.2572 seconds)	2.9 (0.2573 seconds)
	Yaw	-22.9 (0.8766 seconds)	-21.2 (0.8245 seconds)

As shown in Figure 24, Figure 25, and Table 9, the change in values for all the data is very small, and the behavior of the truck is not changed significantly. The reaction of the barrier when the truck collides though does change. When the window opening width is increased, the amount of resistance that the barrier is able to provide decreases dramatically. With the posts spaced further apart, the amount of resistance per linear foot of barrier decreases because there is less reinforcing steel per linear of foot. This, in turn, makes the barrier more susceptible to damage than it otherwise would be. This decrease in steel per unit length means the concrete of the posts will crack more easily, and the

steel bars may also fail if the collision is severe enough. Figure 26 shows a comparison

of the damage incurred on the barrier for both cases.

(a)

(b)
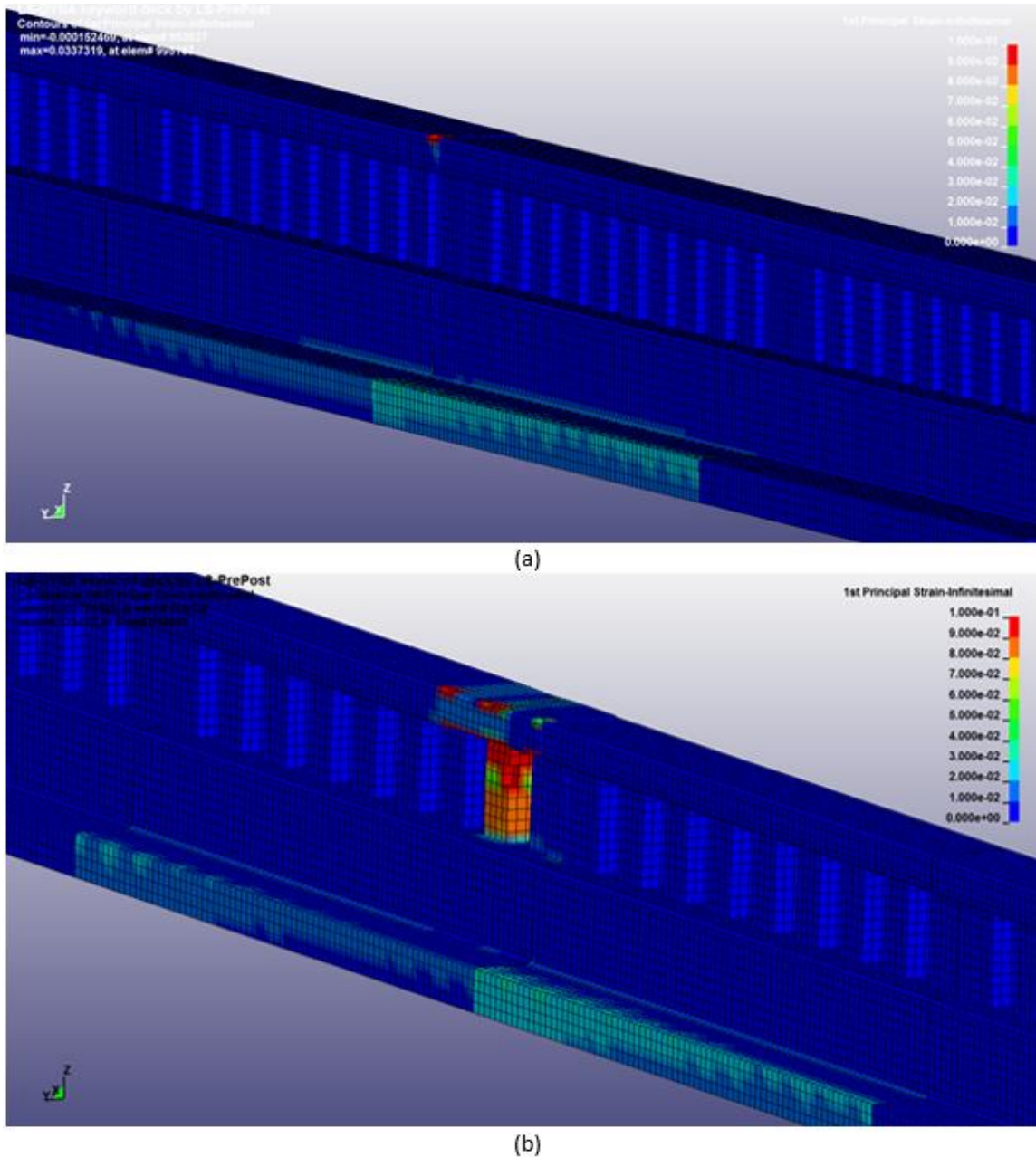
Figure 26: Comparison of damage between 6 in window openings (a) and 8 in window
openings (b) barriers

As shown in Figure 28, the post directly in the line of the collision with the truck

in the 8 in window case is completely destroyed, while that same post in the in the 6 inch

window case is virtually unharmed. This is due to the fact that the rebar in this post was put under too much stress, and yielded because there was not enough contribution from other posts because they were too far away to share the load of the impact. This permanent deformation of the steel bars caused cracking and failing of concrete in that post. Another reason the post is severely damaged is because having the opening widened to be 8 in increases the likelihood for components to get in between the posts and hit the post sideways.

After looking at the results of these two collisions, it is very clear that with an 8 inch post width, the 6 inch window opening performs much better than the 8 inch opening does. After reviewing the results for all barriers, it was decided that the final design would have a height of 44 in, post width of 8 in, and a window opening of 6 in. Even though the ratio of post width to window opening is not exactly 1:1, it is close enough to the original Pulaski barrier to satisfy the aesthetic requirements of the Historical Preservation Office, and is more durable than the 8 in window opening.

The collisions of the pickup truck and the passenger car are both much less severe than the SUT collision because these vehicles are significantly lighter. This means that in this parametric study, the damage incurred on the barrier is only a concern for the SUT collisions.

3.4.3. Pickup Truck Collision

The AASHTO MASH TL-4 criteria calls for a pickup truck impacting at 62 miles per hour at an angle of 25 degrees. The parametric study for the pickup truck was identical to the single unit truck, with the only differences being the vehicle, impact speed, and angle. Because this vehicle is much smaller and not as tall as the single unit truck, the results do not change throughout the parametric study the same way they did for the single unit truck. Because the bottom of the pickup truck bed is much lower than the top of the barrier (regardless of which height is being tested), the behavior of the truck will not change much when the height is adjusted in 1 inch increments. When the back of the truck swings around and hits the barrier, the body will always hit first, and there is virtually no risk of the tires hitting first because unlike the SUT, the bed of the truck is not completely above the tires. Side views of the SUT and pickup truck are shown in Figure 21. This is different from the single unit truck where the tires may hit first if the barrier height is lower, causing the rolling "tripping" motion over the barrier. Figure 28 shows a comparison of pickup truck collisions with different height barriers. As shown in the figure, the height of the barrier has almost no effect on the behavior of the vehicle during and after collision. This is largely due to the fact that the part of the truck hitting the barrier during the backswing is not dependent on the height difference of two inches. The wall of the truck bed will always be hitting first.
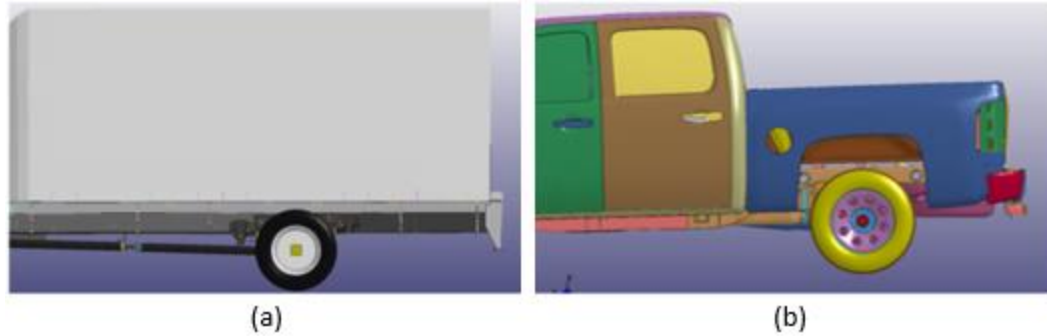
Figure 27: Wheel locations relative to bottom plane of cargo areas for (a) SUT and (b) pickup truck

Figure 29 and Figure 30 show graphs comparing the accelerations in the x, y, and z-axes for different height barrier. As seen in Figure 29, the accelerations in every direction are almost identical. Because the tires are not hitting the barrier first, the truck bounces back towards the traffic side rapidly (like in the 44 in single unit truck collision). This is what the large spike in the y-acceleration is at 0.05 seconds. The accelerations in every direction are almost identical because every collision is very similar.

As seen in Figure 30, the yaw is also very close for all cases. As far as rotations, the parameters with the highest variation is seen in the graphs for roll and pitch. The roll is slightly lower as the height increases because the center of rotation (top point of contact between vehicle and barrier) increases, which makes the rotation about the truck's x-axis lower. This in turn affects the pitch because pitch depends on how long the rear tires stay in the air. The longer the rear tires spend off of the ground, the longer the pitch values are away from the zero degree mark. The maximum values are also compared in Table 10.

42 in barrier	43 in barrier	44 in barrier
0.020 s	0.020 s	0.020 s
0.120 s	0.120 s	0.120 s
0.280 s	0.280 s	0.280 s
0.350 s	0.350 s	0.350 s
0.620 s	0.620 s	0.620 s
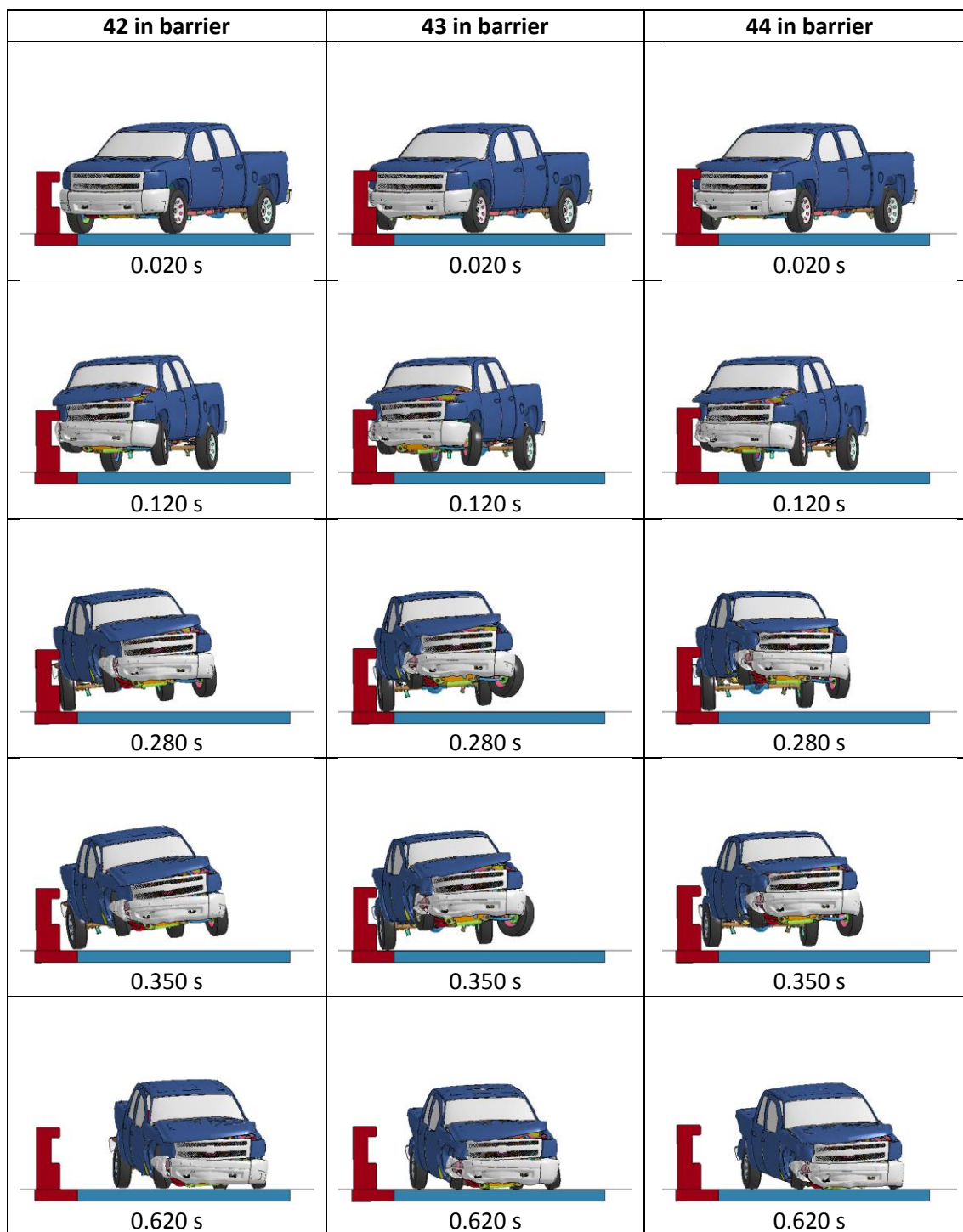
Figure 28: Pickup truck collisions with the 42, 43, and 44 inch barriers, respectively

Figure 29: Pickup truck collision comparison for different height barriers: (a) x-acceleration plots; (b) y-acceleration plots; (c) z-acceleration plots.
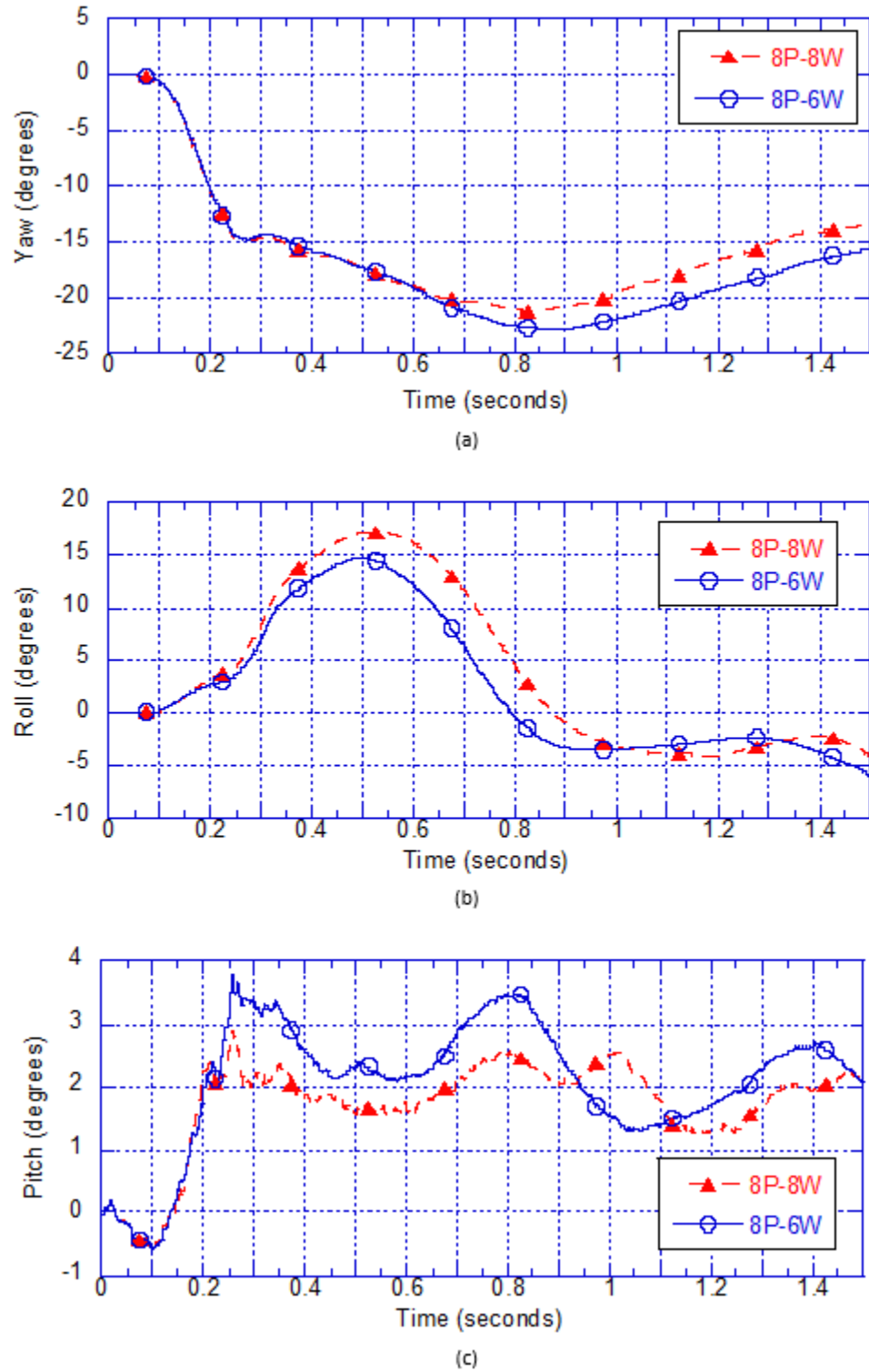
Figure 30: Pickup truck collision comparison of axial rotations for different height barriers: (a) Yaw angles vs time; (b) Roll angles vs time; (c) Pitch angles vs time.

Table 10: Pickup truck collision data for different height barriers

Occupant Risk Factors		42 in barrier	43 in barrier	44 in barrier
		FEA	FEA	FEA
Occupant Impact Velocity (m/s)	x-direction	8.8	9.2	9.3
	y-direction	-8.3	-7.8	-8
	at time	at 0.0851 seconds on left side of interior	at 0.0857 seconds on left side of interior	at 0.0855 seconds on left side of interior
THIV (m/s)		12.1	12	11.8
		at 0.0851 seconds on left side of interior	at 0.0857 seconds on left side of interior	at 0.0855 seconds on left side of interior
Ridedown Acceleration (g's)	x-direction	-9.5 (0.0959 - 0.1059 seconds)	-6.1 (0.0924 - 0.1024 seconds)	-8.7 (0.2738 - 0.2838 seconds)
	y-direction	8.1 (0.2619 - 0.2719 seconds)	10.6 (0.3070 - 0.3170 seconds)	11.1 (0.2821 - 0.2921 seconds)
PHD (g's)		9.5 (0.0959 - 0.1059 seconds)	10.7 (0.3070 - 0.3170 seconds)	12.9 (0.2746 - 0.2846 seconds)
ASI		1.97 (0.0270 - 0.0770 seconds)	2.02 (0.0272 - 0.0772 seconds)	2 (0.0288 - 0.0788 seconds)
Maximum Angular Disp. (deg)	Roll	11.4 (0.4891 seconds)	8.7 (0.4534 seconds)	9 (0.9206 seconds)
	Pitch	4.1 (0.5502 seconds)	-4.7 (0.2985 seconds)	-4.1 (0.3240 seconds)
	Yaw	35.2 (0.4664 seconds)	33.3 (0.3198 seconds)	36.3 (0.6071 seconds)

Table 10 shows very little variation in the collision data when the height of the barrier is changed. Also, the damage to the barrier for all three heights is very minimal and not a concern for collisions with this vehicle. The only visible damage incurred on the barrier is seen on the top of the bottom rail. Other than at this location, there doesn't seem to be a high risk of cracking or damage. The damage for all three height cases is

almost identical, and Figure 31 shows the damage that is incurred on the 44 inch barrier when the pickup truck collides.
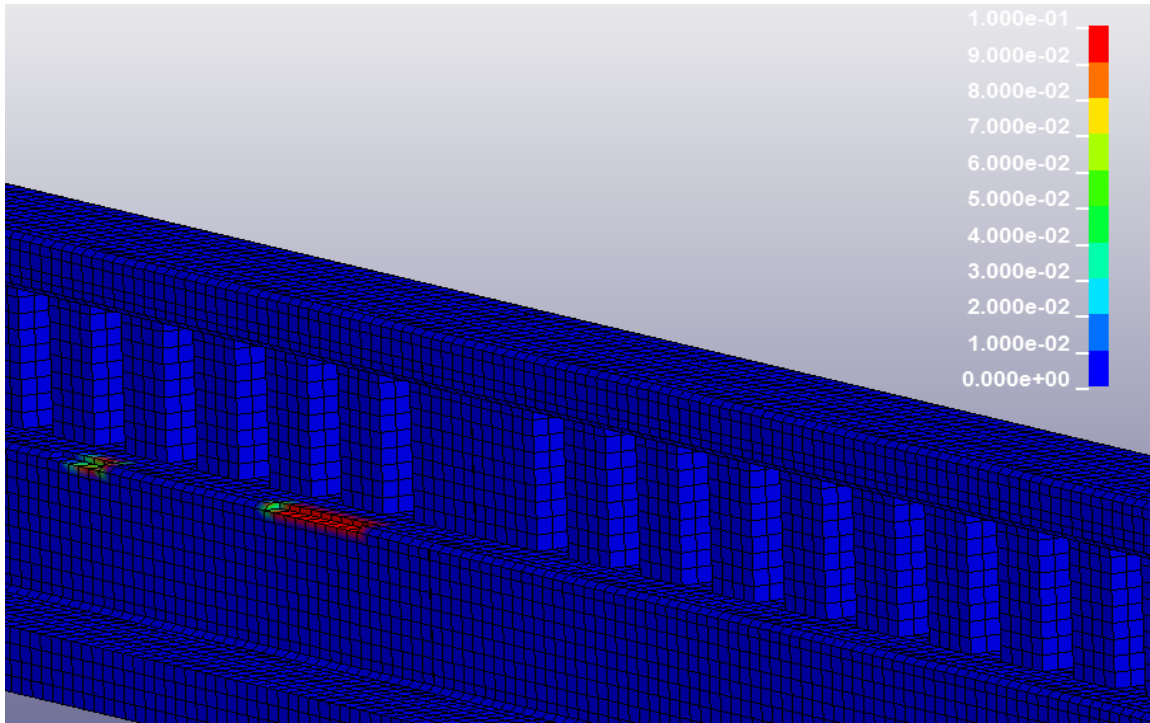
Figure 31: Damage incurred on 44 in barrier after pickup truck collision

The barrier with an 8 inch window opening which was tested with the single unit truck would have probably performed very well in the pickup truck collision, and most likely would not have been severely damaged. The reason that barrier was not simulated with the pickup truck is because it was severely damaged in the SUT collision, which is more severe and controls in this parametric study. Because it was already eliminated in the SUT collision, a successful performance with this vehicle would be moot.

3.4.4. Passenger Car Collision

The AASHTO MASH TL-4 criteria calls for a passenger car impacting at 62 miles per hour at an angle of 25 degrees. The parametric study for the passenger car was identical to the pickup truck's, with the only difference being the vehicle. This vehicle is much smaller than the others, which means the height of the barrier will have virtually no effect on the behavior of the vehicle. Because the vehicle is very short, the behavior of it will not change much when the height is changed in 1 in increments. When the vehicle collides with the barrier, it bounces back almost immediately and the back barely touches when it swings around. Figure 32 shows a comparison of passenger car collisions with different height barriers. As shown in Figure 32, the height of the barrier has almost no effect on the behavior of the vehicle during and after collision.

Figure 33 shows graphs comparing the accelerations in the x, y, and z-axes for different height barriers. As seen in the graphs, the accelerations in every direction are almost identical. Just like the pickup truck, the barriers being different heights had virtually no effect on the behavior of the vehicle during or after the collision. The height difference did not change which part of the vehicle was hit, and in each case, the vehicle trajectory remained constant across each case. This consistency is also shown in the accelerometer data gathered that was collected during the simulation.

As seen in Figure 34, the yaw, roll, and pitch are also very close for all cases. Because the same part of the vehicle is hitting in each collision, the rotations about every axis have very little variation. Because the passenger car is very short and the center of gravity is well-below the top of the barrier, the collisions are minimally effected by the change in height. The maximum values are also compared in Table 11.

42 in barrier	43 in barrier	44 in barrier
0.010 s	0.010 s	0.010 s
0.065 s	0.065 s	0.065 s
0.305 s	0.305 s	0.305 s
0.395 s	0.395 s	0.395 s
0.535 s	0.535 s	0.535 s
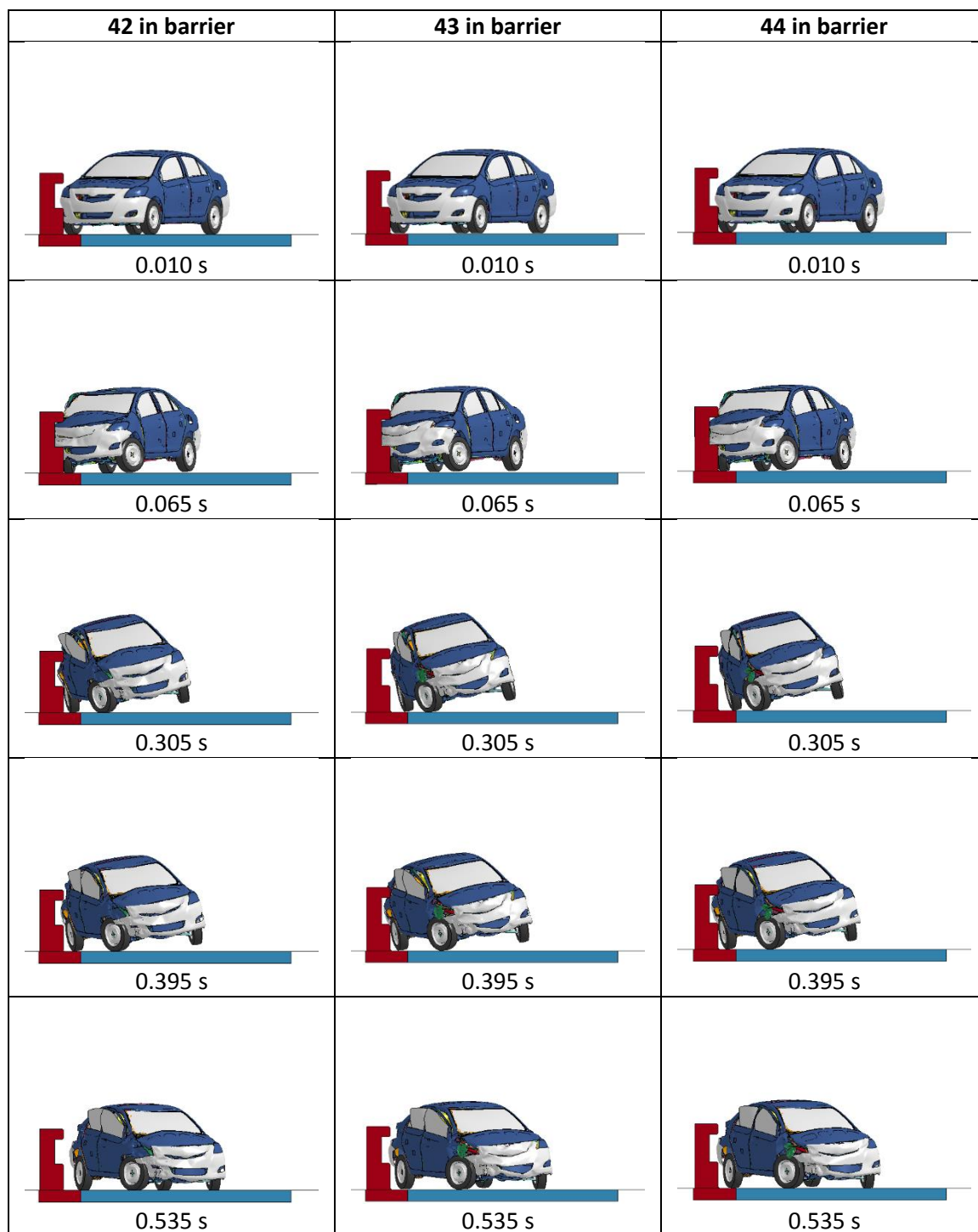
Figure 32: Passenger car collisions with the 42, 43, and 44 inch barriers, respectively
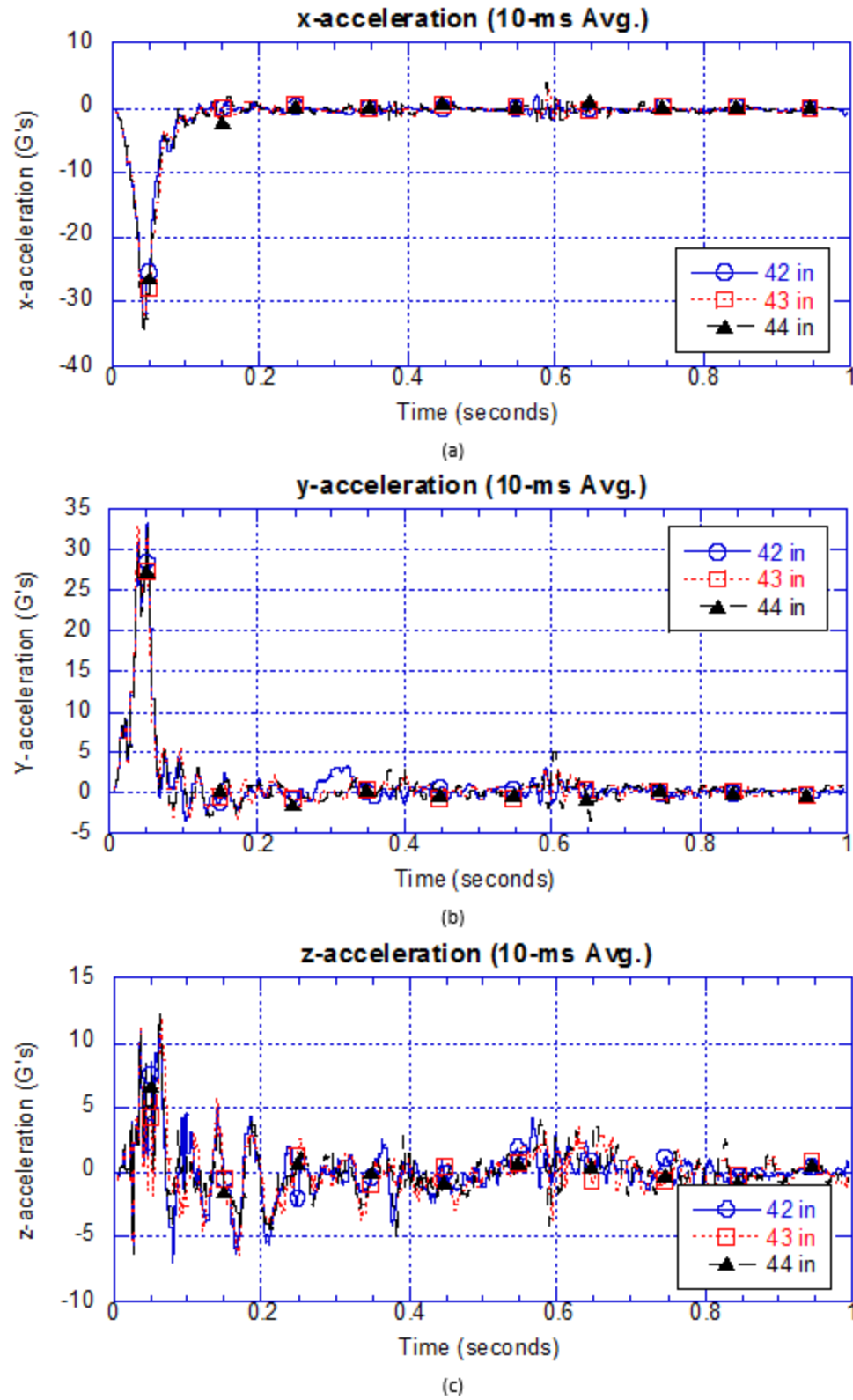
Figure 33: Passenger car collision comparison for different height barriers: (a) x-acceleration plots; (b) y-acceleration plots; (c) z-acceleration plots)
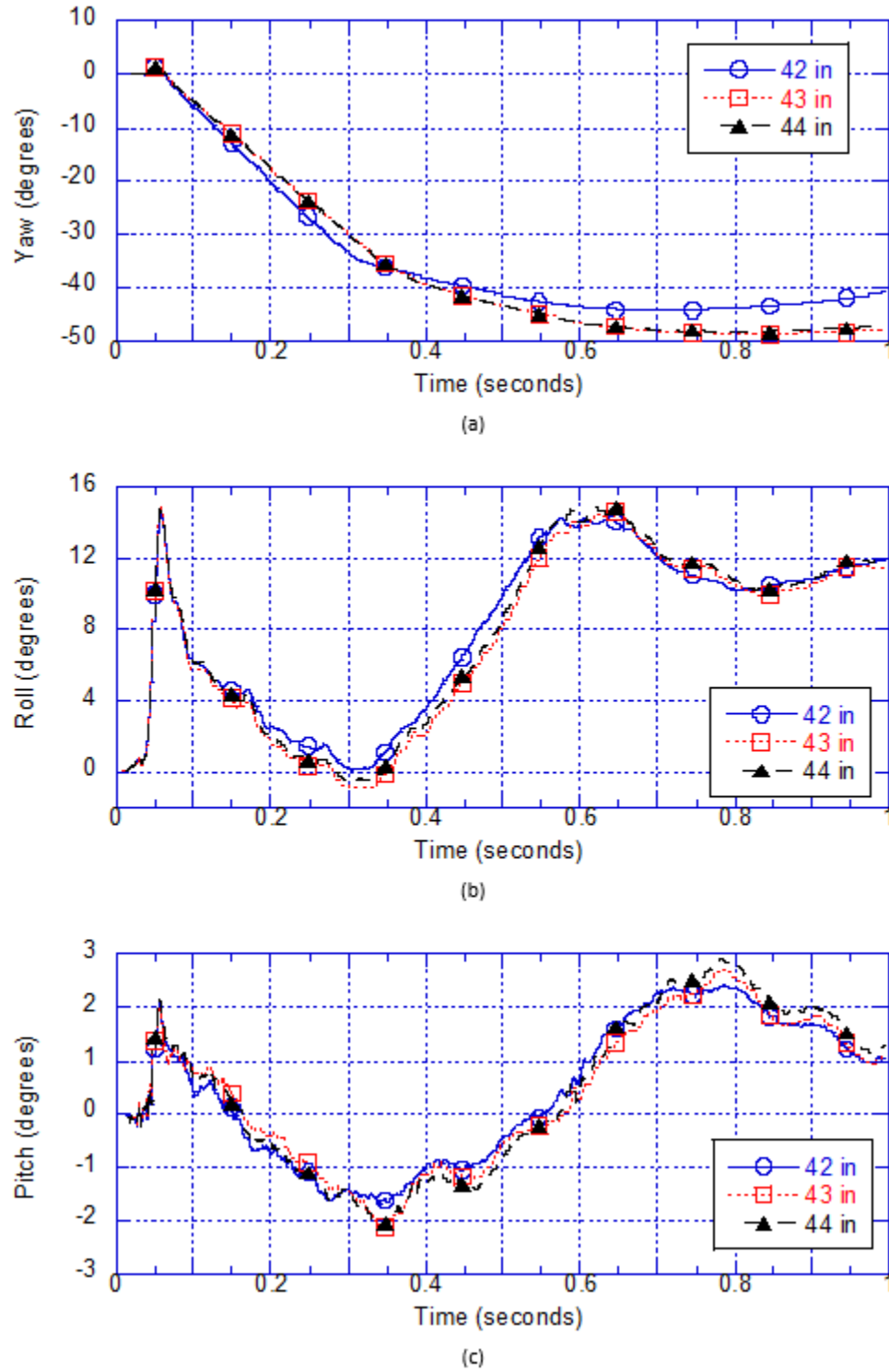
Figure 34: Passenger car collision comparison of axial rotations for different height barriers: (a) Yaw angles vs time; (b) Roll angles vs time; (c) Pitch angles vs time.
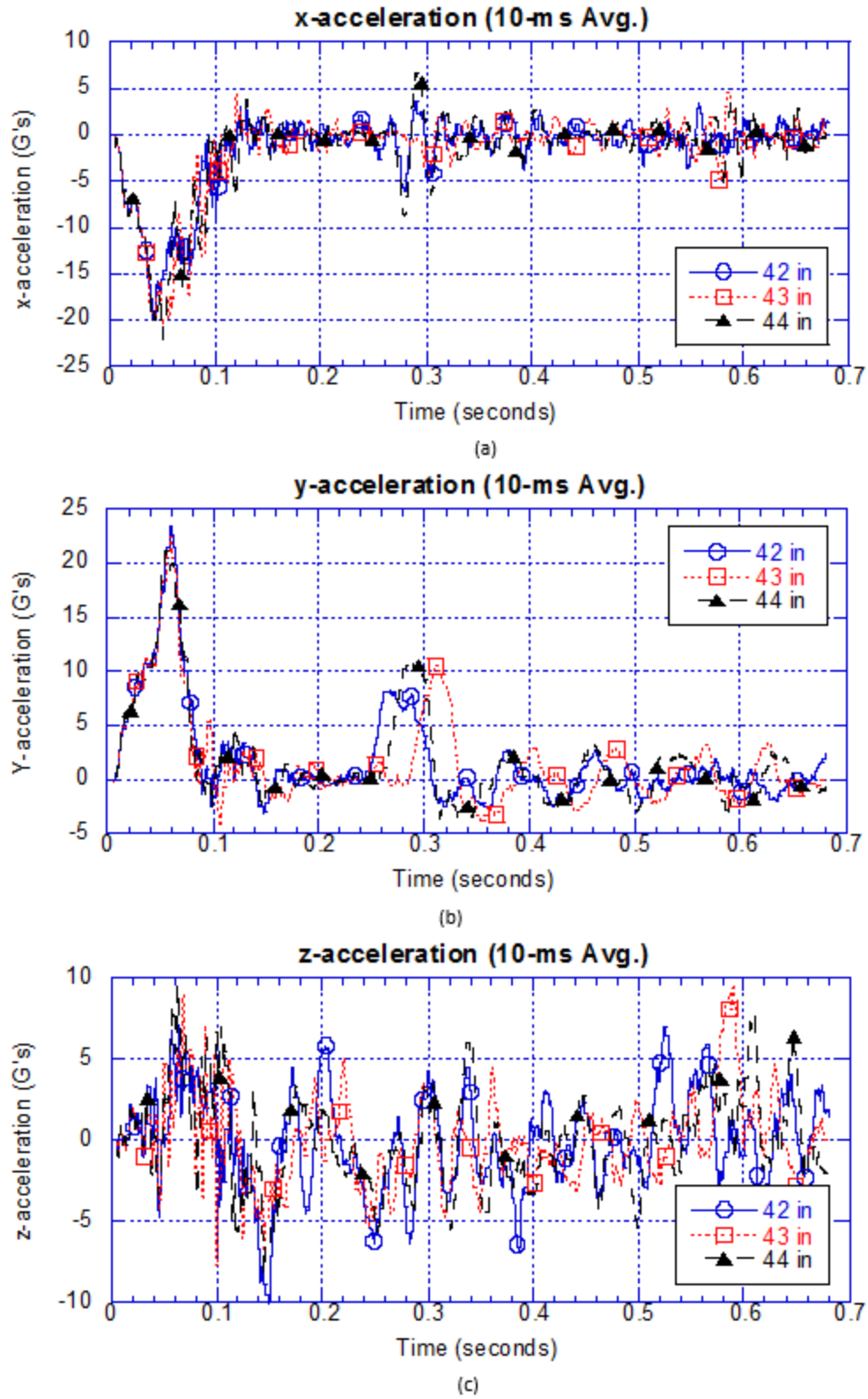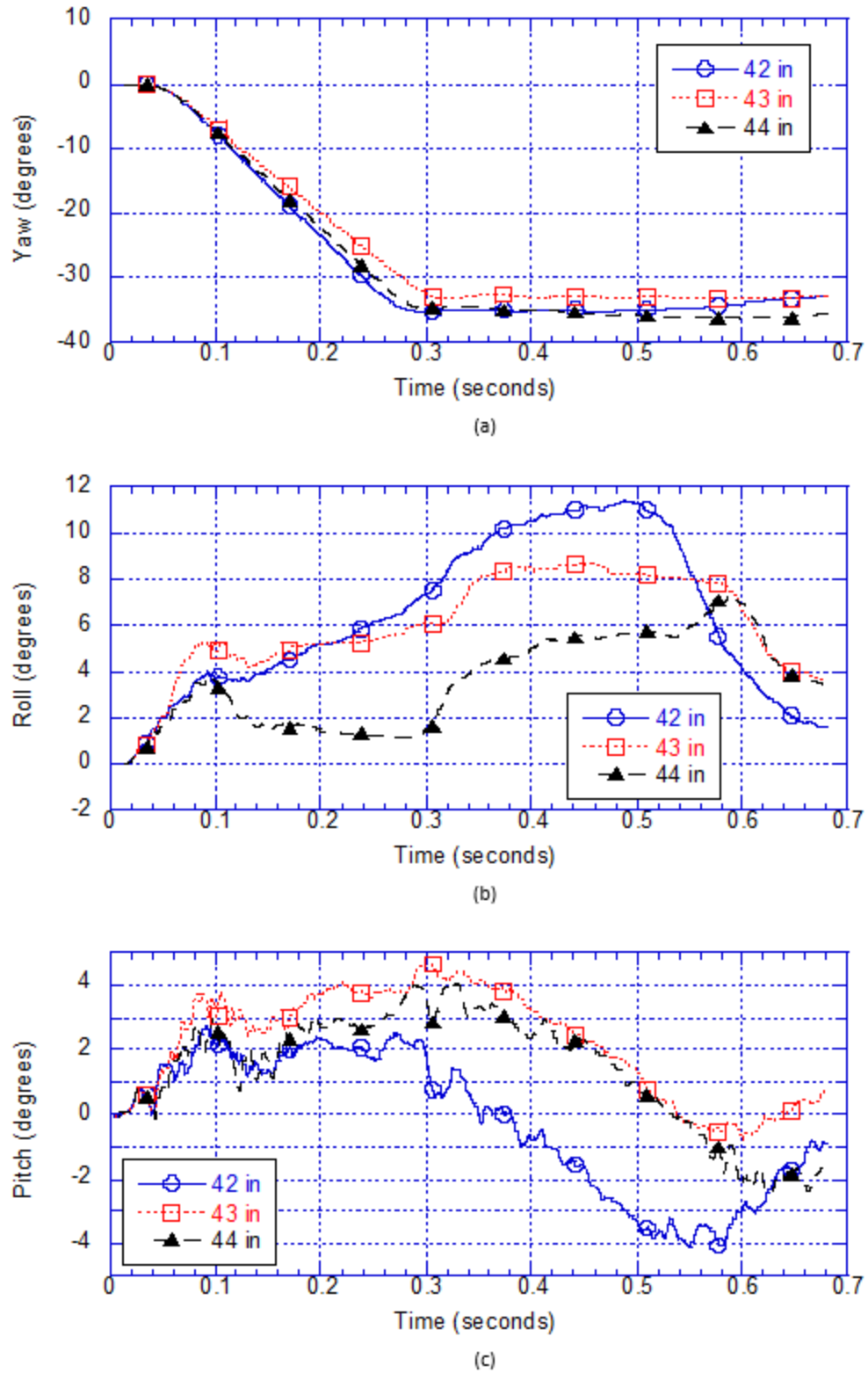
Table 11: Passenger car collision data for different height barriers

Occupant Risk Factors		42 in barrier	43 in barrier	44 in barrier
		FEA	FEA	FEA
Occupant Impact Velocity (m/s)	x-direction	8.9	9.9	9.9
	y-direction	-8.8	-8.9	-8.9
	at time	at 0.0749 seconds on left side of interior	at 0.0751 seconds on left side of interior	at 0.0754 seconds on left side of interior
THIV (m/s)		12.5	13.3	13.2
		at 0.0749 seconds on left side of interior	at 0.0751 seconds on left side of interior	at 0.0754 seconds on left side of interior
Ridedown Acceleration (g's)	x-direction	-5.1 (0.0763 - 0.0863 seconds)	-5.3 (0.0776 - 0.0876 seconds)	-6.5 (0.0767 - 0.0867 seconds)
	y-direction	4.7 (0.0874 - 0.0974 seconds)	5.5 (0.0906 - 0.1006 seconds)	4.9 (0.5985 - 0.6085 seconds)
PHD (g's)		6.3 (0.0749 - 0.0849 seconds)	5.8 (0.0785 - 0.0885 seconds)	6.7 (0.0759 - 0.0859 seconds)
ASI		2.43 (0.0148 - 0.0648 seconds)	2.46 (0.0165 - 0.0665 seconds)	2.5 (0.0165 - 0.0665 seconds)
Maximum Angular Disp. (deg)	Roll	-14.6 (0.0569 seconds)	-14.9 (0.0566 seconds)	-15 (0.6501 seconds)
	Pitch	-2.4 (0.7864 seconds)	-2.7 (0.7834 seconds)	-2.9 (0.7840 seconds)
	Yaw	44.3 (0.7064 seconds)	48.8 (0.8274 seconds)	48.4 (0.8064 seconds)

Table 11 shows very little variation in the collision data collected when the height of the barrier is changed. Also, the damage to the barrier for all three heights is non-existent and not a concern for collisions with this vehicle. There doesn't seem to be a high risk of noticeable cracking or damage when this vehicle collides with the barrier. Figure 35 shows the damage that is incurred on the 44 inch barrier when the passenger car collides.
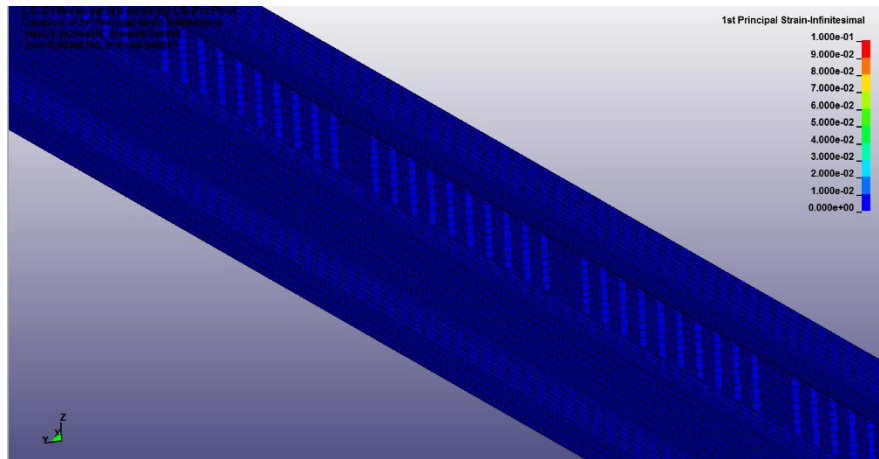
Figure 35: Damage incurred on 44 in barrier after passenger car collision

3.5. FINAL DESIGN

After conducting the parametric study, it was found that all collisions meet the requirements to pass MASH TL-4. The accelerations all fall below the maximum permissible values for the pickup truck and passenger car, and there is no acceleration requirement for the single unit truck. Table 12 shows the maximum permissible values for occupant impact velocity, ridedown acceleration, roll, pitch, and yaw. The single unit truck does not have any required values. The only requirement in MASH for the single unit truck collision is that the barrier contains and redirects the vehicle in a controlled manner. It is preferred, although not essential, that the vehicle remains upright during and after the collision.

After analyzing all the results and seeing the behavior of the vehicle, the final design was chosen for testing. The modified design shown in Figure 15 and Figure 16 was chosen to be tested under MASH impact conditions.

Table 12: Preferred and maximum permissible acceleration values

Acceleration Parameter		MASH Test 4-10 Small Car		MASH Test 4-11 Pickup Truck		MASH Test 4-12 Single Unit Truck	
		Pref.	Max	Pref.	Max	Pref.	Max
Occupant Impact Velocity (m/s)	x-direction	9.1	12.2	9.1	12.2	n/a	n/a
	y-direction	9.1	12.2	9.1	12.2	n/a	n/a
Ridedown Acceleration (g's)	x-direction	15	20.49	15	20.49	n/a	n/a
	y-direction	15	20.49	15	20.49	n/a	n/a
Maximum Angular Disp. (deg)	Roll	-	75	-	75	n/a	n/a
	Pitch	-	75	-	75	n/a	n/a
	Yaw	n/a	n/a	n/a	n/a	n/a	n/a

CHAPTER IV

4. FULL SCALE CRASH TESTING AND MODEL VALIDATION

4.1.   TESTING FACILITY

The full-scale tests were performed at Texas A&M's Texas Transportation Institute (TTI). Founded in 1950, TTI has become a world leader in roadway safety studies, and since 1965 has conducted over 2,000 full scale crash tests. Their test facility is a 2,000-acre complex where they perform a variety of crash tests, ranging from small passenger cars to large tractor-trailers and tanker trucks, into a variety of roadside safety hardware such as bridge rails, and signs. Their vast experience and knowledge in the field of roadside safety hardware is what led the RIME Team to pick them as the facility to perform these tests. After sharing the details of the barrier with them, their engineers generated their own construction drawings and renderings, and experimental setup. They also handle all construction, vehicle data collection and processing, and photography/videography.

4.2.   CONSTRUCTION AND FEM DEVELOPMENT

To construct the barrier, conditions of being on a bridge must be simulated. TTI performs many of these tests at their facilities, and they are all built using the same

method. There is a rigid concrete apron that all concrete bridge barriers to be tested are attached too. Because of this, the finite element model needs to be modified to reflect this. Initially, the model being used was simply a barrier attached to a deck, but the new setup must be replicated to produce the best representation. Figure 36 shows a Solidworks rendering view from the end of the barrier to show how it will be laid out. The face of the wall at the level of the deck and below is where the interface of the apron and assembly are attached via anchor bars.
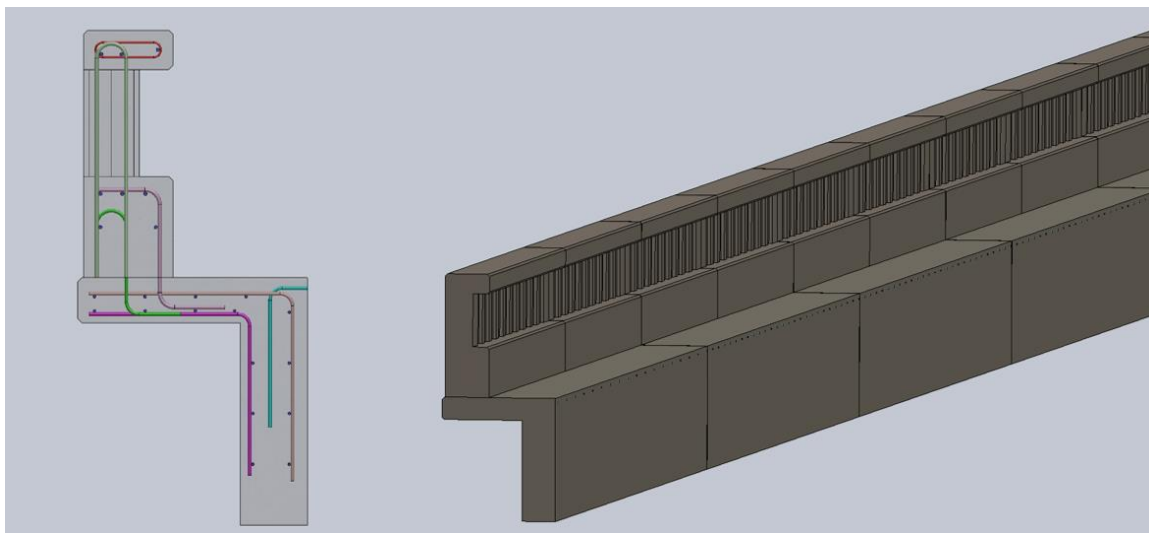
Figure 36: Solidworks rendering of barrier-rebar layout and isometric view of barrier attachment. (Provided by William Williams at TTI)

On the edge of this rigid apron, there are dowels sticking out at 18 in along the length of the barrier, and 15 ft upstream and downstream of the impact locations, they are located every 12 in. Anchor bars are welded to each of these dowels and are developed in the concrete wall to secure it to the rigid block. Figure 37 shows these anchor bars welded to the dowels, and the finite element representation of them.

Figure 37: (a) Anchor bars welded to dowels, and epoxy coated deck bars (TTI) and (b) FEM representation

Also shown in Figure 37 are the deck bars. Because the rigid apron concrete is preexisting, the deck bars are bent and developed in the wall portion of the setup. The bottom deck bars are placed at 8 in as they will be in the one built on a bridge, and the top deck bars are placed at 4 in. They are placed at 4 in because in the barrier specifications, there is a 5 ft bar alternating with the regular deck reinforcement to provide additional strength to the connection with the deck. All the longitudinal #4 bars are tied to the deck bars. After this part of the rebar assembly is finished, the vertical wall portion is then poured. This is shown in Figure 38.
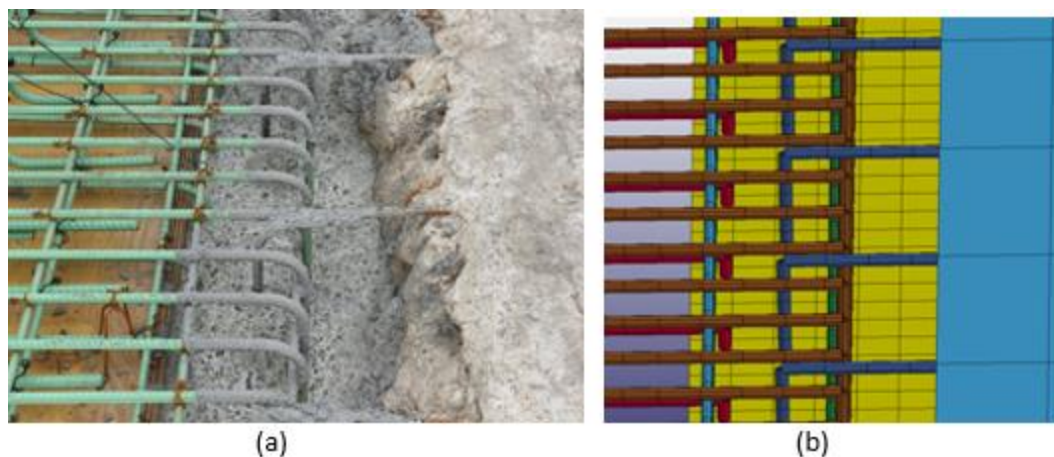
Figure 38: (a) Filled wall portion of barrier setup (TTI) and (b) FEM representation

The c-bars and d-bars that attach the barrier to the deck can be tied to the deck bars before or after the pouring of the wall because they do not come in contact with it. After they are tied to the deck bars, the longitudinal bars in the bottom portion of the barrier can also be tied to them. Figure 39 shows these bars tied in the assembly. When this part of the assembly is completed, the remaining portion of the deck is poured, leaving only the c-bars and d-bars protruding up from the concrete. This is shown in Figure 40.
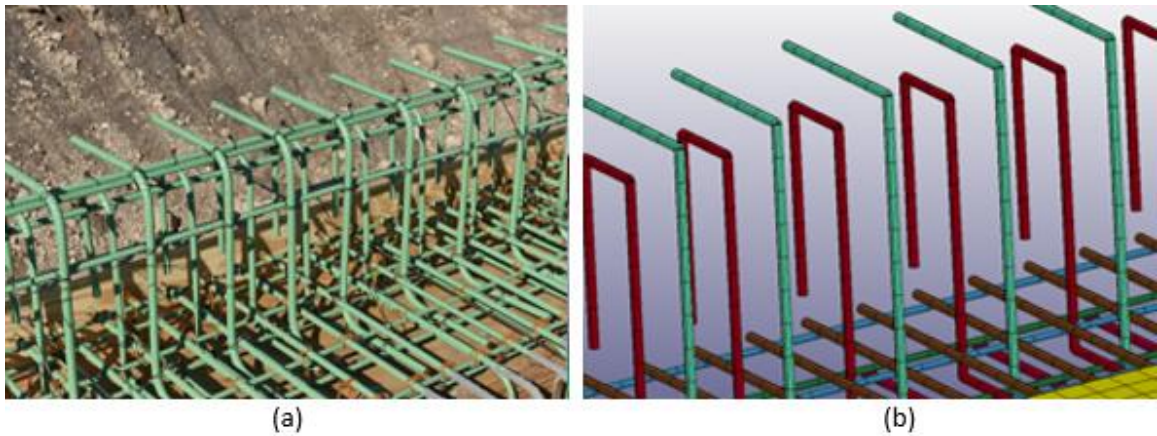
Figure 39: (a) C-bars and D-bars tied to deck bars (TTI) and (b) FEM representation
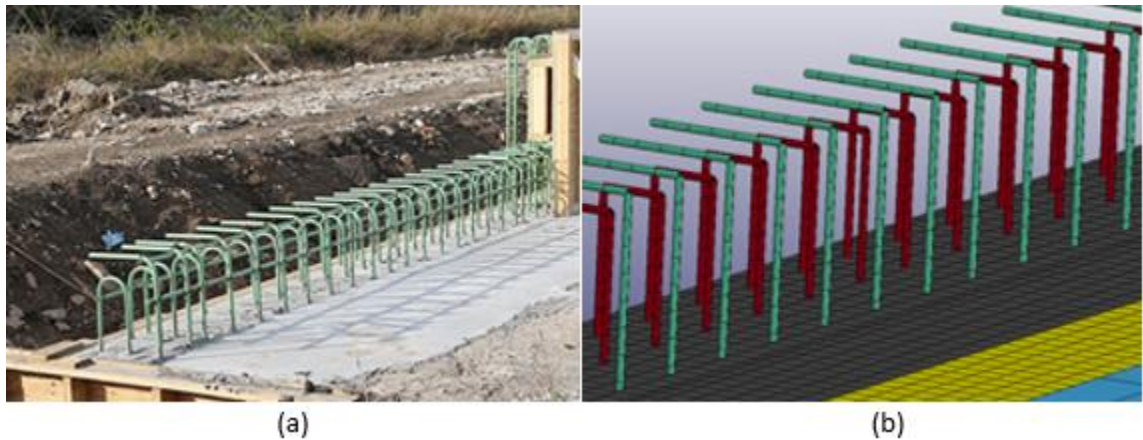
Figure 40: (a) C-bars and D-bars protruding up from finished deck (TTI) and (b) FEM representation

After the deck is poured, the inside part of the formwork is assembled and set into place. The vertical b-bars, the a-bars in the top rail, and the longitudinal e-bars are then

tied into place and secured to the formwork to ensure proper placement. This setup is shown in Figure 41. To create the openings needed between the posts, foam blocks are cut and then glued into the appropriate position on the formwork. When the concrete for the barrier is poured, it will flow around the blocks leaving behind the iconic openings required for this historic looking barrier. The placement of these foam blocks is shown in Figure 42.

Figure 41: Vertical bars and top rail reinforcement secured to formwork (TTI)

Figure 42: Foam blocks for openings being glued to formwork (TTI)

The other side of the formwork and the ends are set into place and the concrete is then poured. After the concrete is hard enough, the formwork is removed and the foam blocks can be removed easily. Once the foam blocks are removed, the barrier construction is complete. Figure 43 shows a picture of the finished product and its FEM counterpart. Figure 44 displays the attachment mechanism of the original and modified models.
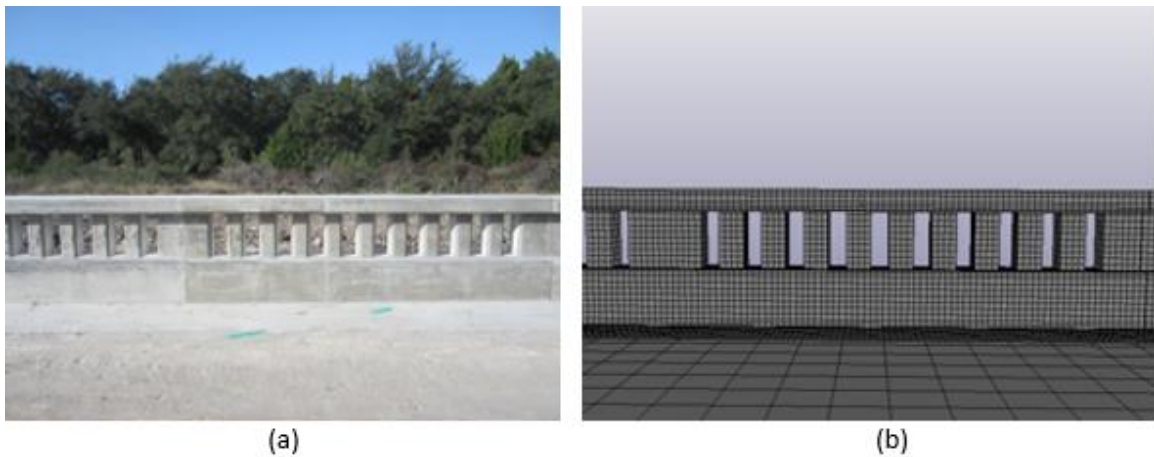
Figure 43: (a) Fully constructed barrier and (b) FEM representation
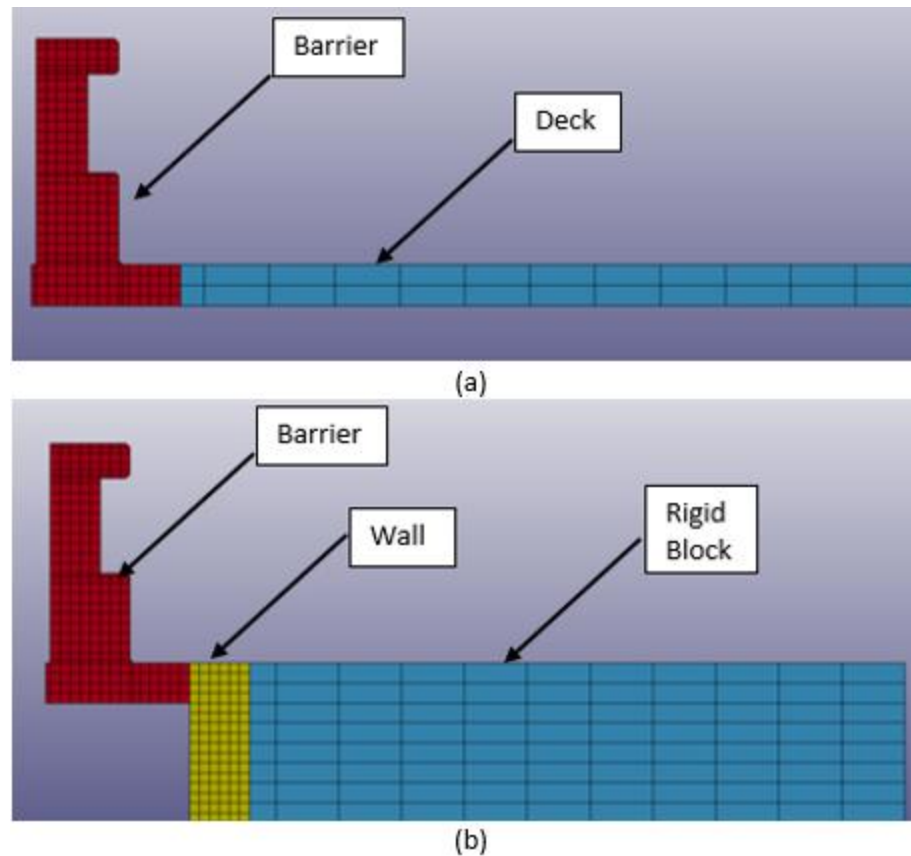
Figure 44: (a) Original assembly and (b) final barrier model assembly

Because the concrete for many components was poured at different times, there were many cold joints that needed to be simulated. This included the portions of barrier that were touching at their ends forming contraction joints, and at the interface of the deck and barrier. Figure 45 displays the location of the cold joint created when the barrier is poured after the deck. This cold joint was modeled by unmerging the nodes of these elements that were coincident such that the barrier does not act as if it was all poured at the same time.
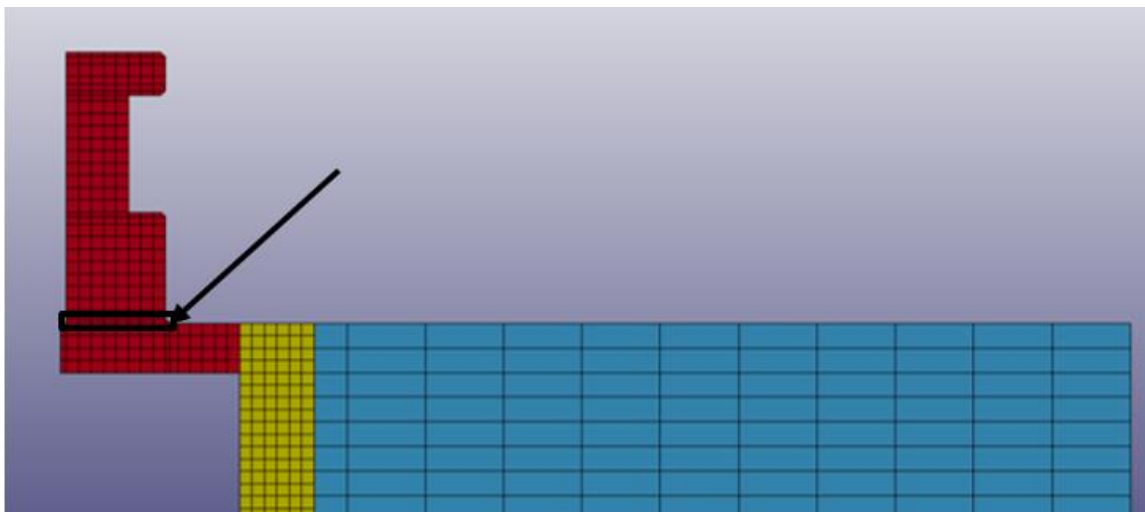
Figure 45: Location of cold joint interface between deck and barrier

4.2.1. MATERIAL SPECIFICATIONS

For this barrier design, the only material specifications listed are the concrete axial compressive strength, steel rebar grade and yield strength, and steel rebar corrosion protection. All of these minimum design requirements must be met to give the designed resistance and meet all NJDOT specifications in order to be implemented.

4.2.2. Concrete Specifications

The concrete used for the barrier was supplied by Martin Marietta, and was a P gravel mix containing Type C fly ash. The required minimum concrete compressive strength for this barrier design is 4,000 psi. The first pour of the deck took place on November 17, 2016 and the last occurred on December 9, 2016. The strength on the day of the first test with the single unit truck fulfilled the minimum requirement with a strength of 5,850 psi.

4.2.3. Reinforcing Steel Specifications

The reinforcement specified for this barrier is grade 60 epoxy coated steel bars. As per NJDOT specifications, the bars are all corrosion protected with a protective layer of epoxy, and the tensile yield strength is 60,000 psi. The steel supplier for this barrier

was CMC Steel in Allen, TX. The bars were delivered coated with epoxy, and were then cut and bent by the construction team at TTI.

4.3.   VEHICLES

As per AASHTO MASH TL-4 requirements, three vehicles must be tested to determine the crashworthiness of the longitudinal barrier. The first vehicle to be tested is a 10,000 kg single unit truck. Next is a 2,270 kg pickup truck, and finally a 1,100 kg passenger car. After these vehicles are received by TTI, the inside of the vehicles are stripped down leaving only the necessities. Usually the back seats are removed and a data acquisition system and accelerometers are put in the place of them, and the front seats remain in order to place a crash test dummy. Under MASH, the crash test dummy does not play a role in determining whether the barrier passes or fails, but is there for the research purposes of TTI (Fang et. al, 2016) and (AASHTO, 2016). The only vehicle that is required to have a crash test dummy under MASH is the passenger car. It is required because the vehicle is very light, and the 165 lb dummy in the driver's seat makes up a significant portion of the total system mass, about 6.5 percent. The vehicles used are described in this section.

4.3.1. SINGLE UNIT TRUCK (10000S)

Before the crash scenario was modeled, the vehicle needed modifications. The first vehicle crash tested was the 2006 International 4200 single unit box truck, shown in Figure 46, and the vehicle model used was downloaded from the National Crash Analysis Center (NCAC) which is now the Center for Collision Safety and Analysis (CCSA) George Mason University. It was a truck that fulfilled the requirements of a TL-4 vehicle under NCHRP Report 350. To make this vehicle usable, dimensions and the mass were

modified to fulfill the requirements of MASH. In order to achieve the required 10,000 kg and center of mass height, a concrete block ballast was cast and mounted in the middle of the truck box. Accelerometers were mounted in the box of the truck in front of the concrete ballast, and in the cab of the truck on the floor between the driver and passenger seats.

Figure 46: (a) 10000S single unit truck and (b) FEM representation

There were very small differences in some dimensions of the vehicle, but none of them were large enough to warrant making any major modifications. One modification that was made includes the fuel tank location. It was originally on the impact side in the model, but on the outside in the full-scale test. The truck model was completely reflected in order to match the full-scale test. Another simple modification that was made was the ballast location. In the model, it was originally placed about 1.5 ft forward from the actual location, and was moved to the correct location. Additional rigid constraints were added to the ballast to attach it more firmly to the cargo box. More rigid constraints were also added to the accelerometer to reduce noise recorded by it, and to increase the accuracy. Figure 47 show the original ballast and accelerometer locations with limited

rigid constraints around the ballast and accelerometer, and the modified model with many rigid constraints around the ballast and for the accelerometer.

(a)   (b)
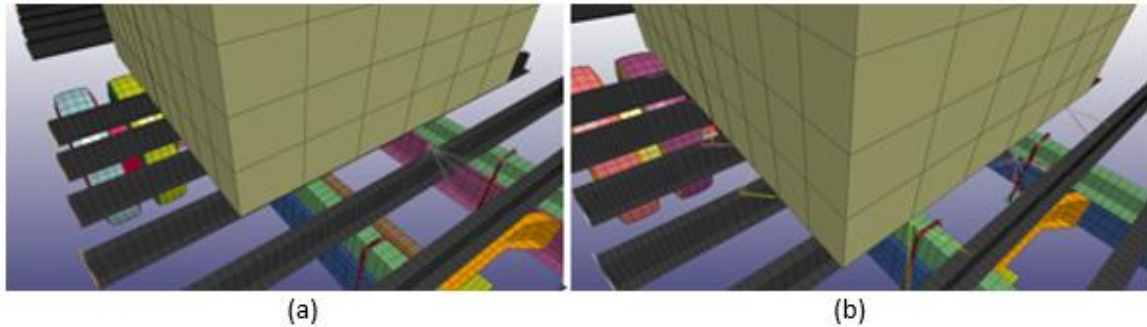
Figure 47: Original (a) and modified (b) ballast and accelerometer constraints

When running the simulations, the axle was detaching from the suspension leafs, which did not occur in the full-scale test. Upon further investigation, it was found that the u-bolts connecting the axle to the suspension leafs were failing in the simulation. To correct this problem, the u-bolts were strengthened to ensure this failure and detaching would not occur. After these modifications were performed, the vehicle model was ready to be simulated.

The final changes to the simulation were modifications to the contact frictions. The friction between surfaces plays an integral role in determining how the vehicle will behave during and after impact. They were iteratively modified until the behavior was as representative of the full-scale test as possible. The original and modified friction values are listed in Table 13.

Table 13: Original and modified friction coefficients for 10000S simulation

Model	Tires to Rail	Tires to Deck	Vehicle to Rail
Original	0.300	0.600	0.25
Modified	0.900	0.800	0.15

4.3.2. PICKUP TRUCK (2270P)

The second vehicle used for crash testing was a 2011 Dodge Ram 1500 quad-cab pickup truck shown in Figure 48. The rear seats of this vehicle were removed and data collection hardware, including accelerometers, were mounted on the floor in their place. A crash test dummy was also placed in this vehicle in the driver's seat. Unlike the single unit truck, there was no need to add a ballast in the back to achieve the required 2,270 kg required for the test. The model used to simulate this collision was a 2007 Chevy Silverado. The dimensions of the Chevy Silverado pickup truck model and the Dodge Ram 1500 used in the test are very similar, and therefore no dimensional changes were needed.

(a)   (b)
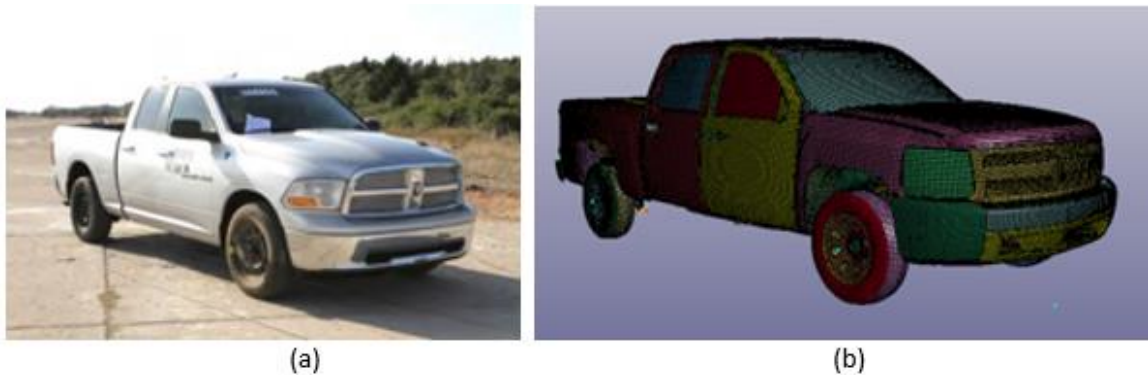
Figure 48: (a) 2270P vehicle used (TTI) and (b) FEM of the Chevy Silverado modeled

The only modification made to this vehicle was the accelerometer mounting. The number of rigid constraints between the accelerometer and the floor of the cab was increased to reduce the noise collected by the accelerometer and to give a more accurate reading. This modified constraint is shown in Figure 49.

(a)

(b)
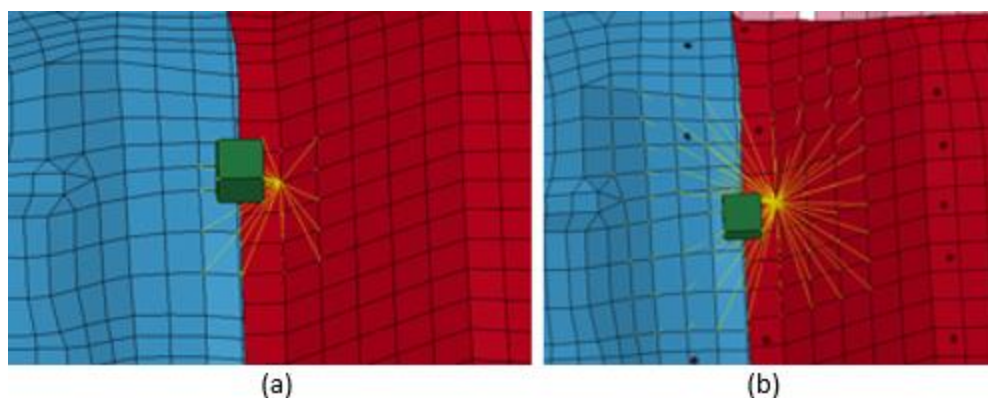
Figure 49: Original 2270P accelerometer constraint (a) and modified constraint (b)

The final changes to the simulation were modifications to the contact frictions. The friction between surfaces plays an integral role in determining how the vehicle will behave during and after impact. They were iteratively modified until the behavior was as representative of the full-scale test as possible. The original and modified friction values are listed in Table 14.

Table 14: Original and modified friction coefficients for 2270P simulation

Model	Tires to Rail	Tires to Deck	Vehicle to Rail (static)	Vehicle to Rail (dynamic)
Original	0.400	0.600	0.200	0.100
Modified	0.160	0.800	0.110	0.110

4.3.3. SMALL CAR (1100C)

The third and final vehicle used to test the barrier was a 2010 Kia Rio shown in Figure 50. The rear seats of the vehicle were removed and data collection hardware, including accelerometers, were mounted to the floor in their place. A required crash test dummy was placed in the driver's seat for the test. There was no need to add additional weight to this vehicle to achieve the required 1,100 kg required for the test. The model used to simulate this collision was a 2010 Toyota Yaris. The dimensions of the Toyota

Yaris model and Kia Rio used in the test are very similar, and therefore no dimensional changes were needed.

Figure 50: (a) 1100C vehicle used (TTI) and (b) Toyota Yaris modeled

The only modification made to this vehicle was the accelerometer mounting. The number of rigid constraints between the accelerometer and the floor of the cab was increased to reduce the noise collected by the accelerometer and to give a more accurate reading. This modified constraint is shown in Figure 51.
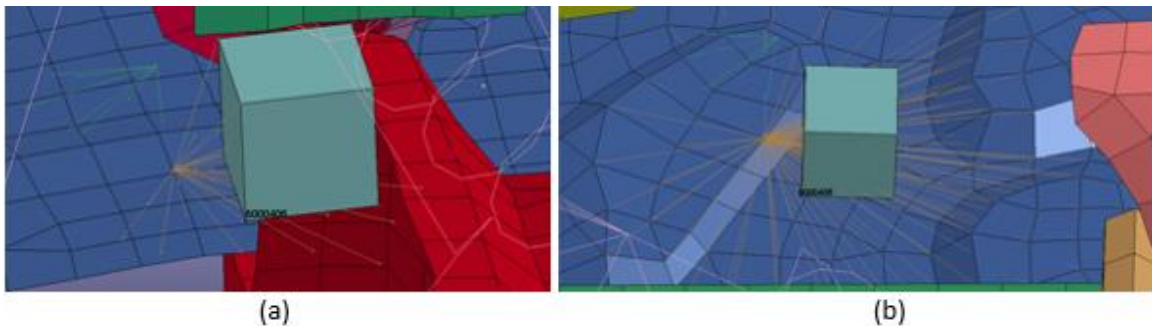
Figure 51: Original 1100C accelerometer constraint (a) and modified constraint (b)

The final changes to the simulation were modifications to the contact frictions. The friction between surfaces plays an integral role in determining how the vehicle will behave during and after impact. They were iteratively modified until the behavior was as representative of the full-scale test as possible. The original and modified friction values are listed in Table 15.

Table 15: Original and modified friction coefficients for the 1100C simulation.

Model	Tires to Rail	Tires to Deck	Vehicle to Rail (static)	Vehicle to Rail (dynamic)
Original	0.400	0.400	0.200	0.100
Modified	0.200	0.700	0.100	0.100

4.4. EXPERIMENTAL SETUP

4.4.1. VEHICLE PROPULSION AND GUIDANCE

After the test vehicle is prepared and accelerometers are installed, it is placed at a set distance far from the barrier, and at the specified angle for the specific test. A two-to-one reverse tow cable pulley system was used to propel the vehicle and a steel guide wire was anchored to the ground and tensioned along the distance that the vehicle was being towed for. Figure 52 shows the vehicle that is used to pull the test vehicles toward the barrier. The system was oriented such that the towing truck drives away from the impact location to pull the test vehicle towards it. The front passenger side wheel of the test vehicle is attached to the guide wire using TTI's proprietary vehicle guidance system, and the vehicle was towed using a cable attached to the front center of the vehicle. Both systems are detached just before impact resulting in a free-moving vehicle colliding with the barrier. After the collision, the vehicle's breaks are applied to bring it to a controlled stop. Figure 53 shows a schematic of how the system was laid out.

Figure 52: TTI truck used to tow vehicles to collision site.
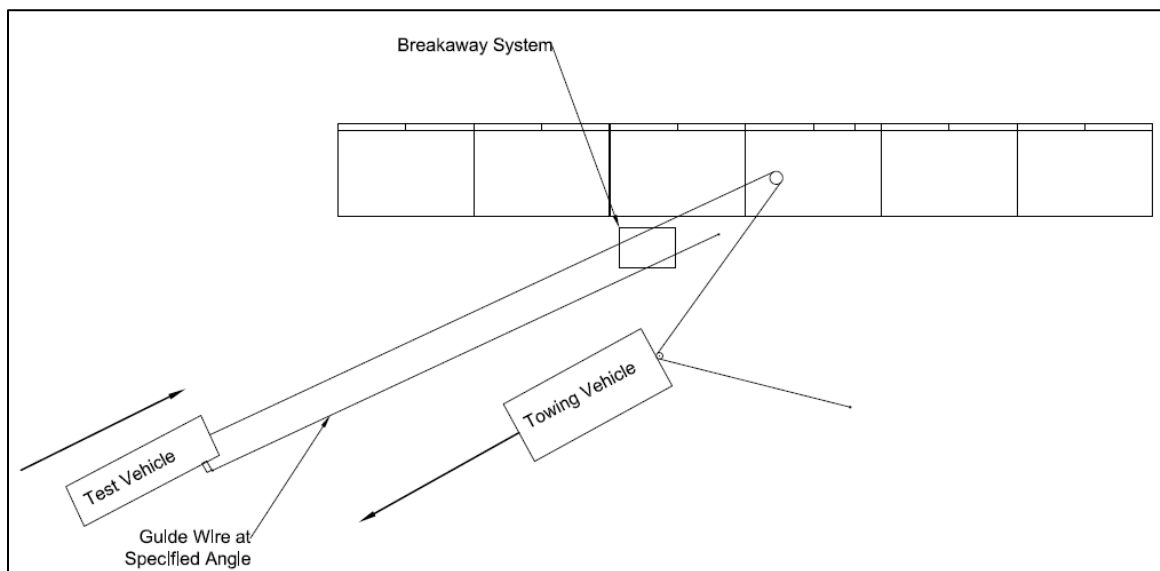
Figure 53: Cable-tow and vehicle guidance system

4.4.2. DATA COLLECTION

The system used to collect data from each collision was the Tiny Data Acquisition System Pro by Diversified Technical Systems, Inc. This system contained accelerometers that recorded acceleration in the x, y, and z directions, and angular rate sensors along each axis recorded the roll, pitch and yaw rates. Data was collected at a rate of 10,000 Hz (Williams et. al, 2017). After the data is collected, the procedure for processing it is identical to the one when data from a simulation is used. The

accelerometer and rotational rate data is then input into the Test Risk Assessment Program (TRAP) which filters the acceleration data and integrates the rotational rates to calculate the angular displacement.

4.5.   RESULTS AND VALIDATION

The three vehicles were all tested according to MASH TL-4 standards and the results the tests were that the barrier satisfactorily met all requirements. Full scale crash tests are typically the last step in proving the crashworthiness of a barrier. The barrier is now on its way to getting FHWA approval, and validating the finite element models is an important last step of the process. A barrier does not need to be modeled and validated to get approval and be implemented, but having validated models makes the process of retrofitting easier than ever. The FHWA recently announced that crash simulation results would be considered acceptable for evaluating improvements to previously tested barriers, which means there would be no need for another crash test (Marzougui et. al, 2012). All three crash tests were successful, and the results of the simulations were in very good agreement.

When validating a finite element model of a vehicle crash using testing data, there are three main steps: (1) solution verification, (2) time-history validation, and (3) Phenomena Importance Verification (PIRT's) (Ray et. al., 2010). It was shown that all criteria was fulfilled and the finite element collision scenarios are valid. The time interval being evaluated is from the moment of impact to 0.6 seconds after impact for the SUT, and from the moment of impact to 0.5 seconds for the small car and pickup truck. The reason these intervals were chosen is because within these times, all important

phenomena and maximum values for rotations and ridedown accelerations occurs, and everything that occurs afterwards is non-significant.

The first step of validating a computer model is the analysis solution verification. Checking the solution verification criteria is a way to determine that the model is stable, and that all laws of physics are being upheld. These checks ensure that energy is conserved, that hourglass energy is not excessive, and that the amount of mass added to the model during analysis does not affect the accuracy of the solution.

The second step in validating a computer model is the time-history validation, which compares parameters such as accelerations and rotational velocities using single-channel comparisons, and a multi-channel weighted comparison. This is accomplished by the use of the Roadside Safety Verification and Validation Program (RSVVP). The comparison method described in NCHRP w179 involves using the Sprague-Geers magnitude-phase-composite (MPC) comparison metrics. In MPC metrics the phase and magnitude components should not be dependent on each other, and should be compared separately (Sprague & Geers, 2003). This allows the person analyzing the curves to identify the aspects that do not agree. The magnitude and phase components of the Sprague-Geers comparison are calculated as:

$$M_G = \sqrt{\frac{\sum c_i^2}{\sum m_i^2}} - 1$$

$$P_{SG} = \frac{1}{\pi} \cos^{-1}\left(\frac{\sum c_i m_i}{\sqrt{\sum c_i^2 \sum m_i^2}}\right)$$

Where M_G is the magnitude comparison, P_{SG} is the phase comparison, c_i represents the computed quantities, and m_i represents the measured quantities. The Sprague-Geers Comprehensive metric comparison is calculated as:

$$\sqrt{M_{SG}^2 + P_{SG}^2}$$

For all three parameters (magnitude, phase, and comprehensive), a value of 40% or lower indicates a pass, and a value greater than 40% indicates a failure (Sprague & Geers, 2003) and (Ray, 1996). Although the comprehensive metric comparison is not used to determine if the model is validated or not, it is still calculated by RSVVP.

In addition to the MPC metric comparisons, Analysis of Variance (ANOVA) metrics are also compared. ANOVA comparisons are based on the assumption that the true curves measured in the field and test curves extracted from the model represent the same event in such a way that any differences between the curves must be attributable to random experimental error only (Ray et. al, 2010) and (Oberkampf & Barone, 2006). These comparisons assess whether the variance between the two curves can be attributed to random error or not. Two ANOVA metrics are compared: average residual error normalized by the peak response (i.e., e^{-r}), and the standard deviation of the normalized residuals (i.e., σ^r), and are calculated as follows:

$$e^{-r} = \frac{\sum(c_i - m_i)/m_{max}}{n} < 0.05 * m_{max}$$

$$\sigma^r = \sqrt{\frac{\sum(e^r - e^{-r})^2}{n-1}} < 0.20 * m_{max}$$

Where c_i represents the computed quantities, m_i represents the measured quantities, and m_{max} represents the peak response of the measured values. In order for ANOVA metrics to be considered passed, the average residual error (e^{-r}) must be less than 5% of the peak value, and the standard deviation of the normalized residuals (σ^r) must be less than 20% of the peak value.

When dealing with vehicle crashes, it is acceptable for some comparison channels in the model to fail, while the overall model can still be considered valid. In order for this to be accounted for, each channel is given a weighting factor that corresponds to the importance, or "weight" each parameter has on the behavior of the vehicle during the collision. The most accurate method for calculating the weighting factors is the Inertial Method that uses a proportion of momentum in each channel to calculate the factor. In order to perform the calculation using this method, the vehicle mass and three angular inertial properties must be known. These exact quantities are not always known for the test vehicles, and calculating these properties is a very time-consuming process that includes a series of very involved calculations.

Because of this, the default method used in RSVVP for calculating the weighting factors is the Area Method, which is a pseudo moment approach. The weighting factors calculated using the Area Method produce similar factors to those calculated using the Inertia Method, making it acceptable to use in validating collision models. The factors are calculated using only measured information from the full-scale crash tests. The factors for linear and rotational momentum are calculated separately from one another because of the unit difference, and each one is assigned an "index" value. This value gauges how important the parameter is relative to other ones. Once each channel's index

value is calculated, the weighting factors are calculated by simply dividing the index value by the summation of all index values. The procedure for calculating the values is as follows:

1.) Evaluate the true curve for each acceleration and rotational channel, a_i and v_i, respectively.

2.) Evaluate the sum of the acceleration and rotational areas, a_{sum} and v_{sum}, respectively.

3.) Evaluate the local weight (index value) for each acceleration and rotational channel:

$$lw_i^{(a)} = \frac{a_i}{a_{sum}}$$

$$lw_i^{(v)} = \frac{v_i}{v_{sum}}$$

4.) Calculate the acceleration and rotational weight factors for the model as follows:

$$w_i^{(a)} = \frac{lw_i^{(a)}}{\sum lw_i^{(a)} + \sum lw_i^{(v)}}$$

$$w_i^{(v)} = \frac{lw_i^{(v)}}{\sum lw_i^{(a)} + \sum lw_i^{(v)}}$$

These factors are then used to compute the multi-channel comparison metrics for the model. If all metrics satisfy the criteria listed above, the time-histories for the vehicle can be considered verified.

The third and final step in validating a computer model is comparing various parameters using a Phenomena Importance Ranking Table (PIRT). The items set forth in the Phenomena Importance Ranking Table include information about structural adequacy, occupant risk, and vehicle trajectory. Each item in the table describes very important events that occur during a vehicle collision, and it is very important that every event occurs in the model and during testing, and that measured values, such as rotations and accelerations, are close enough to one another such that the difference between the model and collision is insignificant.

Once all three steps of the validation process are completed and all criteria is affirmative, then the model is considered validated, and can be accepted as an accurate representation of what occurs during full scale testing.

4.5.1. SINGLE UNIT TRUCK (10000S)

MASH Test 4-12 of the 10000S single unit truck was performed on December 16, 2016. The only requirement for this test to be deemed a pass is that the truck must stay on the correct side of the barrier and not overturn to the other side, or show potential for overturning to the other side. The vehicle must be safely contained and redirected from the barrier and not show any signs of ending on the other side. It is preferable, although not essential, that the vehicle remains upright during and after the test, but is not a requirement for the pass/fail grade (AASHTO, 2016). The truck was successfully contained and redirected on the correct side of the barrier, remained upright, also stayed very close to the barrier for the duration of the collision, and was very stable throughout the whole event. Figure 54 shows a visual comparison between the full-scale crash test and the finite element model. The kinematics of the test and model were very similar to

each other, and were in good agreement. The accelerations and rotations were also in very good agreement, as shown in Figure 55 and Figure 56.

Test	Simulation
0.000 s	0.000 s
0.100 s	0.100 s
0.200 s	0.200 s
0.300 s	0.300 s
0.400	0.400

Figure 54: Sequential views of MASH Test 4-12 and FEA
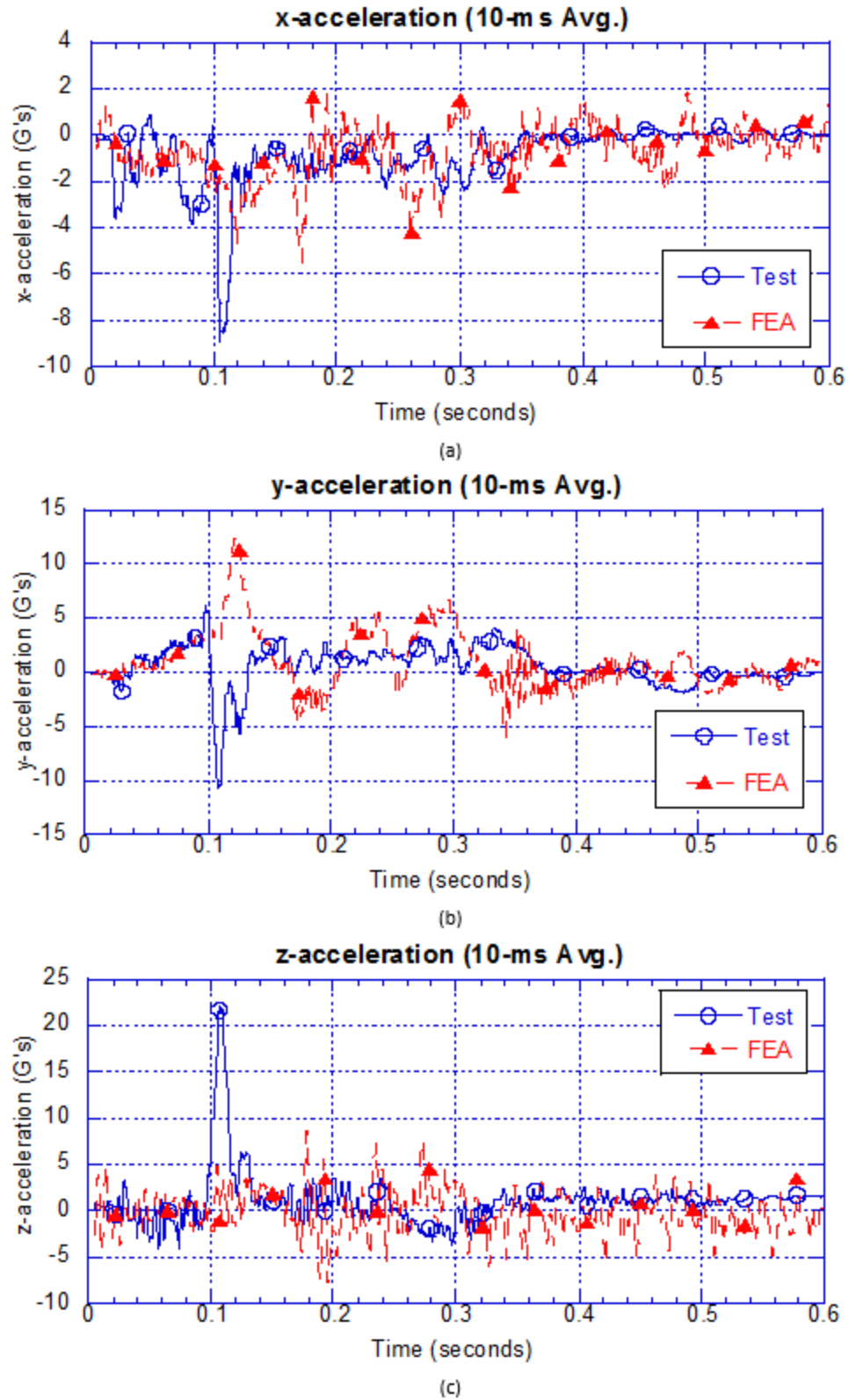
Figure 55: Acceleration comparison between MASH 4-12 test and FEA: (a) x-acceleration plots; (b) y-acceleration plots; (c) z-acceleration plots
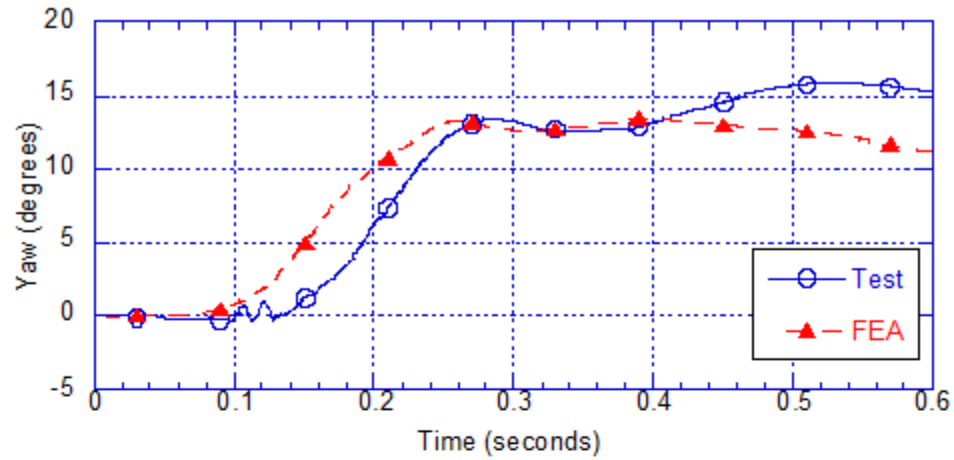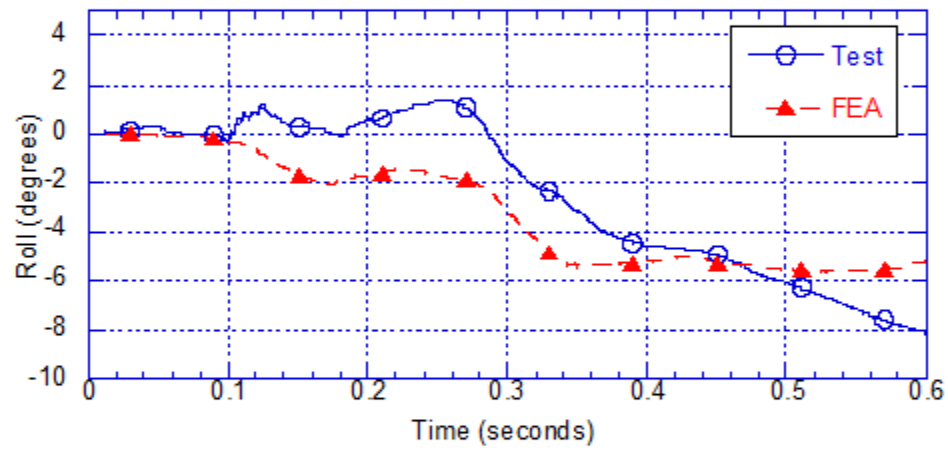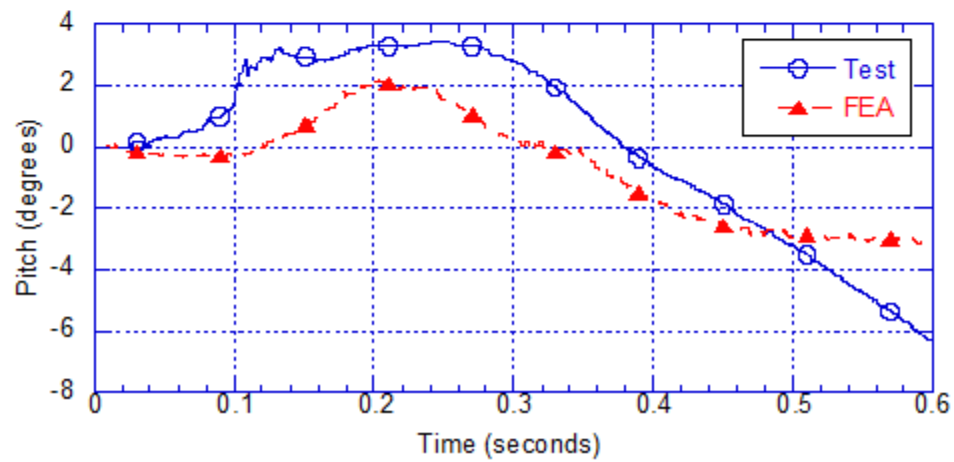
Figure 56: Rotational Angle comparison between MASH 4-12 test and FEA: (a) Yaw angles vs time; (b) Roll angles vs time; (c) Pitch angles vs time.

The first step in validating the model is checking the solution verification criteria to ensure the model is stable and all laws of physics are upheld. Table 16 shows the solution verification table for the single unit truck model, and all criteria passes.

Table 16: Solution verification criteria for model of MASH test 4-12

Verification Evaluation Criteria	Change (%)	Pass?
Total energy of the analysis solution (i.e., kinetic, potential, contact, etc.) must not vary more than 10 percent from the beginning of the run to the end of the run.	<1	YES
Hourglass Energy of the analysis solution at the end of the run is less than 5% of the total initial energy at the beginning of the run.	<1	YES
The part/material with the highest amount of hourglass energy at any time during the run is less than 5% of the total initial energy at the beginning of the run.	<1	YES
Mass added to the total model is less than 5% the total model mass at the start of the run.	<1	YES
The part/material with the most mass added had less than 10% of its initial mass added.	<1	YES
The moving parts/materials in the model have less than 5% of mass added to the initial moving mass of the model.	<1	YES
There are no shooting nodes in the solution?	YES	YES
There are no solid elements with negative volumes?	YES	YES

The next step in validating the model is validating the time-history curves. All accelerations and rotations about the three axes were compared using RSVVP and the theory described in the beginning of this section. Although the Sprague-Geers metrics did not pass for some single-channel comparisons, the multi-channel comparison passed, and therefore the time-histories pass and are validated. Table 17 lists all the scores for the time-history validation of the individual channels, as well as the multi-channel comparison.

Table 17: Time-history validation of MASH test 4-12 Finite Element Analysis

Single Channel Time History Comparison Results		Time interval [0 sec - 0.6 sec]		
	Sprague-Geer Metrics	M	P	Pass?
O	X acceleration	6.5	40.6	Fail
	Y acceleration	20.4	50.4	Fail
	Z acceleration	50.4	48.8	Fail
	Yaw rate	27.9	24.1	Pass
	Roll rate	32.4	35.2	Pass
	Pitch rate	20.7	43.2	Fail
	ANOVA Metrics	Mean	SD	Pass?
P	X acceleration/Peak	0.47	13.51	Pass
	Y acceleration/Peak	2.28	19.4	Pass
	Z acceleration/Peak	-4.45	22.51	Pass
	Yaw rate	-1.95	14.67	Pass
	Roll rate	6	19.7	Fail
	Pitch rate	4.33	16.26	Pass
Multi-Channel Weighting Factors		Time interval [0 sec - 0.6 sec]		
Multi-Channel Weighting Method Peaks Area I Area II Inertial	X Channel	0.16059642		
	Y Channel	0.106453842		
	Z Channel	0.232949738		
	Yaw Channel	0.222019916		
	Roll Channel	0.155941409		
	Pitch Channel	0.122038675		
Sprague-Geer Metrics		M	P	Pass?
	All Channels (weighted)	28.7	39.4	Pass
ANOVA Metrics		Mean	SD	Pass?
	All Channels (weighted)	0.3	17.8	Pass

The third and final step of the validation process is checking that all criteria in the Phenomena Importance Ranking Table (PIRT) is fulfilled. Table 18 lists the criteria that needs to be fulfilled in order for the model to be considered fully validated.

Table 18: Phenomena Importance Ranking Table for MASH Test 4-12

			Evaluation Criteria	Known Result	Analysis Result	Agree?
Structural Adequacy	A	A1	Test article should contain and redirect the vehicle; the vehicle should not penetrate, under-ride, or override the installation although controlled lateral deflection of the test article is acceptable.	YES	YES	YES
		A2	The relative difference in the maximum dynamic deflection is less than 20 percent or the absolute difference is less than 5.9 in.	4.4	0.62	YES
		A3	The relative difference in the time of vehicle-barrier contact is less than 20 percent.	0.6	0.6	YES
		A4	The relative difference in the number of broken or significantly bent posts is less than 20 percent.	n/a	n/a	n/a
		A5	Barrier did not fail (answer Yes or No).	YES	YES	YES
		A6	There were no failures of connector elements.	n/a	n/a	n/a
		A7	There was no significant snagging between the vehicle wheels and barrier elements (Answer Yes or No).	YES	YES	YES
		A8	There was no significant snagging between vehicle body components and barrier elements (Answer Yes or No).	YES	YES	YES
Occupant Risk		D	Detached elements, fragments, or other debris from the test article should not penetrate or show potential for penetrating the occupant compartment, or present an undue hazard to other traffic, pedestrians or personnel in a work zone.	YES	YES	YES
	F	F1	The vehicle should remain upright during and after the collision. The maximum pitch & roll angles are not to exceed 75 degrees.	YES	YES	YES
		F2	Maximum Vehicle roll - relative difference is less than 20% or absolute difference is less than 5 degrees.	8	5.6	YES
		F3	Maximum Vehicle pitch - relative difference is less than 20% or absolute difference is less than 5 degrees.	6.3	3.1	YES
		F4	Maximum Vehicle yaw - relative difference is less than 20% or absolute difference is less than 5 degrees.	15.8	13.5	YES
	H	H1	Longitudinal & lateral occupant impact velocities (OIV) should fall below the preferred value of 30 ft/s (9.1 m/s), or at least below the maximum allowed value of 40 ft/s (12.2 m/s)	YES	YES	YES
		H2	Longitudinal OIV (m/s) - Relative difference is less than 20% or absolute difference is less than 2 m/s	4	2.6	YES
		H3	Lateral OIV (m/s - Relative difference is less than 20% or absolute difference is less than 2 m/s)	2.1	3.5	YES
	I	I1	Longitudinal & lateral occupant ridedown accelerations (ORA) should fall below the preferred value of 15.0 g, or at least below the maximum allowed value of 20.49 g.	YES	YES	YES
		I2	Longitudinal ORA (g) - Relative difference is less than 20% or absolute difference is less than 4 g's	2.4	4.4	YES
		I3	Lateral ORA (g) - Relative difference is less than 20% or absolute difference is less than 4 g's	4.1	6.7	YES
Trajectory		L	The occupant impact velocity in the longitudinal direction should not exceed 40 ft/sec and the occupant ride-down acceleration in the longitudinal direction should not exceed 20 g's	YES	YES	YES
		M	The exit angle from the test article preferable should be less than 60 percent of the test impact angle, measured at the time of vehicle loss of contact with test device.	YES	YES	YES

After all three steps of the validation process are completed, a final determination on whether the model is valid or not can be made. The results of all steps must be affirmative in order for the model to be validated, and every requirement is fulfilled, which means the model is valid. Table 19 summarizes all steps of the validation process for MASH Test 4-12.

Table 19: Composite test comparison for MASH Test 4-12 validation

Composite Test Comparison		
Table 1 - Analysis Solution Verification	Did all solution verification criteria in table pass?	YES
Table 2 - RSVVP Results	Do all the time history evaluation scores from the single channel factors result in a satisfactory comparison (i.e., The comparison passes the criterion)?	NO
	If all the values for Single Channel comparison did not pass, did the weighted procedure result in an acceptable comparison?	YES
Table 3 - Roadside Safety Phenomena Importance Ranking Table	Did all the critical criteria in the PIRT Table pass? Note: Tire deflation was observed in the test but not in the simulation. This was due to the fact that tire deflation was not incorporated into the model. This is considered not to have a critical effect on the outcome of the test.	YES
Overall	Are the results of Steps I through III all affirmative (i.e., YES)? If all three steps result in a "YES" answer, the comparison can be considered validated or verified. If one of the steps results in a negative response, the result cannot be considered validated or verified.	YES

*A "YES" for the weighted procedure but not single channels is acceptable.

4.5.2. PICKUP TRUCK (2270P)

MASH Test 4-11 of the 2270P pickup truck was performed on December 20, 2016. All of the requirements of this test were satisfactorily met, and they are listed in

Table 28. The pickup truck was successfully contained and redirected, and remained upright during and after the collision. Other than non-structural fragments (front grill, pieces of metal from the body, front passenger window) getting taken off of the car, the main damage incurred on the vehicle included the front axle bending and locking the front drivers-side wheel and the tire detaching from the rear driver's side rim, and body damage on the impact side of the vehicle. The intrusions into the occupant compartment were minimal, and did exceed any of the limits specified in MASH. Figure 57 shows a visual comparison between the full-scale crash test and the finite element model. The kinematics of the test and model were very similar to eachother, and were in good agreement. The accelerations and rotations were also in very good agreement, as shown in Figure 58 and Figure 59.

Test	Simulation
0.000 s	0.000 s
0.100 s	0.100 s
0.200 s	0.200 s
0.300 s	0.300 s
0.400	0.400
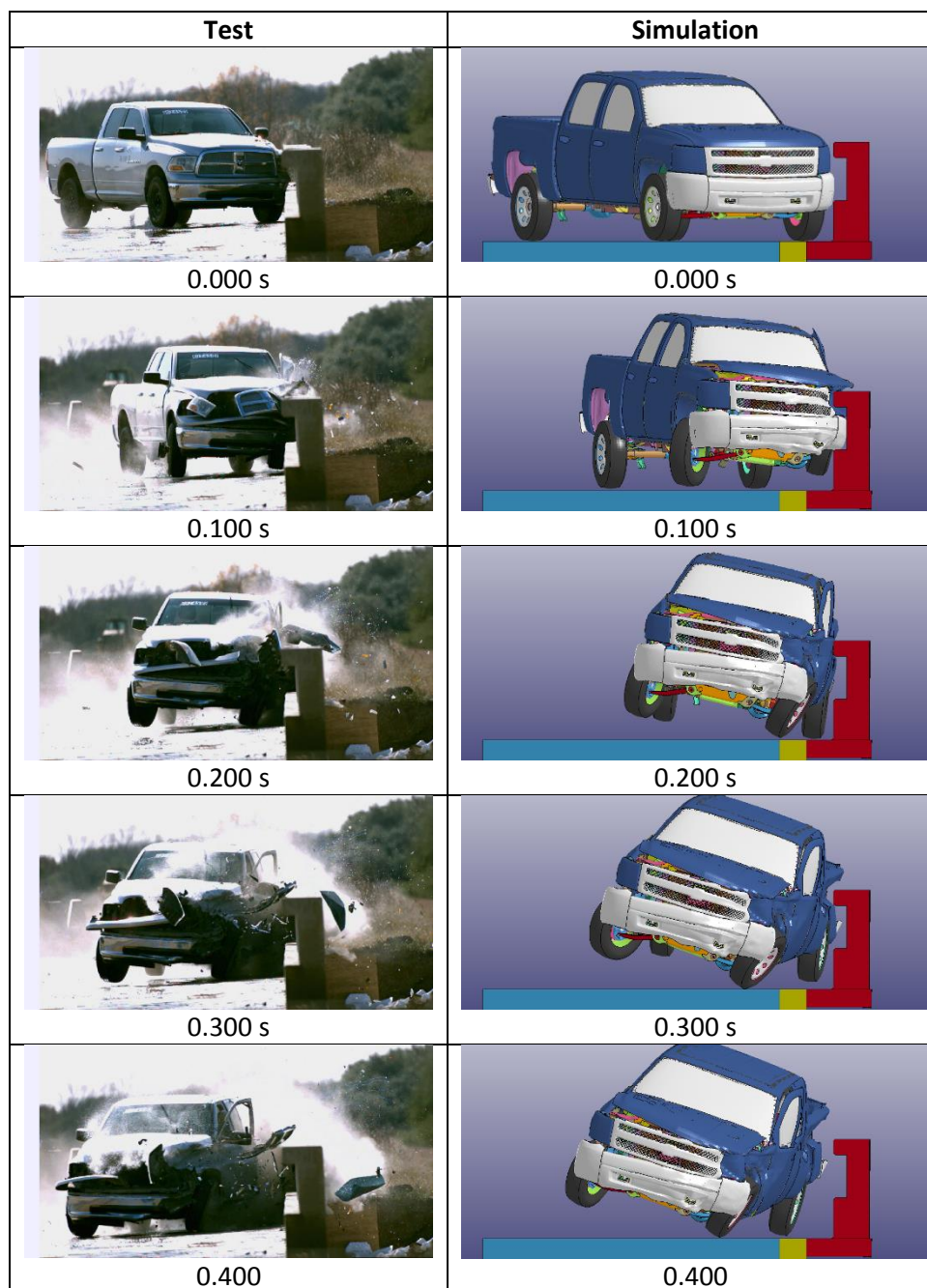
Figure 57: Visual comparison between MASH test 4-11 and FEA
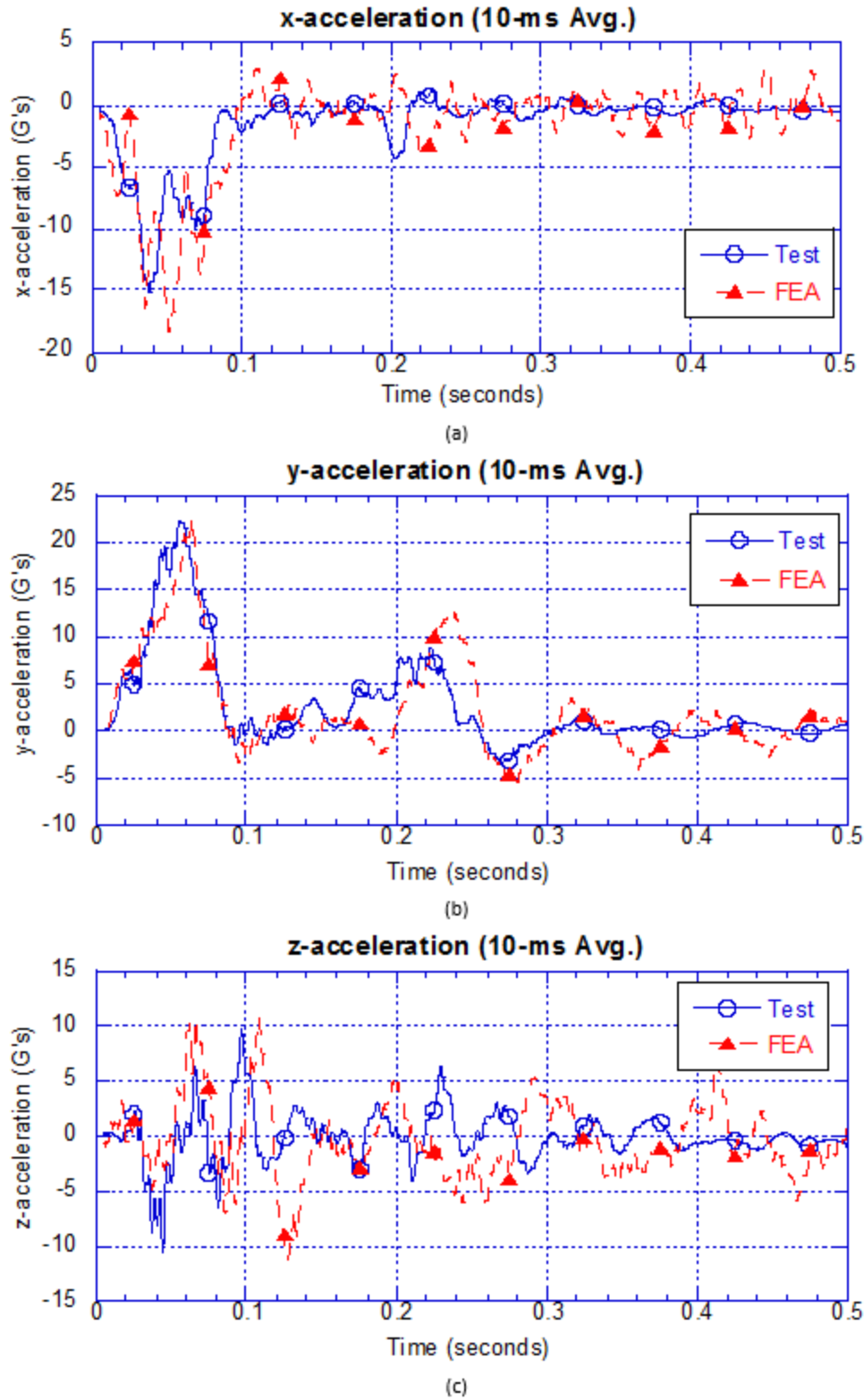
Figure 58: Acceleration comparison between MASH test 4-11 and FEA: (a) x-acceleration plots; (b) y-acceleration plots; (c) z-acceleration plots)
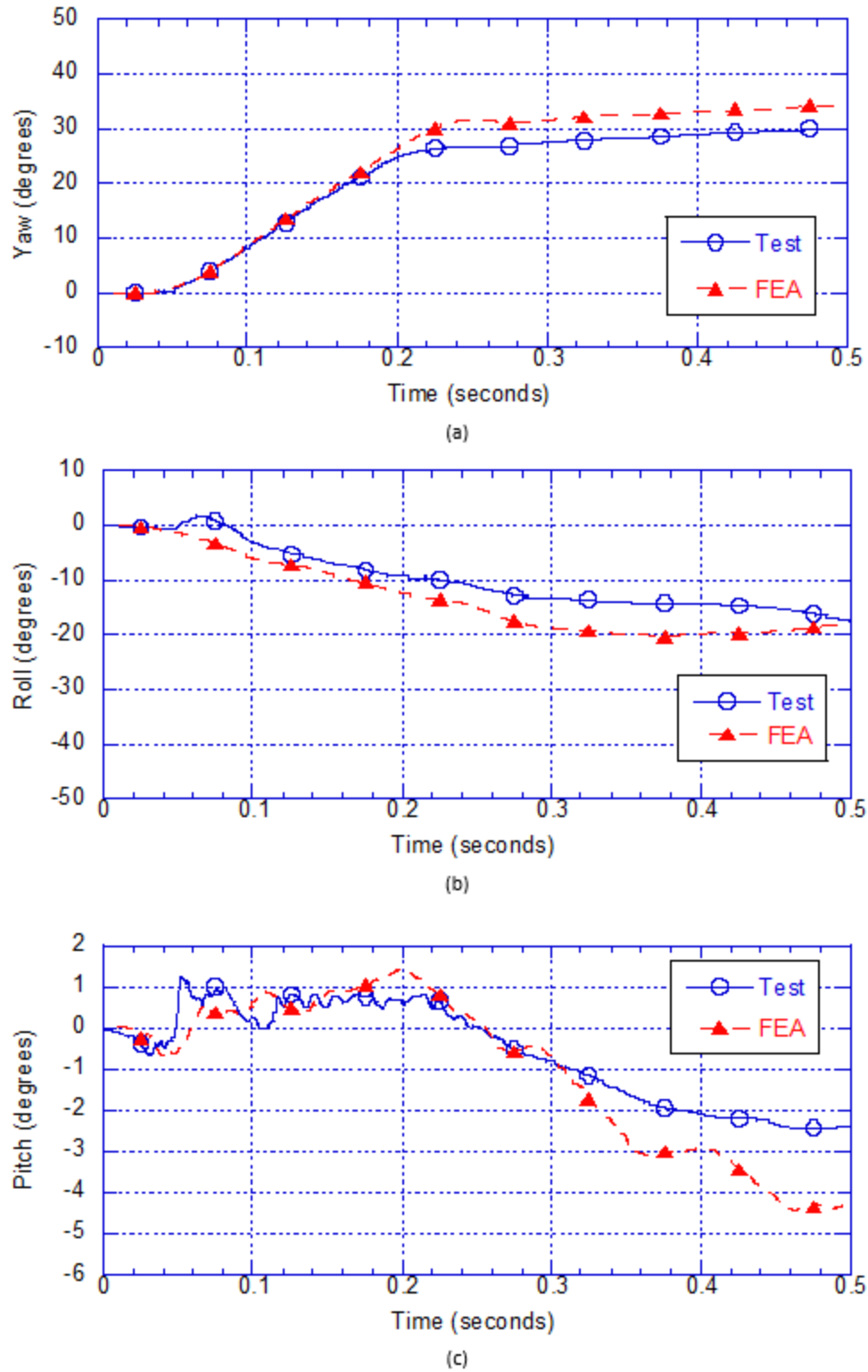
Figure 59: Rotational angle comparison between MASH test 4-11 and FEA: (a) Yaw angles vs time; (b) Roll angles vs time; (c) Pitch angles vs time.

The first step in validating the model is checking the solution verification criteria to ensure the model is stable and all laws of physics are upheld. Table 20 shows the solution verification table for the small car model, and all criteria passes.

Table 20: Solution verification criteria for model of MASH test 4-11

Verification Evaluation Criteria	Change (%)	Pass?
Total energy of the analysis solution (i.e., kinetic, potential, contact, etc.) must not vary more than 10 percent from the beginning of the run to the end of the run.	<1	YES
Hourglass Energy of the analysis solution at the end of the run is less than 5% of the total initial energy at the beginning of the run.	<1	YES
The part/material with the highest amount of hourglass energy at any time during the run is less than 5% of the total initial energy at the beginning of the run.	<1	YES
Mass added to the total model is less than 5% the total model mass at the start of the run.	<1	YES
The part/material with the most mass added had less than 10% of its initial mass added.	<1	YES
The moving parts/materials in the model have less than 5% of mass added to the initial moving mass of the model.	<1	YES
There are no shooting nodes in the solution?	YES	YES
There are no solid elements with negative volumes?	YES	YES

The next step in validating the model is validating the time-history curves. All accelerations and rotations about the three axes were compared using RSVVP and the theory described in the beginning of this section. Although the Sprague-Geers metrics did not pass for the z-acceleration, roll rate, and pitch rate channels, the multi-channel comparison passed, and therefore the time-histories pass and are validated.

Because the magnitudes of the channels that failed the Sprague-Geers comparison had such low magnitudes relative to the other channels, they were given much lower weighting factors in the multi-channel comparison than the other channels that passed. In other words, the channels that failed had a very small effect on the overall behavior and performance of the system. The channels with the most significance on the behavior of

the vehicle were matching in the model and full-scale test, and therefore were deemed acceptable. Table 21 lists all the scores for the time-history validation of the individual channels, as well as the multi-channel comparison.

Table 21: Time-history validation of MASH test 4-11 Finite Element Analysis

Single Channel Time History Comparison Results		Time interval [0 sec - 0.5 sec]		
	Sprague-Geer Metrics	**M**	**P**	**Pass?**
	X acceleration	37.7	26.4	Fail
O	Y acceleration	0.1	19.4	Pass
	Z acceleration	47.2	46.7	Fail
	Yaw rate	9.8	7.6	Pass
	Roll rate	0.7	49.9	Fail
	Pitch rate	13.9	48.8	Fail
	ANOVA Metrics	**Mean**	**SD**	**Pass?**
	X acceleration/Peak	-0.59	17.39	Pass
P	Y acceleration/Peak	-1.06	11.99	Pass
	Z acceleration/Peak	-1.55	34.16	Pass
	Yaw rate	2.03	9.56	Pass
	Roll rate	2.06	24.83	Pass
	Pitch rate	-5.47	13.14	Pass
Multi-Channel Weighting Factors		**Time interval [0 sec - 0.5 sec]**		
Multi-Channel Weighting Method Peaks Area I Area II Inertial	**X Channel**	0.17521272		
	Y Channel	0.302934251		
	Z Channel	0.021853028		
	Yaw Channel	0.363504853		
	Roll Channel	0.118629509		
	Pitch Channel	0.017865638		
Sprague-Geer Metrics		**M**	**P**	**Pass?**
	All Channels (weighted)	11.6	21.2	Pass
ANOVA Metrics		**Mean**	**SD**	**Pass?**
	All Channels (weighted)	-1.2	13.7	Pass

The third and final step of the validation process is checking that all criteria in the Phenomena Importance Ranking Table (PIRT) is fulfilled. Table 22 lists the criteria that needs to be fulfilled in order for the model to be considered fully validated.

Table 22: Phenomena Importance Ranking Table for MASH Test 4-11

			Evaluation Criteria	Known Result	Analysis Result	Agree?
Structural Adequacy	**A**	A1	Test article should contain and redirect the vehicle; the vehicle should not penetrate, under-ride, or override the installation although controlled lateral deflection of the test article is acceptable.	YES	YES	YES
		A2	The relative difference in the maximum dynamic deflection is less than 20 percent or the absolute difference is less than 0.15 m (5.9 in).	1	0.58	YES
		A3	The relative difference in the time of vehicle-barrier contact is less than 20 percent.	0.33	0.27	YES
		A4	The relative difference in the number of broken or significantly bent posts is less than 20 percent.	n/a	n/a	n/a
		A5	Barrier did not fail (answer Yes or No).	YES	YES	YES
		A6	There were no failures of connector elements.	n/a	n/a	n/a
		A7	There was no significant snagging between the vehicle wheels and barrier elements (Answer Yes or No).	YES	YES	YES
		A8	There was no significant snagging between vehicle body components and barrier elements (Answer Yes or No).	YES	YES	YES
Occupant Risk		**D**	Detached elements, fragments, or other debris from the test article should not penetrate or show potential for penetrating the occupant compartment, or present an undue hazard to other traffic, pedestrians or personnel in a work zone.	YES	YES	YES
	F	F1	The vehicle should remain upright during and after the collision. The maximum pitch & roll angles are not to exceed 75 degrees.	YES	YES	YES
		F2	Maximum Vehicle roll - relative difference is less than 20% or absolute difference is less than 5 degrees.	24	20.2	YES
		F3	Maximum Vehicle pitch - relative difference is less than 20% or absolute difference is less than 5 degrees.	6	4.4	YES
		F4	Maximum Vehicle yaw - relative difference is less than 20% or absolute difference is less than 5 degrees.	32	36	YES
	H	H1	Longitudinal & lateral occupant impact velocities (OIV) should fall below the preferred value of 30 ft/s (9.1 m/s), or at least below the maximum allowed value of 40 ft/s (12.2 m/s)	YES	YES	YES
		H2	Longitudinal OIV (m/s) - Relative difference is less than 20% or absolute difference is less than 2 m/s	5.5	7.2	YES
		H3	Lateral OIV (m/s - Relative difference is less than 20% or absolute difference is less than 2 m/s)	8.8	8.1	YES
	I	I1	Longitudinal & lateral occupant ridedown accelerations (ORA) should fall below the preferred value of 15.0 g, or at least below the maximum allowed value of 20.49 g.	YES	YES	YES
		I2	Longitudinal ORA (g) - Relative difference is less than 20% or absolute difference is less than 4 g's	4.4	4.2	YES
		I3	Lateral ORA (g) - Relative difference is less than 20% or absolute difference is less than 4 g's	8.9	12.5	YES
Trajectory		**L**	The occupant impact velocity in the longitudinal direction should not exceed 40 ft/sec and the occupant ride-down acceleration in the longitudinal direction should not exceed 20 G's.	YES	YES	YES
		M	The exit angle from the test article preferable should be less than 60 percent of the test impact angle, measured at the time of vehicle loss of contact with test device.	YES	YES	YES

After all three steps of the validation process are completed, a final determination on whether the model is valid or not can be made. The results of all steps must be affirmative in order for the model to be validated, and every requirement is fulfilled, which means the model is valid. Table 23 summarizes all steps of the validation process for MASH Test 4-11.

Table 23: Composite test comparison for MASH Test 4-11 validation

Composite Test Comparison		
Table 1 - Analysis Solution Verification	Did all solution verification criteria in table pass?	YES
Table 2 - RSVVP Results	Do all the time history evaluation scores from the single channel factors result in a satisfactory comparison (i.e., The comparison passes the criterion)?	NO
	If all the values for Single Channel comparison did not pass, did the weighted procedure result in an acceptable comparison?	YES
Table 3 - Roadside Safety Phenomena Importance Ranking Table	Did all the critical criteria in the PIRT Table pass? Note: Tire deflation was observed in the test but not in the simulation. This was due to the fact that tire deflation was not incorporated into the model. This is considered not to have a critical effect on the outcome of the test.	YES
Overall	Are the results of Steps I through III all affirmative (i.e., YES)? If all three steps result in a "YES" answer, the comparison can be considered validated or verified. If one of the steps results in a negative response, the result cannot be considered validated or verified.	YES

*A "YES" for the weighted procedure but not single channels is acceptable.

4.5.3. SMALL CAR (1100C)

MASH Test 4-10 of the 1100C passenger car was performed on December 21, 2016. All of the requirements of this test were satisfactorily met, and they are listed in Table 28. The car was successfully contained and redirected, and remained upright during and after the collision. The intrusions into the occupant compartment were minimal, and did exceed any of the limits specified in MASH. Figure 60 shows a visual comparison between the full-scale crash test and the finite element model. The kinematics of the test and model were very similar to each other, and were in good agreement. The accelerations and rotations were also in very good agreement, as shown in Figure 61 and Figure 62.

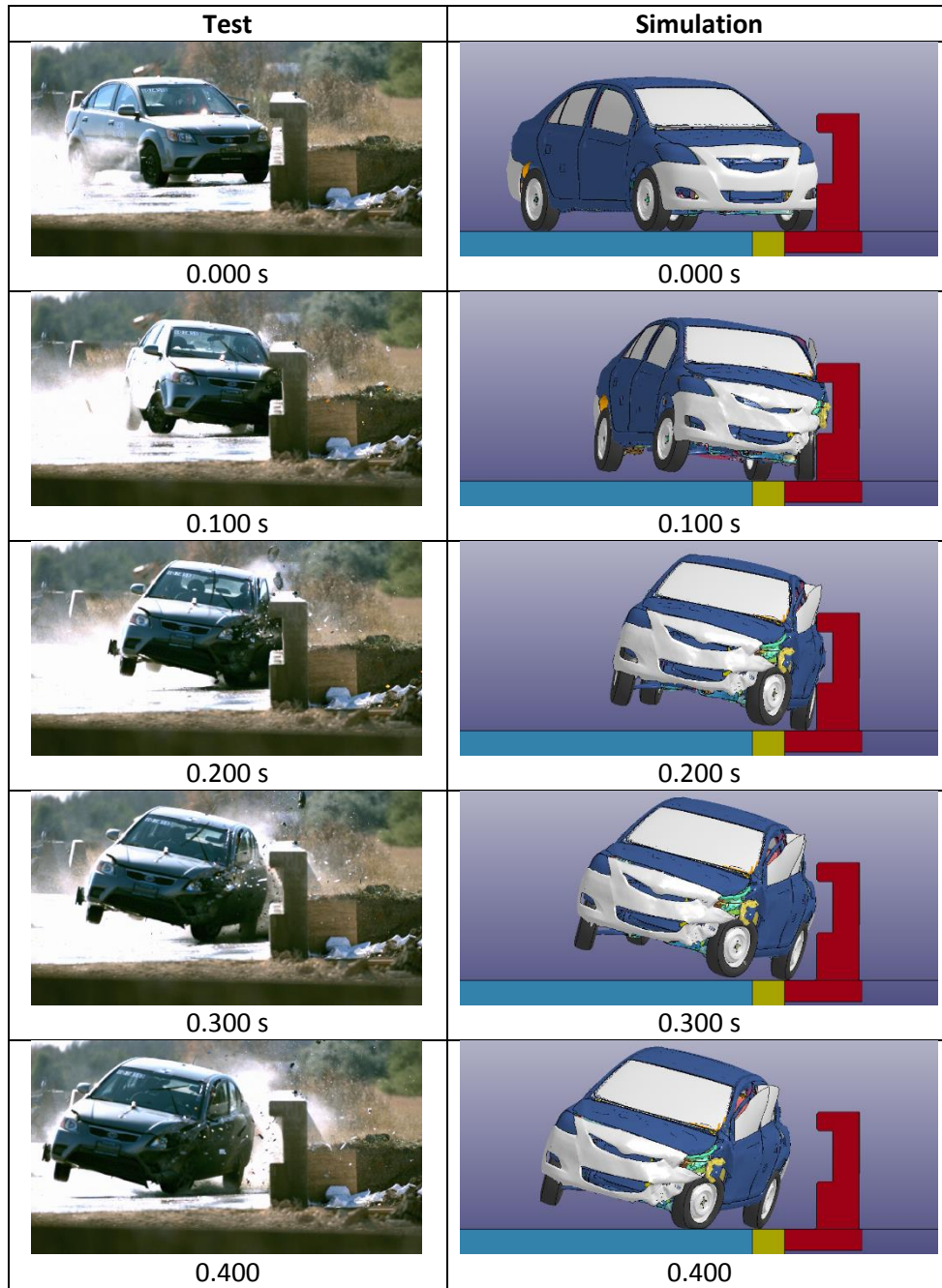| Test	Simulation
0.000 s	0.000 s
0.100 s	0.100 s
0.200 s	0.200 s
0.300 s	0.300 s
0.400	0.400

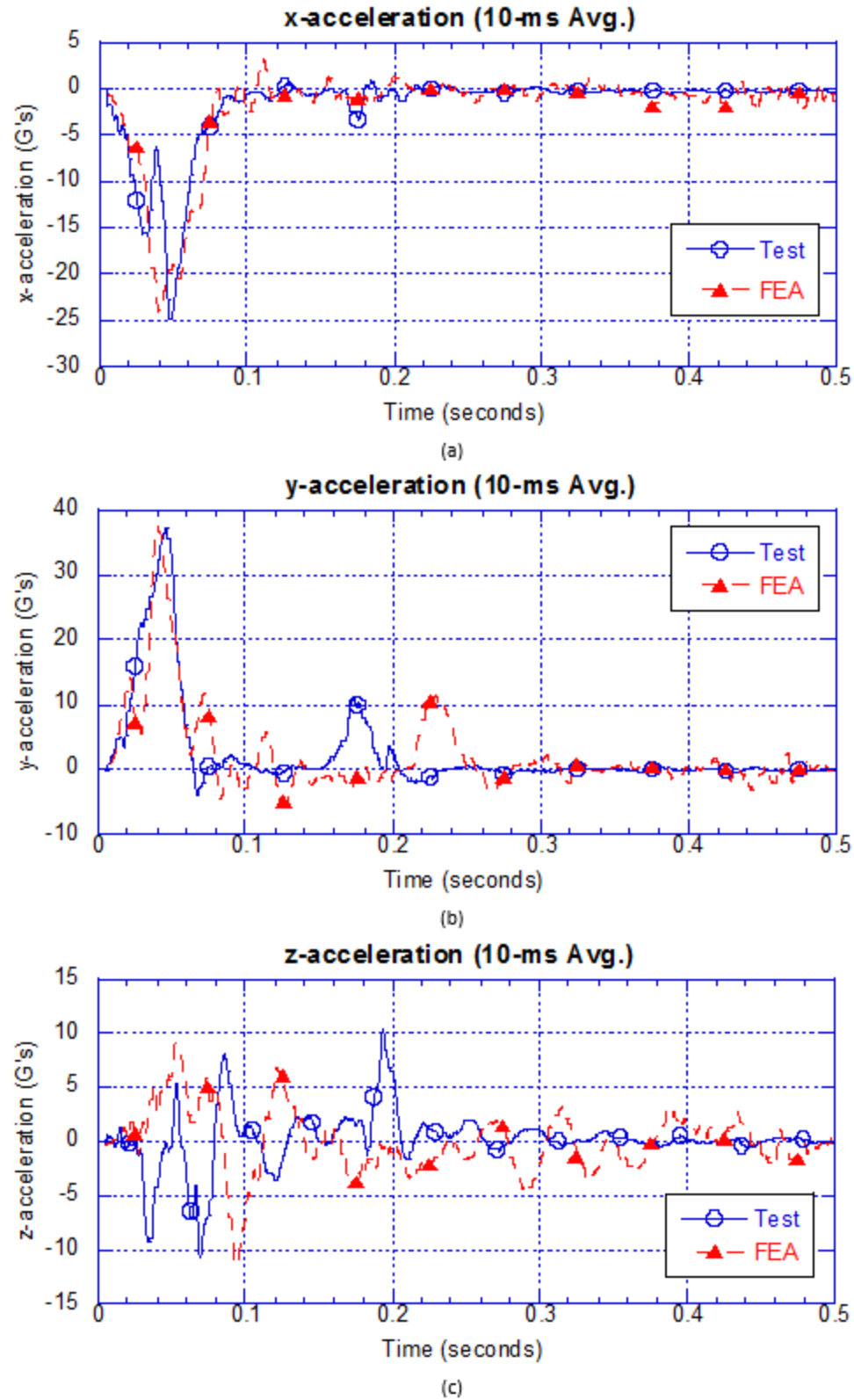Figure 60: Visual comparison between MASH test 4-10 and FEA

Figure 61: Acceleration comparison between MASH test 4-10 and FEA: (a) x-acceleration plots; (b) y-acceleration plots; (c) z-acceleration plots)
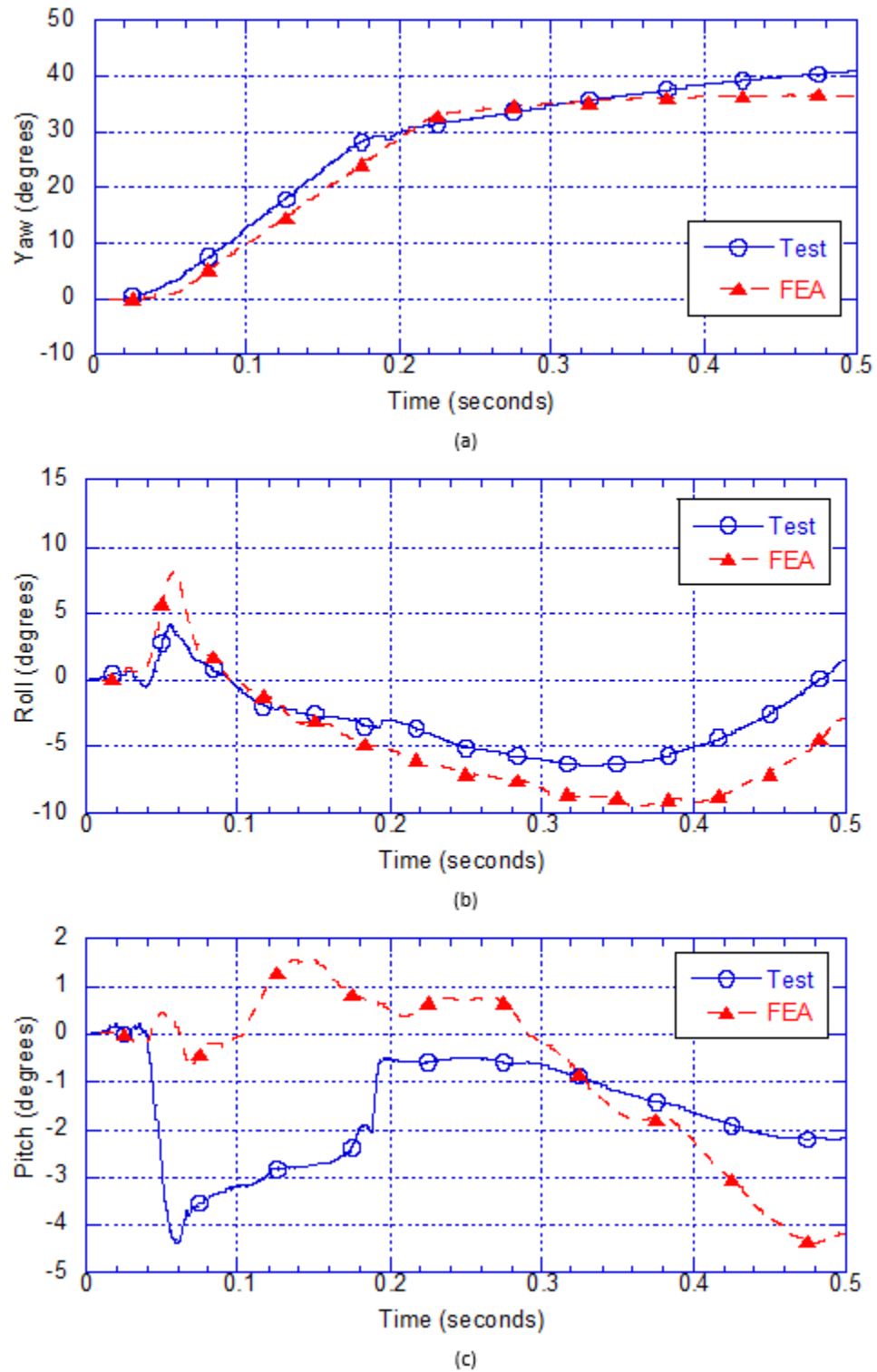
Figure 62: Rotational angle comparison between MASH test 4-10 and FEA: (a) Yaw angles vs time; (b) Roll angles vs time; (c) Pitch angles vs time.

The first step in validating the model is checking the solution verification criteria to ensure the model is stable and all laws of physics are upheld. Table 24 shows the solution verification table for the small car model, and all criteria passes.

Table 24: Solution verification criteria for model of MASH test 4-10

Verification Evaluation Criteria	Change (%)	Pass?
Total energy of the analysis solution (i.e., kinetic, potential, contact, etc.) must not vary more than 10 percent from the beginning of the run to the end of the run.	5.39	YES
Hourglass Energy of the analysis solution at the end of the run is less than 5% of the total initial energy at the beginning of the run.	<1	YES
The part/material with the highest amount of hourglass energy at any time during the run is less than 5% of the total initial energy at the beginning of the run.	<1	YES
Mass added to the total model is less than 5% the total model mass at the start of the run.	<1	YES
The part/material with the most mass added had less than 10% of its initial mass added.	<1	YES
The moving parts/materials in the model have less than 5% of mass added to the initial moving mass of the model.	3.8	YES
There are no shooting nodes in the solution?	YES	YES
There are no solid elements with negative volumes?	YES	YES

The next step in validating the model is validating the time-history curves. All accelerations and rotations about the three axes were compared using RSVVP and the theory described in the beginning of this section. Although the Sprague-Geers metrics did not pass for the z-acceleration, roll rate, and pitch rate channels, the multi-channel comparison passed, and therefore the time-histories pass and are validated.

Because the magnitudes of the channels that failed the Sprague-Geers comparison had such low magnitudes relative to the other channels, they were given much lower weighting factors in the multi-channel comparison than the other channels that passed. In other words, the channels that failed had a very small effect on the overall behavior and performance of the system. The channels with the most significance on the behavior of

the vehicle were matching in the model and full-scale test, and therefore were deemed acceptable. Table 25 lists all the scores for the time-history validation of the individual channels, as well as the multi-channel comparison.

Table 25: Time-history validation of MASH test 4-10 Finite Element Analysis

Single Channel Time History Comparison Results		Time interval [0 sec - 0.5 sec]		
	Sprague-Geer Metrics	M	P	Pass?
O	X acceleration	10.2	23.4	Pass
	Y acceleration	1.2	24.8	Pass
	Z acceleration	1.6	42.4	Fail
	Yaw rate	3.1	15.2	Pass
	Roll rate	42.1	18.8	Fail
	Pitch rate	40.7	53.6	Fail
	ANOVA Metrics	Mean	SD	Pass?
P	X acceleration/Peak	-0.34	9.63	Pass
	Y acceleration/Peak	-0.37	10.29	Pass
	Z acceleration/Peak	-0.38	18.37	Pass
	Yaw rate	-4.26	13.25	Pass
	Roll rate	-0.7	13.13	Pass
	Pitch rate	-0.86	16.74	Pass
Multi-Channel Weighting Factors		Time interval [0 sec - 0.5 sec]		
Multi-Channel Weighting Method **Peaks Area I** **Area II Inertial**	X Channel	0.219987577		
	Y Channel	0.273368452		
	Z Channel	0.006643971		
	Yaw Channel	0.428663933		
	Roll Channel	0.066102883		
	Pitch Channel	0.005233184		
Sprague-Geer Metrics		M	P	Pass?
	All Channels (weighted)	6.9	20.3	Pass
ANOVA Metrics		Mean	SD	Pass?
	All Channels (weighted)	-2.1	11.7	Pass

The third and final step of the validation process is checking that all criteria in the Phenomena Importance Ranking Table (PIRT) is fulfilled. Table 26 lists the criteria that needs to be fulfilled in order for the model to be considered fully validated.

Table 26: Phenomena Importance Ranking Table for MASH Test 4-10

Evaluation Criteria			Known Result	Analysis Result	Agree?
Structural Adequacy / **A**	A1	Test article should contain and redirect the vehicle; the vehicle should not penetrate, under-ride, or override the installation although controlled lateral deflection of the test article is acceptable.	YES	YES	YES
	A2	The relative difference in the maximum dynamic deflection is less than 20 percent or the absolute difference is less than 5.9 in.	0.5	0.22	YES
	A3	The relative difference in the time of vehicle-barrier contact is less than 20 percent.	0.23	0.255	YES
	A4	The relative difference in the number of broken or significantly bent posts is less than 20 percent.	n/a	n/a	n/a
	A5	Barrier did not fail (answer Yes or No).	YES	YES	YES
	A6	There were no failures of connector elements.	n/a	n/a	n/a
	A7	There was no significant snagging between the vehicle wheels and barrier elements (Answer Yes or No).	YES	YES	YES
	A8	There was no significant snagging between vehicle body components and barrier elements (Answer Yes or No).	YES	YES	YES
Occupant Risk	**D**	Detached elements, fragments, or other debris from the test article should not penetrate or show potential for penetrating the occupant compartment, or present an undue hazard to other traffic, pedestrians or personnel in a work zone	YES	YES	YES
	F F1	The vehicle should remain upright during and after the collision. The maximum pitch & roll angles are not to exceed 75 degrees.	YES	YES	YES
	F2	Maximum Vehicle roll - relative difference is less than 20% or absolute difference is less than 5 degrees.	11	10.8	YES
	F3	Maximum Vehicle pitch - relative difference is less than 20% or absolute difference is less than 5 degrees.	4	4.6	YES
	F4	Maximum Vehicle yaw - relative difference is less than 20% or absolute difference is less than 5 degrees.	44	36	YES
	H H1	Longitudinal & lateral occupant impact velocities (OIV) should fall below the preferred value of 30 ft/s (9.1 m/s), or at least below the maximum allowed value of 40 ft/s (12.2 m/s)	YES	YES	YES
	H2	Longitudinal OIV (m/s) - Relative difference is less than 20% or absolute difference is less than 2 m/s	7	8.4	YES
	H3	Lateral OIV (m/s - Relative difference is less than 20% or absolute difference is less than 2 m/s)	9.6	9.3	YES
	I I1	Longitudinal & lateral occupant ridedown accelerations (ORA) should fall below the preferred value of 15.0 g, or at least below the maximum allowed value of 20.49 g.	YES	YES	YES
	I2	Longitudinal ORA (g) - Relative difference is less than 20% or absolute difference is less than 4 g's	4.2	3.1	YES
	I3	Lateral ORA (g) - Relative difference is less than 20% or absolute difference is less than 4 g's	11	11.4	YES
Trajectory	**L**	The occupant impact velocity in the longitudinal direction should not exceed 40 ft/sec and the occupant ride-down acceleration in the longitudinal direction should not exceed 20 G's.	YES	YES	YES
	M	The exit angle from the test article preferable should be less than 60 percent of the test impact angle, measured at the time of vehicle loss of contact with test device.	YES	YES	YES

After all three steps of the validation process are completed, a final determination on whether the model is valid or not can be made. The results of all steps must be affirmative in order for the model to be validated, and every requirement is fulfilled, which means the model is valid. Table 27 summarizes all steps of the validation process for MASH Test 4-10.

Table 27: Composite test comparison for MASH Test 4-10 validation

Composite Test Comparison		
Table 1 - Analysis Solution Verification	Did all solution verification criteria in table pass?	YES
Table 2 - RSVVP Results	Do all the time history evaluation scores from the single channel factors result in a satisfactory comparison (i.e., The comparison passes the criterion)?	NO
	If all the values for Single Channel comparison did not pass, did the weighted procedure result in an acceptable comparison?	YES
Table 3 - Roadside Safety Phenomena Importance Ranking Table	Did all the critical criteria in the PIRT Table pass? Note: Tire deflation was observed in the test but not in the simulation. This was due to the fact that tire deflation was not incorporated into the model. This is considered not to have a critical effect on the outcome of the test.	YES
Overall	Are the results of Steps I through III all affirmative (i.e., YES)? If all three steps result in a "YES" answer, the comparison can be considered validated or verified. If one of the steps results in a negative response, the result cannot be considered validated or verified.	YES

*A "YES" for the weighted procedure but not single channels is acceptable.

Table 28: List of requirements for passing MASH tests 4-10 and 4-11 (AASHTO, 2016)

- Test article should contain and redirect the vehicle or bring the vehicle to a controlled stop; the vehicle should not penetrate, underride, or override the installation although controlled lateral deflection of the test article is acceptable
- Detached elements, fragments, or other debris from the test article should not penetrate or show potential for penetrating the occupant compartment, or present undue hazard to other traffic, pedestrians, or personnel in a work zone. Deformations of, or intrusions into, the occupant compartment should not exceed limits set forth in Section 5.2.2 and Appendix E.
- The vehicle should remain upright during and after collision. The maximum roll and pitch angles are not to exceed 75 degrees.
- Occupant impact velocities (OIV) should satisfy the following limits:
  - Preferred: 30 ft/s
  - Maximum: 40 ft/s
- The occupant ridedown acceleration should satisfy the following limits:
  - Preferred: 15.0 G
  - Maximum: 20.49 G

Deformations and intrusions should be limited as follows:
- Roof ≤4 in
- Windshield—no tear of plastic liner and maximum deformation of 3 in.
- Window—no shattering of a side window resulting from direct contact with a structural member of the test article, except for special considerations pertaining to tall, continuous barrier elements discussed below. In cases where side windows are laminated, the guidelines for windshields will apply.
- A- and B-pillars—no complete severing of support member and maximum resultant deformation of 5 in. Lateral deformation should be limited to 3 in.
  - Wheel/foot well and toe pan areas≤9 in.
  - Side front panel (forward of A-pillar) ≤12 in.
  - Front side door area (above seat) ≤ 9 in.
  - Front side door area (below seat) ≤ 12 in.
  - Floor pan and transmission tunnel areas ≤ 12 in.

CHAPTER VI

5. SUMMARY AND CONCLUSIONS

5.1.   SUMMARY

The purpose of this study was to provide an open-faced concrete balustrade design as part of Pulaski Skyway Contract 2. After a preliminary design performed according to AASHTO design procedures was approved by the Historic Preservation Office, it was used as the basis for a parametric study.   Using computer simulations, the parametric study adjusted three parameters to investigate their effect on the collision: (1) total barrier height, (2) post width, and (3) window opening width. Based on the results from the parametric study, the final design was constructed and crash tested at TTI testing facility to AASHTO MASH TL-4 standards. All three required crash tests were successful. Once approved by FHWA, the barrier could be adopted by various agencies in NJ and other states.

The models for each crash test have been validated in accordance with NCHRP W179, and have very close agreement with the full-scale tests. These models can be used in the place of full-scale tests to evaluate improvements and retrofits to the rail in the future.

5.2.   CONCLUSIONS

Based on the results of the study, the following conclusions can be made:

1. As the total height of the barrier increases, the likelihood of a truck overturning is decreased;

2. As posts get closer, the capacity of the barrier increases;

3. Wide post openings can cause components of the vehicle to snag and get caught inside.

Because barrier height decides which part of the vehicle comes in contact with the barrier, if the height is increased the parts impacting the barrier will be higher and more easily keep the vehicle upright. This is especially true for the box truck test because if the box, instead of the tires, hits, the truck will not start the tripping motion that causes leaning over the barrier. If the post openings are too wide, components of the vehicles may get caught inside and cause more damage to the barrier or vehicles. It was found that changing the spacing of the posts did not have a large effect on the kinematics of the truck, and that height was the main factor that affected how the truck responded. The final result of this project is that a balustrade with a height of 44 inches, post width of 8 inches, and window opening of 6 inches is the optimal design for a TL-4 collision.

REFERENCES

1. Demond, G. (1996). Aesthetic guidelines for older bridges. *Transportation Research Record: Journal of the Transportation Research Board*, (1549), 42-47.

2. Eskandarian, A., Marzougui, D., & Bedewi, N. E. (1997). Finite element model and validation of a surrogate crash test vehicle for impacts with roadside objects. *International Journal of Crashworthiness*, *2*(3), 239-258.

3. Consolazio, G. R., Chung, J. H., & Gurley, K. R. (2003). Impact simulation and full scale crash testing of a low profile concrete work zone barrier. *Computers & structures*, *81*(13), 1359-1374.

4. Borovinšek, M., Vesenjak, M., Ulbin, M., & Ren, Z. (2007). Simulation of crash tests for high containment levels of road safety barriers. *Engineering failure analysis*, *14*(8), 1711-1718.

5. Ren, Z., & Vesenjak, M. (2005). Computational and experimental crash analysis of the road safety barrier. *Engineering Failure Analysis*, *12*(6), 963-973.

6. Itoh, Y., Liu, C., & Kusama, R. (2007). Dynamic simulation of collisions of heavy high-speed trucks with concrete barriers. *Chaos, Solitons & Fractals*, *34*(4), 1239-1244.

7. Marzougui, D., Mohan, P., Kan, C. D., & Opiela, K. S. (2012). *Assessing options for improving barrier crashworthiness using finite element models and crash simulations* (Vol. 8). Final Report NCAC-2012-W.

8. Marzougui, D., Kan, C. D., & Opiela, K. S. (2014). Crash test & simulation comparisons of a pickup truck & a small car oblique impacts into a concrete barrier. In *13th International LS-DYNA Users Conference.*

9. Abu-Odeh, A. (2008). Modeling and Simulation of Bogie Impacts on Concrete Bridge Rails using LS-DYNA®. In *10th international LS-DYNA Users Conference, Livermore Software Technology Corporations, June* (pp. 8-10).

10. Borrvall, T., & Riedel, W. (2011, May). The RHT concrete model in LS-DYNA. In *Proceedings of the 8th European LS-DYNA Users Conference, Strasbourg.*

11. Schwer, L. (2014). Modeling Rebar: The Forgotten Sister in Reinforced Concrete Modeling. *Constitutive Modeling*, *13*.

12. H.E. Ross, JR., D.L. Sicking, and R.A. Zimmer. *Recommended Procedures for the Safety Performance Evaluation of Highway Features.* National Cooperative Highway Research Program (NCHRP), NCHRP Report 350. Dynatech Engineering Inc.

13. *Manual for Assessing Safety Hardware (MASH),* American Association of State Highway and Transportation Officials (AASHTO), Washington, D.C., 2016.

14. D. L. Bullard, R. P. Bligh, and W. L. Menges, Appendix A: MASH-08 TL-4 Testing and Evaluation of the New Jersey Safety Shape Bridge Rail. NCHRP Project 22-14, College Station, Texas, 2008.

15. Sheikh, N. M., Bligh, R. P., & Menges, W. L. (2011). *Determination of minimum height and lateral design load for MASH test level 4 bridge rails* (No. FHWA/TX-12/9-1002-5).

16. Sheikh, N., Bligh, R., & Holt, J. (2012). Minimum Rail Height and Design Impact Load for MASH TL-4 Longitudinal Barriers. In *TRB Annual Meeting* (pp. 1-16).

17. AASHTO LRFD Bridge Design Specifications. American Association of State Highway and Transportation Officials (AASHTO), 2012.

18. Pfeifer, B. G., Faller, R. K., Holloway, J. C., & Rosson, B. T. (1996). Test level 4 evaluation of the Minnesota combination bridge rail.

19. Buth, C. E., Bligh, R. P., & Menges, W. L. (1998). *NCHRP Report 350 Test 3-11 of the Texas Type T411 Bridge Rail* (No. FHWA/TX-98/1804-3).

20. Bullard Jr, D. L., Williams, W. F., Menges, W. L., & Haug, R. R. (2002). *Design and evaluation of the TxDOT F411 and T77 Aesthetic Bridge Rails* (No. FHWA/TX-03/4288-1,).

21. Alberson, D. C., Menges, W. L., & Haug, R. R. (2004). TEXAS TRANSPORTATION INSTITUTE THE TEXAS A&M UNIVERSITY SYSTEM COLLEGE STATION, TEXAS 77843.

22. S. K. Tay, J. K. Poon, R. Chan., *Modeling Rebar in Reinforced Concrete for ALE Simulations. 14th International LS-DYNA Users Conference,* June 2016.

23. New Jersey Department of Transportation Design Manual for Bridges and Structures (5th edition). New Jersey Department of Transportation (NJDOT), 2009.

24. *LS-DYNA R8.0.0 Release Notes,* Livermore Software Technology Corporation (LSTC), Livermore, CA., 2016.

25. Dynasupport.com

26. Ray, M.H., Mongiardini, M., Plaxico, C.A., Anghileri, M., *Procedures for Verification and Validation of Computer Simulations Used for Roadside Safety Applications*, Final Report to the National Cooperative Highway Research Program (NCHRP), NCHRP Report No. W179, Project No. 22-24, Worcester Polytechnic Institute, March, 2010.

27. Sprague, M. A., & Geers, T. L. (2003). Spectral elements and field separation for an acoustic fluid subject to cavitation. *Journal of Computational Physics*, *184*(1), 149-162.

28. Oberkampf, W. L., & Barone, M. F. (2006). Measures of agreement between computation and experiment: validation metrics. *Journal of Computational Physics*, *217*(1), 5-36.

29. Ray, M. (1996). Repeatability of full-scale crash tests and criteria for validating simulation results. *Transportation Research Record: Journal of the Transportation Research Board*, (1528), 155-160.

30. LS-DYNA R7.0 Keyword User's Manuals I & II, February 2013.

31. Williams, W. F., Menges, W. L., & Kuhn, D. L. (2017). *MASH TL-4 Evaluation of the Pulaski Skyway Bridge Parapet*.